AD_____

Award Number: W81XWH-08-1-0774

TITLE: N-Acetyltransferase 1 Polymorphism and Breast Cancer Risk

PRINCIPAL INVESTIGATOR: Lori Millner

CONTRACTING ORGANIZATION: University of Louisville Research Foundation
Louisville, Y 40292

REPORT DATE: October 2011

TYPE OF REPORT: Final

PREPARED FOR: U.S. Army Medical Research and Materiel Command
Fort Detrick, Maryland 21702-5012

REPORT DOCUMENTATION PAGE

Form Approved
OMB No. 0704-0188

1. REPORT DATE *(DD-MM-YYYY)*	2. REPORT TYPE	3. DATES COVERED *(From - To)*
01-10-2011	Final	29 sep 2008 - 28 Sep 2011

4. TITLE AND SUBTITLE
N-Acetyltransferase 1 Polymorphism and Breast Cancer Risk

5a. CONTRACT NUMBER

5b. GRANT NUMBER
W81XWH-08-1-0774

5c. PROGRAM ELEMENT NUMBER

6. AUTHOR(S)
Lori Millner

E-Mail: lmmill10@louisville.edu

5d. PROJECT NUMBER

5e. TASK NUMBER

5f. WORK UNIT NUMBER

7. PERFORMING ORGANIZATION NAME(S) AND ADDRESS(ES)
University of Louisville Research Foundation
Louisville, KY 40292

8. PERFORMING ORGANIZATION REPORT NUMBER

9. SPONSORING / MONITORING AGENCY NAME(S) AND ADDRESS(ES)
U.S. Army Medical Research and Materiel Command
Fort Detrick, Maryland 21702-5012

10. SPONSOR/MONITOR'S ACRONYM(S)

11. SPONSOR/MONITOR'S REPORT NUMBER(S)

12. DISTRIBUTION / AVAILABILITY STATEMENT
Approved for Public Release; Distribution Unlimited

13. SUPPLEMENTARY NOTES

14. ABSTRACT
Abstract on next page.

15. SUBJECT TERMS
N-acetyltransferase, metabolism, aryl amines

16. SECURITY CLASSIFICATION OF:			17. LIMITATION OF ABSTRACT	18. NUMBER OF PAGES	19a. NAME OF RESPONSIBLE PERSON
a. REPORT	b. ABSTRACT	c. THIS PAGE			USAMRMC
U	U	U	UU		19b. TELEPHONE NUMBER *(include area code)*

14. ABSTRACT

N-acetyltransferase 1 (NAT1) catalyzes *N*-acetylation of aryl amine carcinogens resulting in their activation or inactivation. *NAT1*10* and NAT1*14, common variant alleles have been associated with increased risk for numerous cancers including breast. NAT1 is also upregulated in breast cancer. We employed a novel approach to study functional differences caused by *NAT1*10* and NAT1*14 polymorphisms by using constructs that mimic complete human mRNAs by including the 5′-UTR, coding region and 3′-UTR. Significantly more enzymatic activity, protein expression, mRNA levels and 4-aminobiphenyl-induced DNA adducts and mutants were observed in all constructs containing the NATb 5′-UTR compared to those containing the NATa 5′-UTR. After treatment with 4-aminobiphenyl(ABP), more DNA adducts and mutagenesis was observed in cells transfected with NATb constructs than cells transfected with NATa constructs. Kinetic parameters for *NAT1*14B* compared to *NAT1*4* were determined. The NAT1*14B v_{max} for PABA, ABP, and N-OH-ABP was less than *NAT1*4* v_{max}. The NAT1*14B v_{max}/k_m, or instrinsic clearance, was lower for PABA when compared to NAT1*4 v_{max}/k_m. The *NAT1*14B* v_{max}/k_m was not different compared to NAT1*4 v_{max}/k_m for ABP, but the *NAT1*14B* v_{max}/k_m was higher for *N*-OH-ABP compared to v_{max}/k_m *NAT1*4*. This indicates that clearance for the NAT1 variant, NAT1*14B, is substrate dependent. Consequently, cancer risk related to *NAT1*14B* is likely also substrate dependent. NATb/*NAT1*10* and NATb/*NAT1*10B* transiently and stably transfected cells resulted in higher mRNA levels, protein expression, ABP induced cytotoxicity and *hprt*-mutants. This indicates that individuals possessing a *NAT1*10* or *NAT1*10B* genotype are associated with an increased cancer risk than individuals who possess a NAT1*4 genotype.

Table of Contents

Introduction

Human arylamine *N*-acetyltransferases 1 (NAT1) is a phase II cytosolic enzyme responsible for the biotransformation of many arylamine compounds including pharmaceuticals and environmental carcinogens. A common environmental carcinogen found in cigarette smoke is an aromatic amine, 4-aminobiphenyl (ABP). Arylamines such as ABP can either be inactivated via *N*-acetylation or activated via *O*-acetylation by NAT1. ABP can be *N*-acetylated and then excreted from the body. However, if ABP is first hydroxylated by cytochrome p450 1A1 (CYP1A1), the hydroxyl-ABP then can be further activated by NAT1-catalyzed *O*-acetylation resulting in *N*-acetoxy-ABP. This compound is very unstable and spontaneously degrades to form a nitrenium ion that can react with DNA to produce bulky adducts. If these adducts are not repaired, mutagenesis can occur and result in cancer initiation.

This study examines effects of ABP on NAT1 metabolism. ABP is a confirmed bladder carcinogen (IARC, 1987) and strict federal regulations have banned industrial uses of ABP. However, ABP can still be found as a contaminant in color additives, paints, food colors, leather, textile dyes, diesel-exhaust particles, cooking oil fumes and commercial hair dyes (Nauwelaers et al., 2011). Mainstream cigarette smoke has been reported to contain up to 23 ng per cigarette and sidestream smoke has been reported to contain up to 140 ng per cigarette (Hoffmann et al., 1997).

The only known endogenous NAT1 substrate is p-aminobenzoylglutamate (PABG), a catabolite of folate. *NAT1* has been associated with various birth defects that may be related to deficiencies in folate metabolism. *NAT1* polymorphisms and maternal smoking have been associated with increased incidence of oral clefts, spina bifidia and increased limb deficiency defects. *NAT1* polymorphisms have also been associated with increased risk for breast, pancreatic, prostate, urinary bladder and colorectal cancers non-Hodgkin lymphoma, mammary cell growth and breast cancer survival.

*NAT1*4* is referred to as the referent allele because it was the most common allele in the population in which it was first identified. To date, 26 human *NAT1* alleles have been identified (http://louisville.edu/medschool/pharmacology/consensus-human-arylamine-n-acetyltransferase-gene-nomenclature/). Although the effects of *NAT1* polymorphisms on catalytic activity have been studied, the results are ambiguous. Within single NAT1 genotypes, conflicting phenotypes have been reported, and the relationship between phenotype and genotype remains poorly

understood. Genotype as well as other factors are likely affecting phenotype, therefore it is important to understand transcriptional and translational control of *NAT1*.

*NAT1*14B*

The most common NAT1 variant allele associated with reduced acetylator phenotype is *NAT1*14B.* The allelic frequency for *NAT1*14*B in the Lebanese population was determined to be 23.8% (Dhaini and Levy, 2000). *NAT1*14B* is likely to be very prevalent in other countries in the middle east, however allelic frequencies for many of those populations are not available. *NAT1*14B* has been associated with an increased risk of smoking-induced lung cancer (Bouchardy et al., 1998).

*NAT1*14B* is characterized by a single nucleotide polymorphism (SNP) G560A (rs4986782) located in the coding region. G560A results in an amino acid substitution R187Q. Computational homology modeling based on the NAT1 crystal structure indicate that the side chain of R187 is partially exposed to the domain II beta barrel, the protein surface, and the active site pocket (Walraven et al., 2008). Interactions with these domains serve to stabilize the protein and help shape the active site pocket. The substitution of arginine for glutamine results in at least partial loss of these stabilizing hydrogen bonds resulting in destabilization of the NAT1 structure. Therefore, homology modeling predicts that NAT1 binding of acetyl coenzyme A (AcCoA), active site acetylation, substrate specificity and catalytic activity could be affected by the R187Q substitution (Walraven et al., 2008).

Previous studies have reported *NAT1*14B* to be associated with a reduced *N*-acetylation phenotype. For example, in peripheral blood mononuclear cells, NAT1 14B was reported to result in reduced *N*-acetyltransferase activities and protein levels (Hughes et al., 1998). Recombinant NAT1 14B expression in yeast demonstrated reduced *N*- and *O*-acetylation, protein levels and increased proteasomal degradation (Butcher et al., 2004; Fretland et al., 2001; Fretland et al., 2002). NAT1 14 expressed in mammalian cells also resulted in decreased NAT1 *N*- acetylation of PABA and *O*-acetylation *N*-OH-PhIP (Zhu and Hein, 2008). Zhu also reported that NAT1 14 resulted in reduced V_{max} of PABA and AcCoA and increased substrate K_m of PABA.

Modifications in NAT1 protein activity are biologically relevant because formation of DNA adducts, tumor growth and drug resistance could be altered by differences in enzymatic activity. This study reports findings in constructs that completely mimic NAT1 mRNA by including the 5'- and 3'-UTRs and coding region of the referent, *NAT1*4* and of the most common allele associated with reduced acetylation, *NAT1*14B*. This report describes NAT1 14B *N*- and *O*-acetylation of the urinary bladder carcinogen (Feng et al., 2002), 4-aminobiphenyl (ABP).

*NAT1*10* and *NAT1*10B*

The most common NAT1 polymorphisms are located in the region 3' to the open reading frame; however conflicting results about their effect on acetylation capacity have been reported. *NAT1*10* is the most common NAT1 variant allele in many populations and is characterized by two SNPs in the 3'-UTR including $T^{1088}A$ and $C^{1095}A$. Several studies suggest that *NAT1*10* has higher acetylation capacity than the referent allele, *NAT1*4*, (Bell et al., 1995; de Leon et al., 2000; Payton and Sim, 1998), while others have reported no difference (de Leon et al., 2000). There are no amino acid changes due to these polymorphisms, but the $T^{1088}A$ causes a change in the second consensus polyadenylation signal (AATAAA – AAAAAA). It has been speculated that this change in polyadenylation signal may give rise to a difference in mRNA stability and modulated acetylation activity of NAT1 10 (Bell et al., 1995). The 3'-UTR of a gene contains binding sites for important translational regulatory elements that include microRNAs, proteins or protein complexes, cytoplasmic polyadenylation elements (CPE) and polyadenylation signals (AAUAAA) (Mishra et al., 2008). It has been shown that SNPs in 3'-UTRs of dihydrofolate reductase (DHFR), thrombin and resistin genes cause functional affects and alter disease risk (Gehring et al., 2001; Mishra et al., 2008; Pizzuti et al., 2002).

In addition to the high allelic frequency in many populations, *NAT1*10* is also of great interest because it has been associated with increased risk of so many different forms of cancer. *NAT1*10* heterozygous genotype is associated with increased odds ratios for non-Hodgkin lymphoma (Morton et al., 2006), gastric adenocarcinoma (Boissy et al., 2000), prostate cancer (Hein et al., 2002) and breast cancer (Stephenson et al., 2010) when compared to the homozygous *NAT1*4* genotype. It has also been reported that cancer risk associated with *NAT1*10* is further modulated by exposure to environmental carcinogens found in cigarette smoke, meats cooked at high temperatures, and the use of hair dye. For example, frequent

consumption of red meat in combination with *NAT1*10* is associated with an increased odds ratio for colorectal cancer (Lilla et al., 2006) and the use of dark, permanent hair dye in combination with *NAT1*10* is associated with an increased risk for non-Hodgkin lymphoma (Morton et al., 2007). Heavy smokers possessing the *NAT1*10* allele have an increased risk for developing pancreatic cancer compared to non-smokers (Li et al., 2006) and for developing breast cancer (Zheng et al., 1999). The contribution of *NAT1*10* to increased cancer risk is not well understood. It is imperative that the phenotype of *NAT1*10* be clearly defined in order to resolve the association of *NAT1*10* genotype with increased cancer risk.

In addition to polymorphic variation, it may be necessary to consider transcriptional and translational regulation to further understand the variation associated with *NAT1*10* acetylation activity and effect on cancer risk. In contrast to previous studies which included only the NAT1 coding region, this study employs constructs that mimic the most common transcripts originating from the NATb and the NATa promoters. In this study, the constructs are referred to as NATb/NAT1 or NATa/NAT1. NATb or NATa refers to the 5' non-coding exons (NCEs) while NAT1 refers to the specific allele. The constructs contain the coding region, the 3'-UTR and all 5' NCEs found in the most common *NAT1* transcripts originating at the NATb and NATa promoter (Figure 1) (Barker et al., 2006; Husain et al., 2004; Husain et al., 2007). The NATb/NAT1 construct contains exons 4 and 8 (5' NCEs) and exon 9 (coding region) which has been termed transcript Type IIA by Butcher et al., 2005. The NATa/NAT1 construct contains exons 1, 2, 3, 8 (5' NCEs) and 9 (ORF) which has been termed transcript Type 1A by Butcher et al., 2005. In addition to the 5' NCEs and the ORF, the NATb/NAT1 and NATa/NAT1 constructs also contain 888 nucleotides of the 3'-UTR. The NATb/NAT1 and NATa/NAT1 constructs were employed to provide a more comprehensive model of in vivo metabolism and to study any allele specific interactions between the 5'-UTR and the *NAT1*10* polymorphisms. These constructs were utilized to determine *N*- and *O*- acetylation, mRNA levels, protein levels, and polyadenylation patterns between cells transfected with NATb/*NAT1*4*, NATb/*NAT1*10,* NATb*/NAT1*10B,* NATa/*NAT1*4*, NATa/*NAT1*10* or NATa*/NAT1*10B*.

This study has examined the role of NAT1 polymorphisms including SNPs in the coding region and in the 3'-UTR. Polymorphisms examined in this study include T1088A and C1095A *(NAT1*10*), T1571C, A1642C, ΔCT1647, C1716T (*NAT1*10B*) and G560A (*NAT1*14B*). In

addition to SNP effects, this study has also examined effects of the two major 5'-UTRs (NATb and NATa) on NAT1 enzymatic activity, mRNA level and stability, protein expression, ABP-induced DNA adduct formation, and ABP-induced mutants. To accomplish these goals we proposed the following study objectives:

Objective 1: To create pcDNA5/FRT vector constructs that possess the human *NAT* alleles including *NATa* and *NATb* 5'-UTR exons, the coding region, and 885 nucleotides of the 3'-UTR (with 6 potential polyadenylation signals). In addition to the reference *NAT1*4*, alleles possessing individual or combinations of genetic polymorphisms present in *NAT1*10, NAT1*11*, and *NAT1*14* will be constructed.

Objective II. Nucleotide excision repair deficient Chinese hamster ovary cells expressing human CYP1A1 will be transfected with pcDNA5/FRT vectors containing human *NAT1* constructs. The functional effects of genetic polymorphisms in *NAT1*10*, *NAT1*11 and NAT1*14* will be compared to the reference allele *NAT1*4* in transient transfection experiments. Functional assays will include determinations of N- and O-acetylation catalytic activities (HPLC assays), mRNA levels (Taqman assays) and protein (Western blot assays).

Objective III. Where functional effects are observed in the comparison of *NAT1*10*, *NAT1*11*, and *NAT1*14* with the reference allele, *NAT1*4*, stable CHO cell transfectants with these alleles will be constructed and exposed to various aromatic and heterocyclic amine carcinogens to test their effects on levels of covalent DNA adducts (liquid chromatography-mass spectrometry assays) and mutagenicity (*HPRT* mutants).

Body

NATb/*NAT1*4* vs NATa/*NAT1*4*

The *NAT1* gene spans 53 kb and contains nine exons (Figure 1a).

A schematic representation of the NATa/NAT1*4 and NATb/NAT1*4 constructs is included (Figure 1).

Figure 1. (a) Genomic organization of NAT1 gene; (b) Type IIA and Type IA NAT1 RNA (c) and representative NATb/*NAT1*4* and NATa/*NAT1*4* constructs.

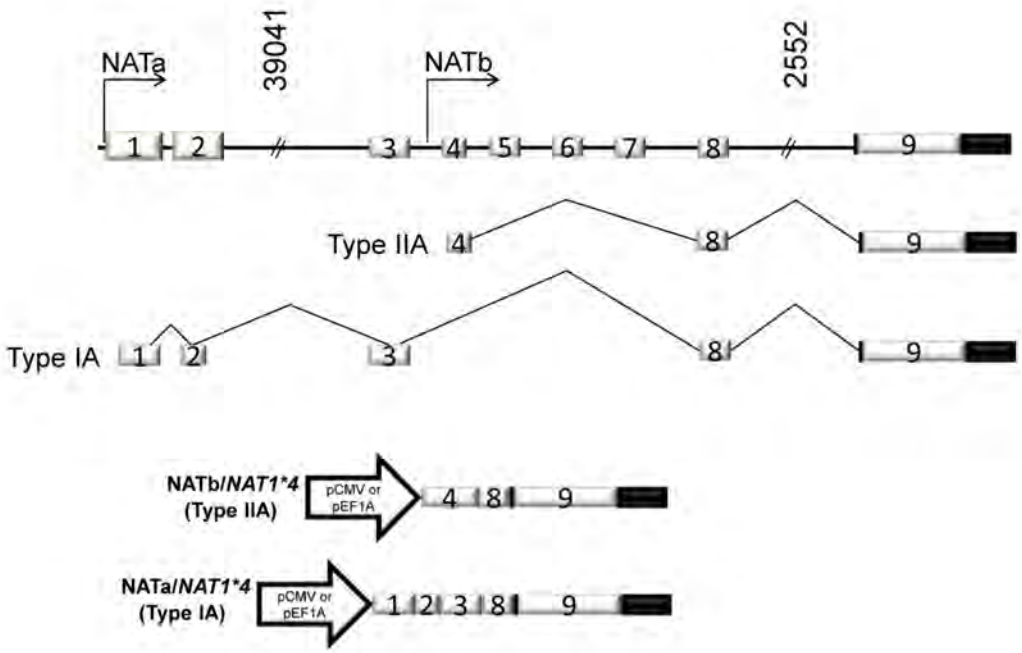

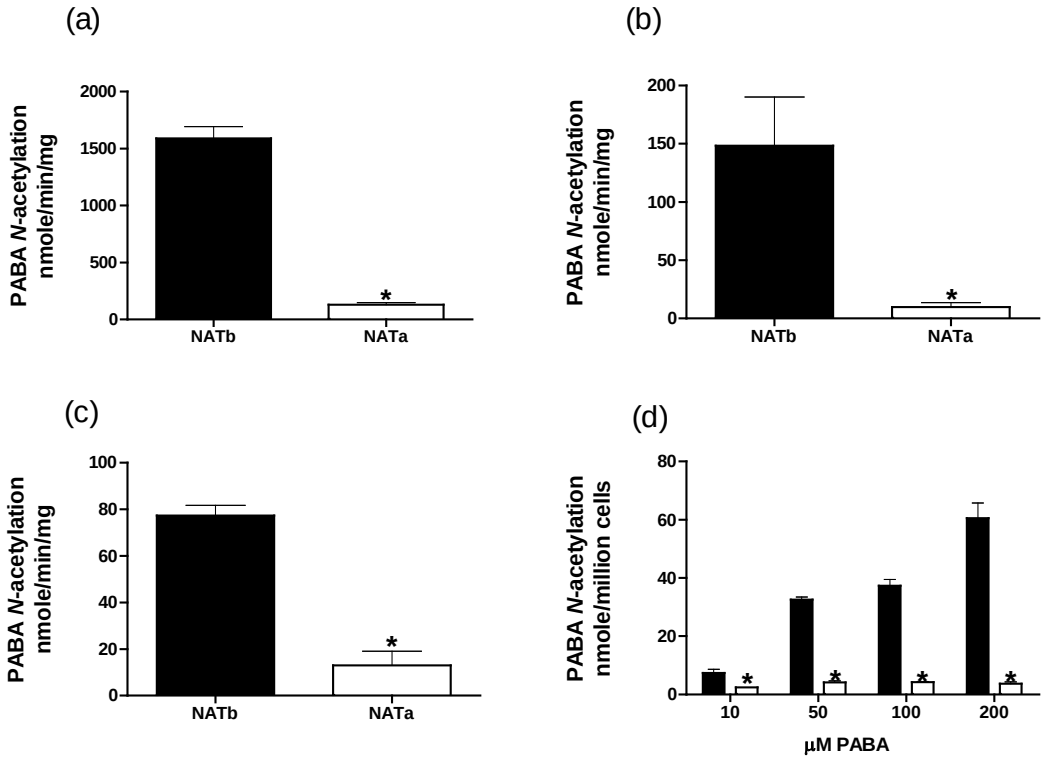

Figure 2. *N*-acetylation of PABA in UV5/1A1 cells expressing *CYP1A1* and NATb/*NAT1*4* (solid bars) or NATa/*NAT1*4* (open bars). (a) PABA *N*-acetylation activity following transient transfection with pcDNA5/FRT; (b) PABA NAT1 catalytic activity following stable transfection with pcDNA5/FRT of 3 different clones of each NATb/*NAT1*4* and NATa/*NAT1*4*; (c) PABA *N*-acetylation activity following transient transfection with pEF1/V5-His; (d) PABA *N*-acetylation *in situ* following stable transfection of pcDNA5/FRT. Each bar represents mean ± S.E.M. for three transient transfections (a, c), 3 separate collections of 3 clones (b) or 3 separate collections of 1 clone (d). Asterisks (*) represent a significant difference ($p<0.05$) (a, b, d) or ($p<0.0001$) (c) following a student's t-test.

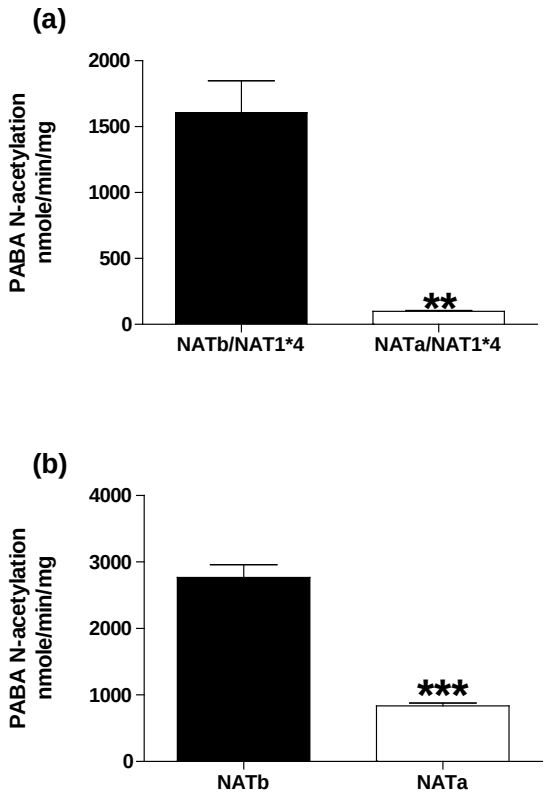

Figure 3. *N*-acetylation of PABA in COS-1 cells transiently transfected with (a) pcDNA5/FRT or pEF1/V5-His (b) containing NATb/*NAT1*4* or NATa/*NAT1*4*. Each bar represents mean ± S.E.M. for three transient transfections. Asterisks represent a significant difference either ($p<.005$) (a) or ($p<.0001$) (b) following a student's t-test.

PABA *N*-acetylation activity was 9- to 12-fold ($p<0.05$) higher in CHO cells transfected with NATb/*NAT1*4* than NATa*/NAT1*4* following both transient and stable transfections (Figure 2 a,b) utilizing the CMV promoter. Figure 2b shows average PABA *N*-acetylation for 3 stable clones of each NATb/*NAT1*4* and NATa/*NAT1*4.* One clone representative was selected from each group to conduct all further assays. To ensure that the difference was not promoter specific, *N*-acetylation activity was also measured following transfection with constructs utilizing the EF1α promoter. PABA *N*-acetylation activity was 6-fold ($p<0.0001$) higher in CHO cells transiently transfected with NATb/*NAT1*4* than NATa/*NAT1*4* (Figure 2c) utilizing the EF1α promoter. To more accurately model *in vivo N*-acetylation and to confirm the *in vitro* results, an *in situ* assay was performed using PABA as the substrate in a dose response experiment (Figure 2d). The *in situ* assay showed that significantly ($p<0.05$) more PABA *N*-acetylation activity was observed in cells stably transfected with NATb/*NAT1*4* than NATa*/NAT1*4* at all

concentrations tested (Figure 2d) utilizing the CMV promoter. As shown in figure 3, PABA *N*-acetylation activity also was significantly higher in COS-1 cells transiently transfected with NATb/*NAT1*4* than with NATa/*NAT1*4* utilizing either the CMV ($p<0.005$) (Figure 3a) or EF1α ($p<0.0001$) (Figure 3b) promoters.

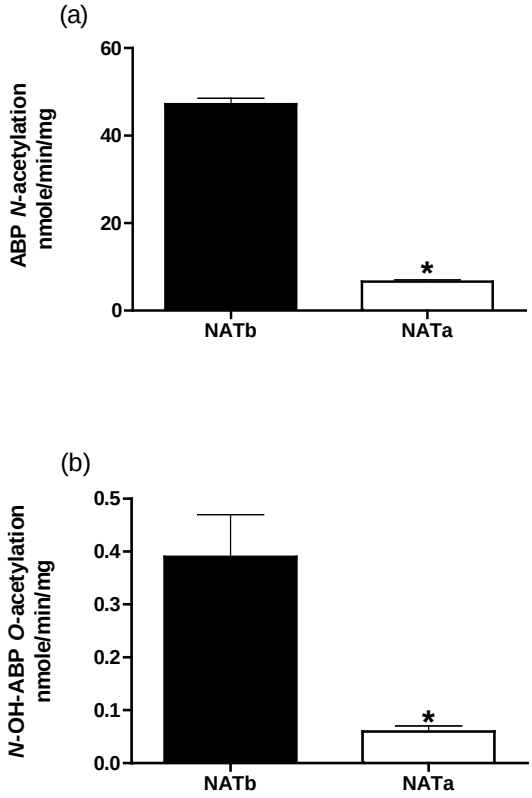

Figure 4. (a) *N*-acetylation of ABP and (b) *O*-acetylation of *N*-hydroxy-ABP in UV5/1A1 cells stably expressing *CYP1A1* and either NATb/*NAT1*4* (solid bars) or NATa/*NAT1*4* (open bars) in pcDNA5/FRT. Each bar represents mean ± S.E.M. for three separate collections. Asterisks (*) represent a significant difference ($p<0.0001$) (a) or ($p<0.05$) (b) following a student's t-test.

Cells stably transfected with NATb/*NAT1*4* were found to have 7-fold ($p<0.0001$) higher ABP *N*-acetylation activity than cells stably transfected with NATa/*NAT1*4* (Figure 4a) utilizing the CMV promoter. *O*-acetyltransferase activity using *N*-OH-ABP as the substrate also was found to be 7-fold ($p<0.05$) higher in cells stably transfected with NATb/*NAT1*4* than NATa*/NAT1*4* (Figure 4b) utilizing CMV promoter.

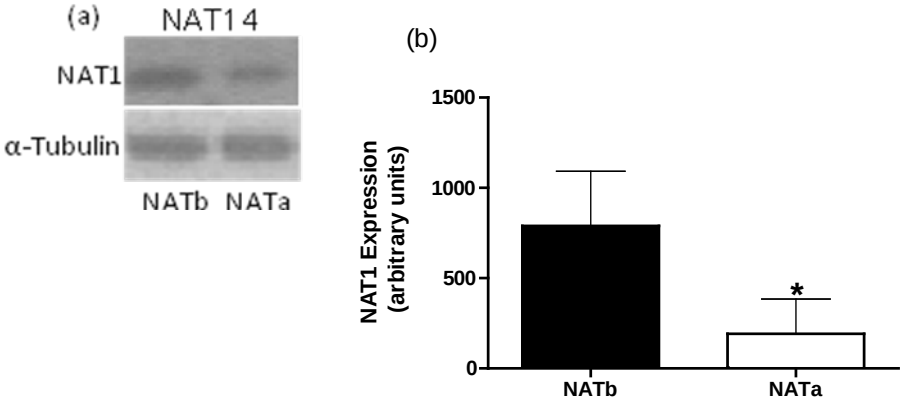

Figure 5. NAT1 protein expression in UV5/1A1 cells stably expressing *CYP1A1* and NATb/*NAT1*4* (solid bars) or NATa/*NAT1*4* (open bars) in pcDNA5/FRT. (a) Representative western blot of 20 µg of total protein loaded; (b) Percent intensity units (NATb defined as 100%) of densitometric analysis perfomed on three independent Western blots. Asterisks (*) represent a significant difference ($p<0.05$) following a student's t-test.

NAT1 expression was determined by western blot in cells stably transfected with NATb/*NAT1*4* and NATa/*NAT1*4* utilizing the CMV promoter. Four-fold ($p<0.05$) more NAT1 was found in cells stably transfected with NATb/*NAT1*4* than cells transfected with NATa/*NAT1*4* following densitometric analysis (Figure 5).

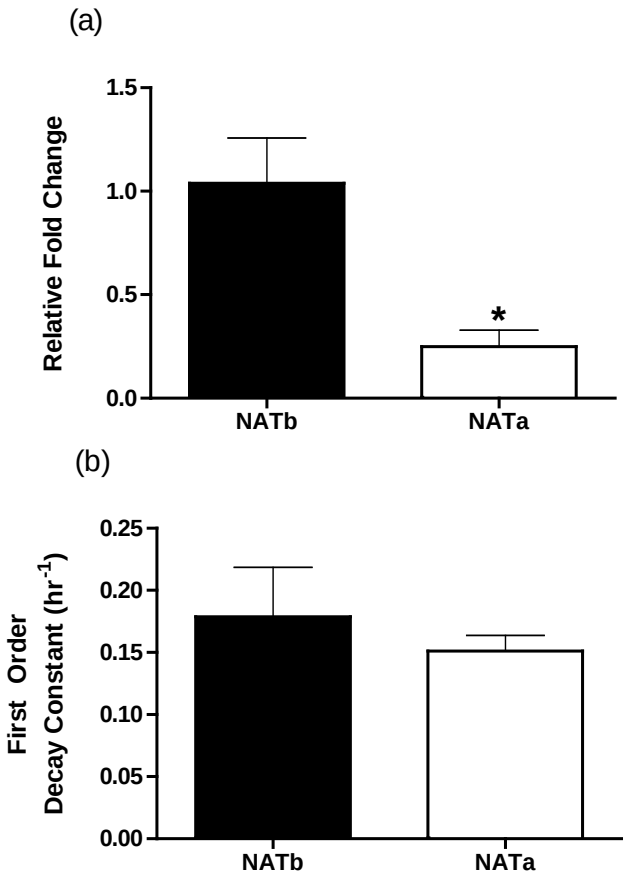

Figure 6. (a) NAT1 mRNA expression levels; (b) mRNA stability in UV5/1A1 cells stably expressing *CYP1A1* and NATb/*NAT1*4* (solid bars) or NATa/*NAT1*4* (open bars) in pcDNA5/FRT. Each bar represents mean ± S.E.M. for (a) three or (b) nine determinations. Asterisks (*) represent a significant difference ($p<0.05$) following a student's t-test.

As shown in Figure 6a, 4-fold more NAT1 mRNA was detected in cells stably transfected with NATb/*NAT1*4* than in cells transfected with NATa*/NAT1*4* ($p<0.05$) utilizing the CMV promoter. To determine the cause of the difference in NAT1 steady-state mRNA between cells stably transfected with NATb/*NAT1*4* and in cells transfected with NATa*/NAT1*4*, an mRNA stability assay was performed in the presence of actinomycin-D. No significant ($p>0.05$) difference in the NAT1 mRNA first-order decay constant was observed between NAT1 mRNA derived from cells stably transfected with NATb/*NAT1*4* versus NATa*/NAT1*4* (Figure 6b).

Figure 7. ABP-induced cytotoxicity, mutagenesis, and DNA adduct formation in CHO cells stably expressing *CYP1A1* only (triangles) and NATb/*NAT1*4* (circles) or NATa/*NAT1*4* (squares) in pcDNA5/FRT. Each data point represents mean ± S.E.M. for three determinations. (a) ABP-induced cytotoxicity; (b) ABP-induced dG-C8-ABP adducts/10^8 nucleosides; (c) ABP-induced *hprt* mutant levels.

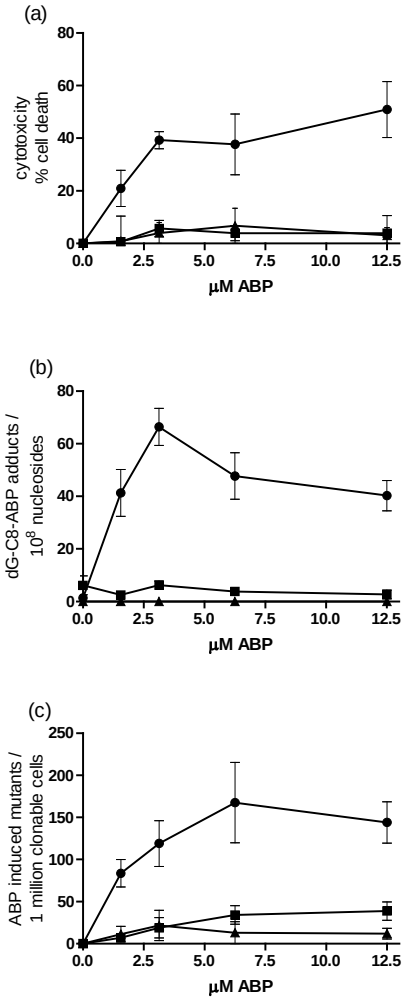

CYP1A1 mediated hydroxylation and NAT1 *O*-acetylation result in DNA adducts and mutations, if not repaired. Significantly ($p<0.05$) greater cytoxicity (Figure 7a), dG-C8-ABP adducts (Figure 7b) and *hprt* mutants (Figure 7c) were detected in cells stably transfected with

NATb/*NAT1*4* than NATa*/NAT1*4* utilizing the CMV promoter at each ABP concentration tested up to 12.5 μM.

All methods for figures 1 – 7 can be found in that attached manuscript, appendix 1.

Discussion

Significantly more NAT1 activity, protein, mRNA, ABP-induced cytoxicity, DNA adducts and mutagenesis were detected in cells stably transfected with NATb/*NAT1*4* than in cells transfected with NATa*/NAT1*4* ($p<0.05$). DNA adduct and mutant levels following exposure to ABP are biological endpoints that are very relevant to cancer risk. The findings that ABP-mediated DNA adduct and mutant levels were significantly higher in cells transfected with elevated NAT1 catalytic activity emphasizes the relative importance of NAT1-catalyzed *O*-acetylation of *N*-hydroxy-ABP in cancer risk. Associations between higher N-acetyltransferase 2 catalytic activity with higher ABP-mediated cytoxicity, DNA adduct formation, and mutagenesis also were recently reported [51]. The finding that these cancer risk indicators were higher in cells transfected with NATb/*NAT1*4* than cells transfected with NATa/*NAT1*4* suggest that differential regulation in the *NAT1* 5'-UTR also may modify ABP-mediated cancer risk. Because NATb transcripts are expressed ubiquitously, the minor transcript, NATa, may be expressed following environmental exposures or under certain disease states resulting in increased mutagenesis, enhanced tumor growth, and decreased chemotherapeutic sensitivity. For example, expression of NATa transcripts have recently been reported in several ER-positive breast cancer cell lines (Wakefield et al., 2008).

The findings of this study are significant due to their relevance to ABP-mediated carcinogenesis. However, translation of our results obtained in cell culture to human subjects will require additional studies to investigate tissue specificity. Although our study focused only on the referent allele, *NAT1*4,* future studies should investigate 5'-UTR control with other *NAT1* alleles, particularly those associated with increased cancer risk. Future investigations to determine mechanism(s) and location(s) of the differential regulation in the NAT1 5'-UTR also are needed.

*NAT1*14B vs NAT1*4*

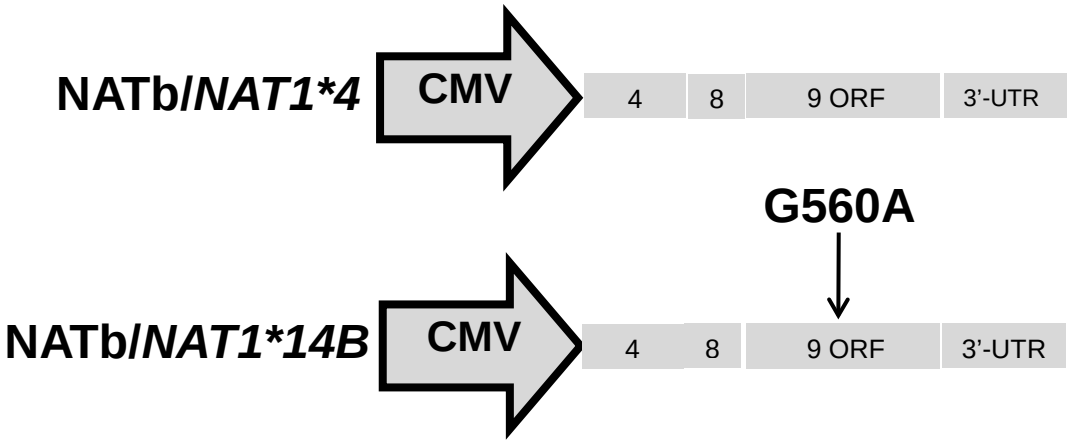

Figure 8. NATb/*NAT1*4* and NATb/*NAT1*14B* constructs. Constructs including 5'-UTR, open reading frame (exon 9) and 3'-UTR.

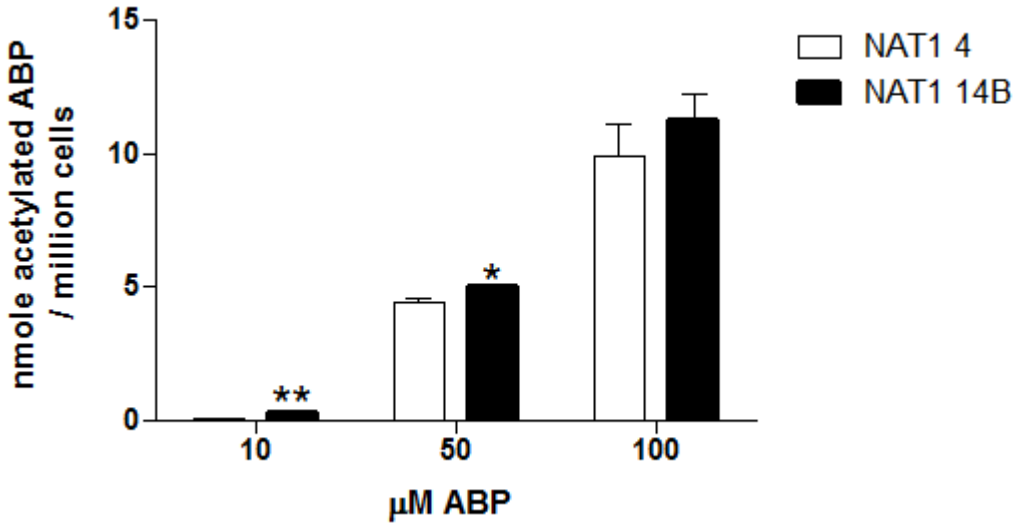

Figure 9. In situ ABP *N*-acetylation assay of yeast cultures recombinantly expressing *NAT1*4* and *NAT1*14B* per million cells. Error bars represent mean of 3 separate collections ± SEM. Difference determined following a Student's t-test and significance denoted by **p<0.001 and *p<.05.

Initial experiments performed in yeast (*in situ*) Resulted in higher NAT1 14B *N*-acetylation at 10 µM (p<0.001) and 50 µM ABP (p<0.05) compared to NAT1 4. There was no difference in *N*-acetylation between NAT1 14B and NAT1 4 following exposure to 100 µM ABP (Figure 9). The results of subsequent experiments performed in CHO cells are described below.

Allele	Substrate	$K_{m(app)}$	$V_{max(app)}$	V_{max}/K_m	$K_{cat(app)}$	K_{cat}/K_m
		μM	nmole min^{-1} mg^{-1}	mL min^{-1} mg^{-1}	min^{-1}	min^{-1} μM^{-1}
*NAT1*4*	PABA	42.9±3.3	116±3	2.72±0.21	2399±57	56.5±4.3
*NAT1*14B*		430±1[a]	18.5±1.5[b]	0.043±0.002[b]	1552±97[b]	3.61±0.20[b]
*NAT1*4*	ABP	273±46	57.7±5.8	0.218±0.018	1200±122	4.52±0.38
*NAT1*14B*		65.6±3.9[b]	18.0±4.3[b]	0.280±.031	1760±128	22.9±0.23[c]
*NAT1*4*	*N*-OH-ABP	141±1.1	2.97±0.19	0.0211±0.0014	35.1±68	0.250±0.02
*NAT1*14B*		46.8±1.3[b]	1.76±0.03[b]	0.038±0.001[c]	147±7[a]	3.15±0.23[c]
*NAT1*4*	AcCoA	6.23±0.75	1.25±0.04	0.204±0.019	25.9±0.7	4.24±0.38
*NAT1*14B*		16.8±2.2[c]	1.50±0.29	0.087±0.005[b]	126±24[c]	7.31±0.45[a]

Table 1. NAT1 4 and NAT1 14B kinetic constants determined *in vitro* (per mg total protein). PABA, ABP, and *N*-OH-ABP constants were determined at a fixed concentration of 100 μM AcCoA. AcCoA kinetic constants were determined at a fixed concentration of 100 μM *N*-OH-ABP. Table values represent mean ± SEM for 3-6 individual determinations. Differences were tested for significance by Student's t-test. [a]significantly higher than NAT1 4 ($p<0.0001$); [b]significantly lower than NAT1 4 ($p<0.0001$); [c]significantly higher than NAT1 4 ($p<0.05$).

Kinetic parameters of the referent, NAT1 4, and the variant, NAT1 14B *in vitro* (per mg total protein in-solution biochemistry) are shown in Table 1. The apparent k_m of NAT1 14B was higher for PABA ($p<0.0001$) compared to NAT1 4 whereas the apparent k_m of NAT1 14B was lower for ABP ($p<0.0001$) and *N*-OH-ABP ($p<0.0001$) when compared to NAT1 4. The apparent v_{max} of NAT1 14B was lower for PABA ($p<0.0001$), ABP ($p<.0001$), and *N*-OH-ABP ($p<0.0001$) when compared to NAT1 4. The apparent v_{max}/k_m of NAT1 14B was lower for PABA ($p<0.0001$), higher for *N*-OH-ABP ($p<0.0001$), and not significantly different for ABP ($p>0.05$) when compared to NAT1 4. The kinetic parameters, apparent k_m and k_{cat} also were determined *in vitro* (per mg NAT1 protein in solution biochemistry) for the referent, NAT1 4 and the variant, NAT1 14B (Table 1). The apparent k_{cat} of NAT1 14B was lower for PABA ($p<0.0001$) but higher for *N*-OH-ABP ($p<0.0001$) when compared to NAT1 4. There was no significant difference in apparent k_{cat} for ABP between NAT1 14B and NAT1 4 ($p>0.05$). The apparent k_{cat}/k_m of NAT1

14B was lower for PABA ($p<0.0001$) but higher for ABP ($p<0.05$) and N-OH-ABP ($p<0.0001$) when compared to NAT1 4.

Allele	Substrate	$K_{m(app)}$	$V_{max(app)}$	V_{max}/K_m
		μM	nmole min^{-1} million $cells^{-1}$	nmole min^{-1} million $cells^{-1}$ μM^{-1}
*NAT1*4*	PABA	95.5±1.1	0.16±0.01	1.71±0.08
*NAT1*14B*		72.1±11.1	0.101±0.018[a]	1.1±0.09[a]
*NAT1*4*	ABP	10.5±0.6	0.024±.0007	2.4±0.1
*NAT1*14B*		2.3±0.2[b]	0.0063±0.0005[b]	2.9±0.1[c]

Table 2. NAT1 4 and NAT1 14B kinetic constants determined *in situ* (per million cells). Table values represent mean ± SEM for 3-6 individual determinations. Differences were tested for significance by Student's t-test. [a]significantly lower than NAT1 4 ($p<0.05$); [b]significantly lower than NAT1 4 ($p<0.0001$); [c]significantly higher than NAT1 4 ($p<0.05$).

Apparent k_m and v_{max} for PABA and ABP also were determined *in situ* (per million cells in a whole cell based assay) for the referent, NAT1 4, and the variant, NAT1 14B (Table 2). The apparent k_m of NAT1 14B was not significantly different for PABA ($p>0.05$) but was significantly lower for ABP ($p<0.0001$) when compared to NAT1 4. The apparent v_{max} of NAT1 14B was lower for PABA ($p<0.05$) and ABP ($p<0.0001$) when compared to NAT1 4. The apparent v_{max}/k_m of NAT1 14B for PABA was significantly less ($p<0.05$) but was significantly higher for ABP ($p<0.05$) when compared to NAT1 4.

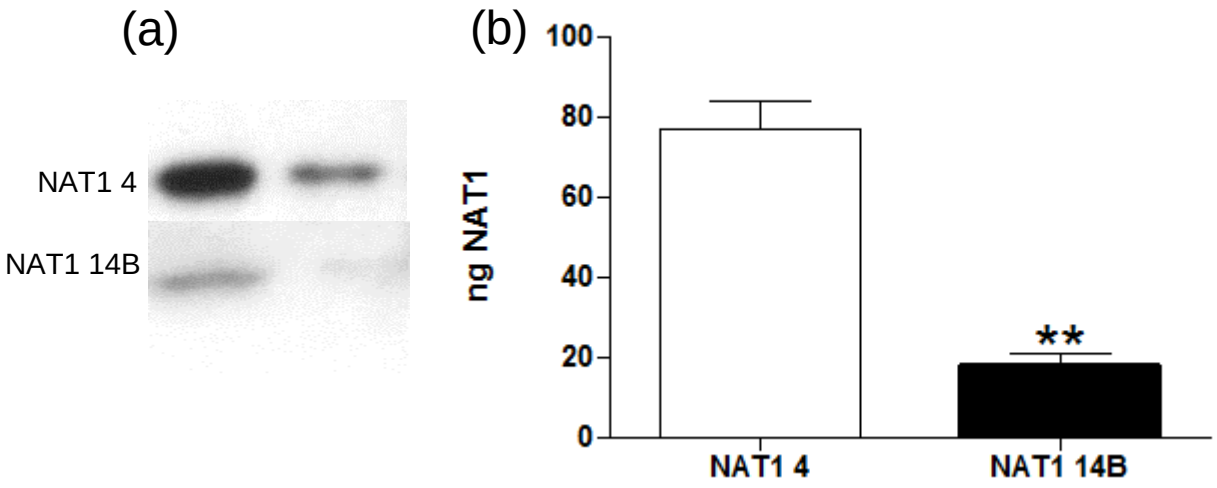

Figure 10. Western blot to determine relative protein expression of NAT1 4 and NAT1 14B. (a) Representative western blot; (b) densitometric analysis of western blot of 28 µg total protein loaded. Loading either 28 or 14 µg of total protein lysate, NAT1 14B resulted in approximately 4-fold less NAT1 protein than NAT1 4 ($p<0.001$). Bars represent mean ± SEM for 3 western blots and significance was determined by Student's t-test.

Expression of NAT1 14B and NAT1 4 was determined by western blot (Figure 10). The standard curve obtained by loading 140 ng – 1.09 ng of purified NAT1 protein (Abnova) was used to compare intensities of lysate from stably transfected cells. 55, 28, or 14 µg of total protein lysate, corresponded to 154, 77, and 38 ng of NAT1 4 protein and 38, 19, and 10 ng of NAT1 14B protein. Overall, NAT1 14B resulted in a 4-fold reduction in NAT1 protein compared to NAT1 4 ($p<0.001$).

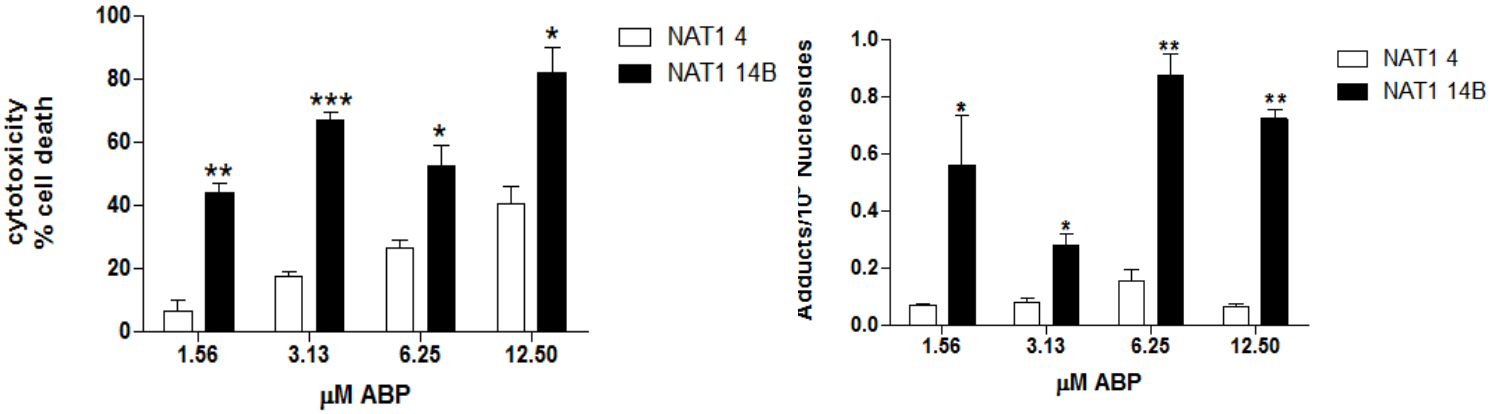

Figure 11. ABP-induced cytotoxicity (a) and dG-C8-ABP adducts (b) in cells stably transfected with *NAT1*4* and *NAT1*14B*. Significantly more cytotoxicity was observed for NAT1 14B than NAT1 4 following all ABP exposures between 1.56 – 12.5 µM. Significantly more adducts were observed following all exposures examined in cells expressing NAT1 14B than in cells expressing NAT1 4. Values were adjusted for baseline values of UV5/*1A1* cells. Bars represent mean ± SEM for 3 determinations and significance was determined by Student's t-test. (*) $p<0.05$, (**) $p<0.001$, and (***) $p<0.0001$.

ABP-induced cytotoxicity was also determined in cells stably transfected with *NAT1*4* or *NAT1*14B* (Figure 11a). Significantly more ABP-induced cytotoxicity was observed in *NAT1*14B* transfected cells following exposures to each ABP concentration. ABP-induced dG-C8-ABP adducts in cells stably transfected with *NAT1*4* and *NAT1*14B* were determined (Figure 11b). Significantly more dG-C8-ABP adducts were observed following exposures between 1.56 – 12.5 µM ABP in cells transfected with *NAT1*14B* than in cells transfected with *NAT1*4.*

All methods for figures 8 – 11 and tables 1 -2 can be found the attached manuscript located in the appendix.

Discussion

Studies performed *in situ* using NAT1 14B and NAT1 4 produced in yeast did not result in lowered NAT1 14B *N*-acetylation of ABP (Figure 2) as previous studies had shown *in vitro* (Fretland et al., 2002). This result was surprising as previous studies reported NAT1 14B activity and protein expression to be lower than NAT1 4. To further explore the NAT1 14B acetylation status, studies were conducted in stably transfected CHO cells.

When comparing apparent v_{max} (*in vitro*), the NAT1 14B apparent v_{max} was lower than the NAT1 4 for all substrates studied. The apparent v_{max} describes the maximum enzyme velocity extrapolated to maximum substrate concentrations. The lower apparent v_{max} for PABA, ABP, and *N*-OH-ABP indicate that at high substrate concentrations, NAT1 14B has a decreased ability to metabolize the substrate when compared to NAT1 4. The apparent v_{max}/k_m, or intrinsic clearance, describes an enzyme's ability to metabolize a substrate at substrate concentrations well below the k_m and has also been shown to correlate well to human liver clearance (Chen et al., 2011; Northrop, 1999). For PABA, the NAT1 14B apparent v_{max}/k_m was lower than NAT1 4. In contrast, no significant difference was observed between NAT1 14B and NAT1 4 apparent v_{max}/k_m towards the *N*-acetylation of ABP. Surprisingly, the NAT1 14B apparent v_{max}/k_m for the *O*-acetylation of *N*-OH-ABP was higher in *NAT1*14B* CHO cell lysate compared to *NAT1*4* CHO cell lysate. This indicates that the status of NAT1 14B intrinsic clearance compared to NAT1 4 intrinsic clearance is substrate dependent.

Transfection of *NAT1*14B* resulted in approximately a 4-fold less NAT1 protein expression compared to *NAT1*4*. When the amount of NAT1 protein was used to calculate apparent k_{cat} (determined *in vitro*), the results suggested that the lower NAT1 14B apparent v_{max} for these substrates is due to a reduction in NAT1 protein, not a reduction in the acetylation rate of the NAT1 14B enzyme. For example, although the NAT1 14B apparent v_{max} for *N*-OH-ABP was lower than the NAT1 4, the NAT1 14B apparent k_{cat} for *N*-OH-ABP was higher than NAT1

4. This difference in v_{max} compared to k_{cat} indicates that the lowered NAT1 14B apparent v_{max} is caused by a reduction in protein expression.

When comparing v_{max} (*in situ*), the NAT1 14B apparent v_{max} was lower than the NAT1 4 4 for PABA and ABP. When evaluated *in situ,* PABA NAT1 14B apparent v_{max}/k_m or intrinsic clearance was lower when compared to NAT1 4. In contrast, for ABP, the *in situ* NAT1 14B apparent v_{max}/k_m was higher when compared to NAT1 4. Because kinetic parameters of *N*-OH-ABP could not be determined *in situ*, an *in vitro* determination was performed. Like ABP, the NAT1 14B apparent v_{max}/k_m for *N*-OH-ABP was higher compared to NAT1 4. These findings indicate that differences in apparent v_{max}/k_m between NAT1 14B and NAT1 4 are substrate dependent. Risk for individuals possessing *NAT1*14B* is also likely exposure dependent. Increased apparent v_{max}/k_m indicates that NAT1 14B has an increased ability to metabolize ABP and *N*-OH-ABP at low substrate concentrations compared to NAT1 4 (Northrop, 1999). Since low substrate concentrations are relevant *in vivo*, the higher NAT1 14B apparent v_{max}/k_m suggests that differences between NAT1 14B and NAT1 4 catalyzed ABP acetylation should be observed *in vivo*. Therefore, risk for individuals possessing *NAT1*14B* is dependent on exposure type and can also be altered depending on exposure level.

In addition to higher apparent v_{max}/k_m for NAT1 14B towards ABP and *N*-OH-ABP when compared to NAT1 4, ABP-induced DNA-adducts and cytoxicity were higher for NAT1 14B compared to NAT1 4. Measurement of DNA adduct levels following exposure to ABP is a biological endpoint very relevant to cancer risk. Because NAT1 14B resulted in increased ABP-induced DNA adducts, our results suggest that individuals possessing the *NAT1*14B* allele likely have increased risk compared to those who are homozygous for *NAT1*4* following low (environmental) dose exposure to ABP. NAT1 14B is not simply associated with “slow acetylation” but rather is substrate dependent, since NAT1 14B exhibits lower *N*-acetylation catalytic efficiency of PABA but higher *N*- and *O*-acetylation catalytic efficiency as well as DNA adducts following exposure to the human carcinogen ABP.

*NAT1*10 and NAT1*10B* compared to *NAT1*4*

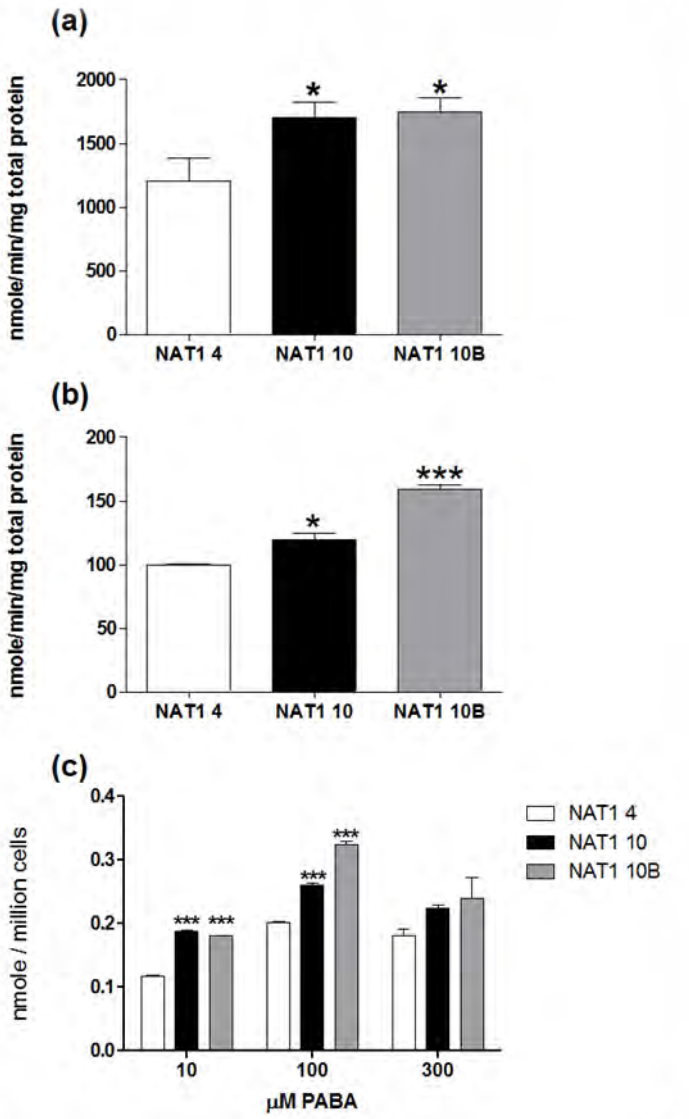

Figure 12. PABA *N*-acetylation by NAT1 4 (open bars), NAT1 10 (closed bars) and NAT1 10B (gray bars). (a) PABA *N*-acetylation (*in vitro*) following transient transfection with pcDNA5/FRT; (b) PABA *N*-acetylation (*in vitro*) following stable transfection with pcDNA5/FRT; (c) PABA *N*-acetylation (*in situ)* following stable transfection with pcDNA5/FRT. Each bar represents mean ± S.E.M. for three transient transfections (a) or three separate collections performed in triplicate (b and c) Significantly higher than NAT1 4 denoted by *p<0.05 and ***p<0.0001 following analysis with one-way ANOVA.

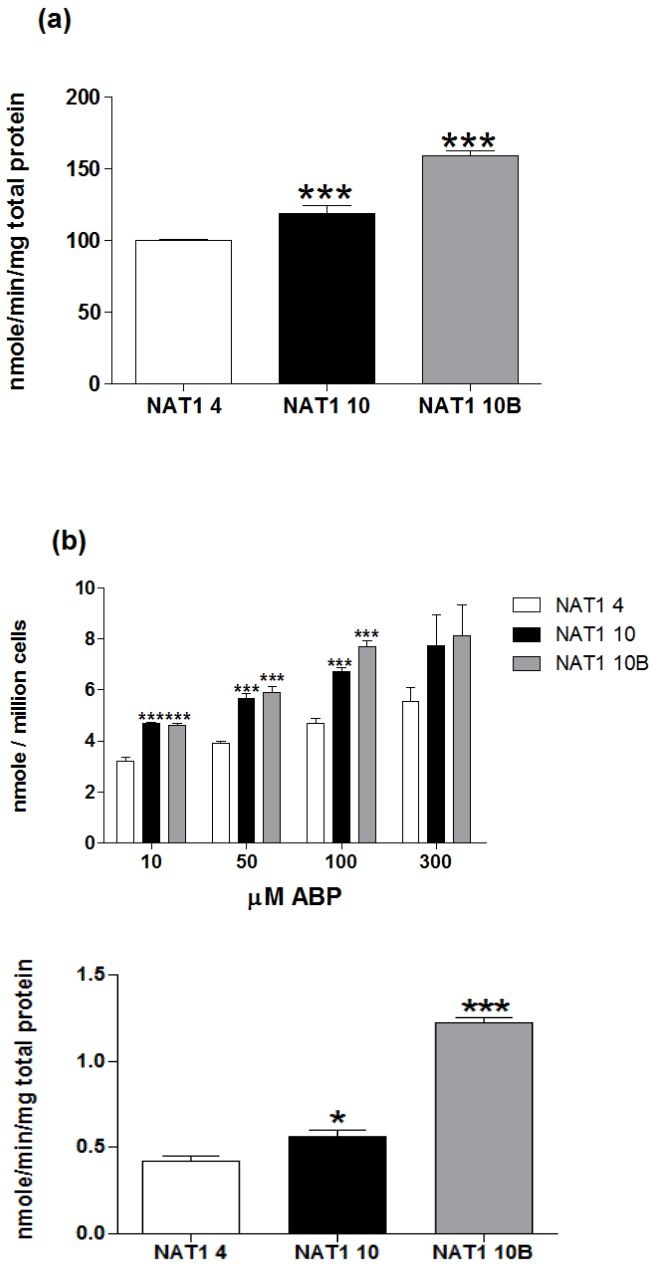

Figure 13. ABP *N*-acetylation and *N*-OH-ABP *O*-acetylaton by NAT1 4 (open bars), NAT1 10 (closed bars) and NAT1 10B (gray bars) in NATb constructs. *N*- and *O*-acetylation of ABP and *N*-OH-ABP following stable transfection in UV5/1A1 cells. (a) ABP *N*-acetylation (*in vitro*); (b) ABP *N*-acetylation (*in situ*); (c) *O*-acetylation of *N*-OH-ABP (*in vitro*). Each bar represents mean ± S.E.M. for three separate collections performed in triplicate. Significantly higher than NAT1 4 denoted by *p<0.05 and ***p<0.0001 following analysis with one-way ANOVA.

NAT1 activity was examined using PABA, ABP, or *N*-OH-ABP as substrates. Significantly more *N*-acetylation of PABA (Figure 12) and ABP (Figure 13) was detected in NATb/*NAT1*10* and NATb/*NAT1*10B* than in NATb/*NAT1*4* ($p<0.05$) in both transiently and stably transfected UV5/1A1 cells. Significantly more *O*-acetylation of *N*-OH-ABP was also detected in *NAT1*10* and *NAT1*10B* than in *NAT1*4* ($p<0.05$) in stably transfected UV5/1A1 cells (Figure 13).

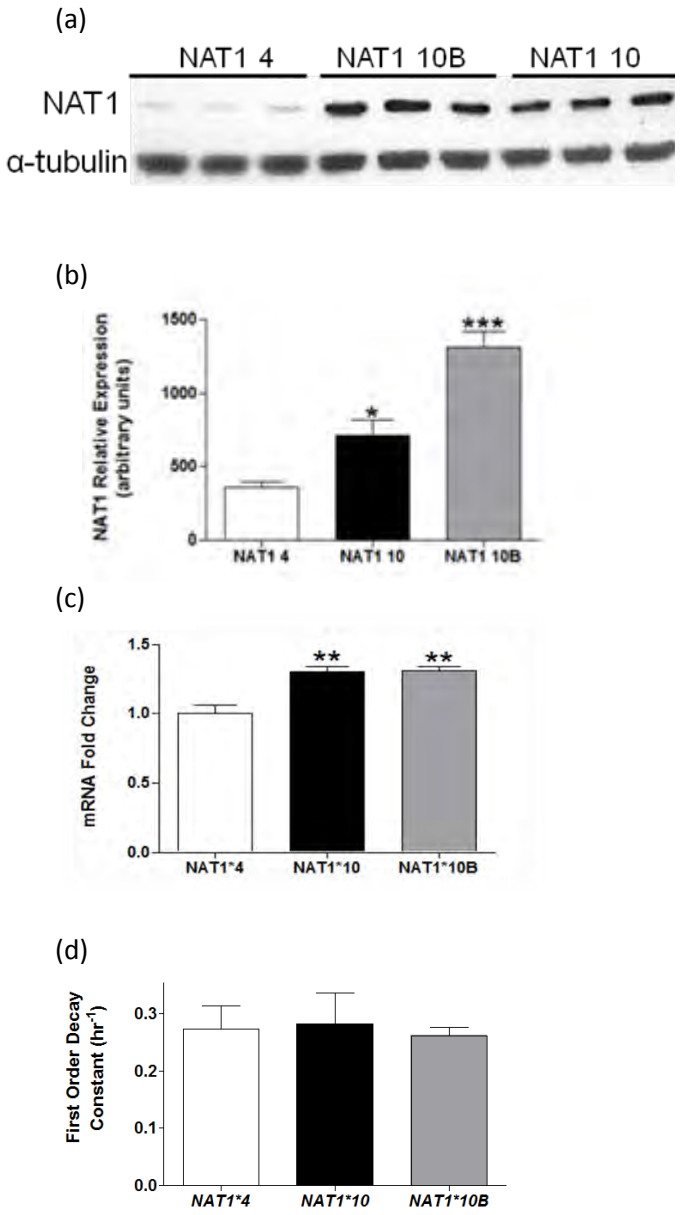

Figure 14. Representative western blot of NAT1 4, NAT1 10, and NAT1 10B stable expression (a) and densitometric analysis (b). NAT1 mRNA expression levels in stably transfected NATb constructs (c). Each bar represents mean ± SEM of 2 western blots or 3 collections of mRNA each performed in triplicate. Analysis done with Quantity One software (BioRad). Significantly higher than NAT1 4 denoted by *$p<0.05$, **$p<0.001$, and ***$p<0.0001$ following analysis with one-way ANOVA.

Western blots were performed to examine NAT1 expression in stably transfected UV5/1A1 cells (Figure 14). Significantly more NAT1 ($p<0.05$) was detected in NATb/*NAT1*10* and *NAT1*10B* than in *NAT1*4* transfected cells (Figure 14b). Significantly ($p<0.001$) more NAT1 mRNA was also observed in *NAT1*10* and *NAT1*10B* than *NAT1*4* transfected cells (Figure 14c). There was no difference between *NAT1*4, NAT1*10* or *NAT1*10B* mRNA stability (Figure 14d).

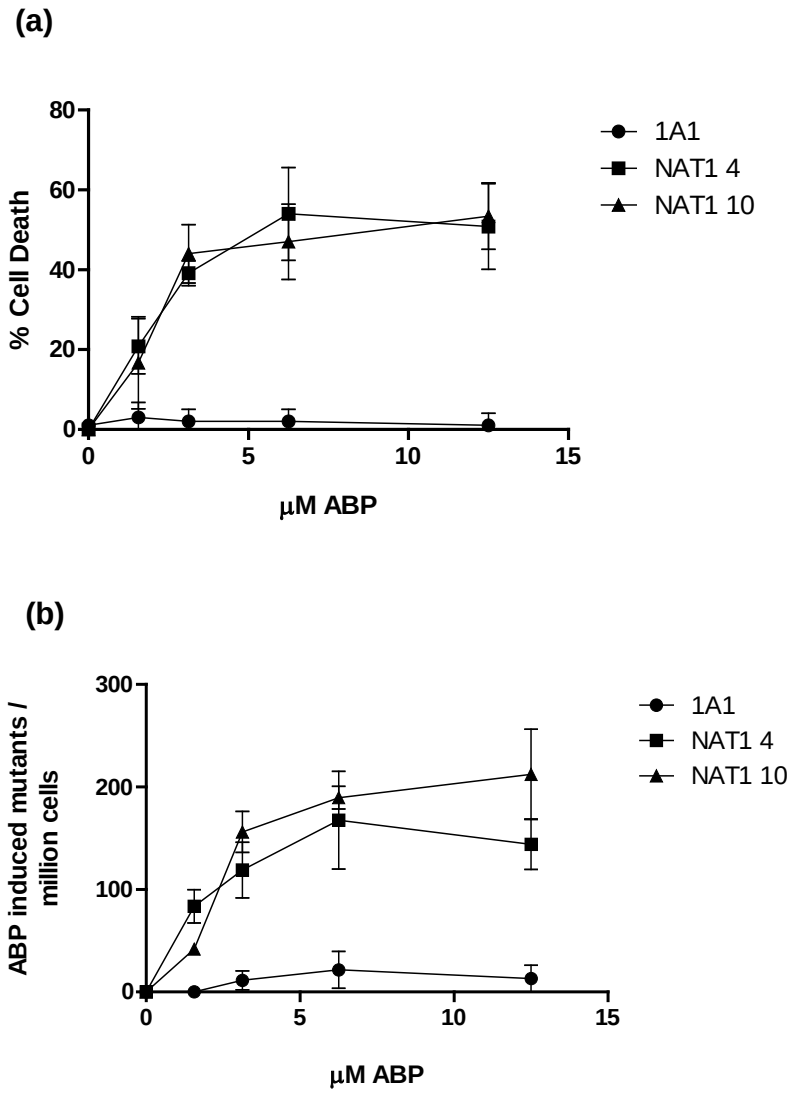

Figure 15. (a) ABP-induced cytotoxicity and (b) ABP-induced *hprt* mutants per million cells in UV5/1A1 cells that were stably transfected. CYP1A1 *only* (●), CYP1A1/NAT1 4 (■), and CYP1A1/NAT1 10 (▲). Each data point represents mean ± S.E.M. for three determinations.

Cytotoxicity and hprt mutants were examined in cells stably transfected with *NAT1*4* and *NAT1*10* following exposure to ABP. Increased ABP-induced cytotoxicity (Figure 15a) and *hprt* mutants (Figure 15b) were observed in all NAT1 transfected cells compared to non-transfected cells. Cells transfected with *NAT1*10* resulted in higher ABP-induced *hprt* mutants than cells transfected with *NAT1*4* for ABP concentrations of 3.2, 6.3 and 12.5 µM.

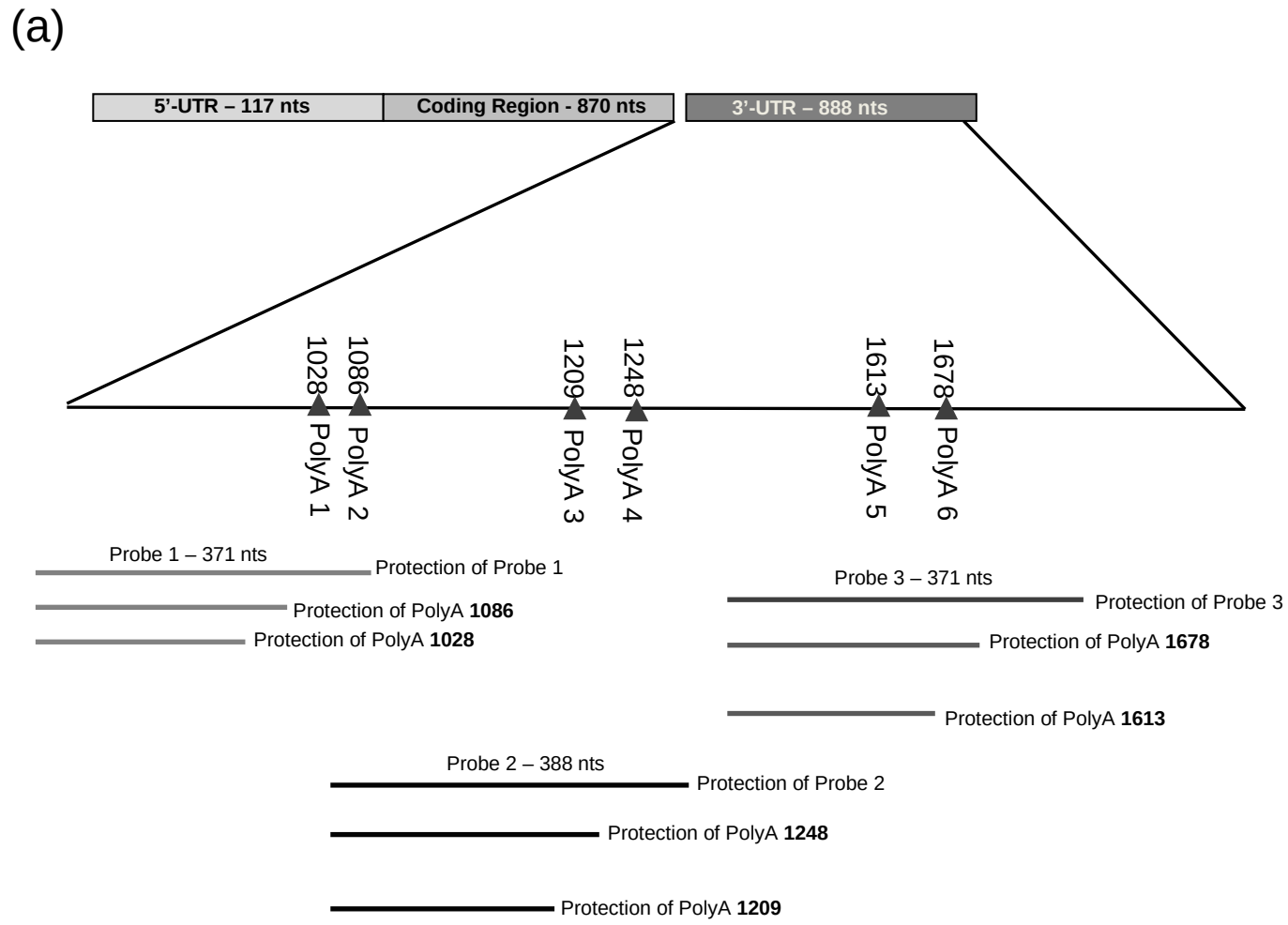

Figure 16. RNase protection assays examining pattern of polyadenylation site usage. (a) Schematic representation of NAT1 3'-UTR and probes . (b) The 1st and 2nd polyadenylation sites mapped with probe 1. (c) The 3rd and 4th polyadenylation sites mapped with probe 2. (d) The 5th and 6th polyadenylation sites mapped with probe 3. Lane 1: biotinylated marker; lane 2: RNA isolated from transiently transfected *NAT1*4*; lane 3: *NAT1*10*; lane 4: *NAT1*10B:* Lanes 5-7 are control lanes; lane 5: yeast (no target) RNA; lane 6: no RNase; lane 7: probe alone. Lanes 2 – 5 were hybridized to probe and treated with RNAse.

(b)

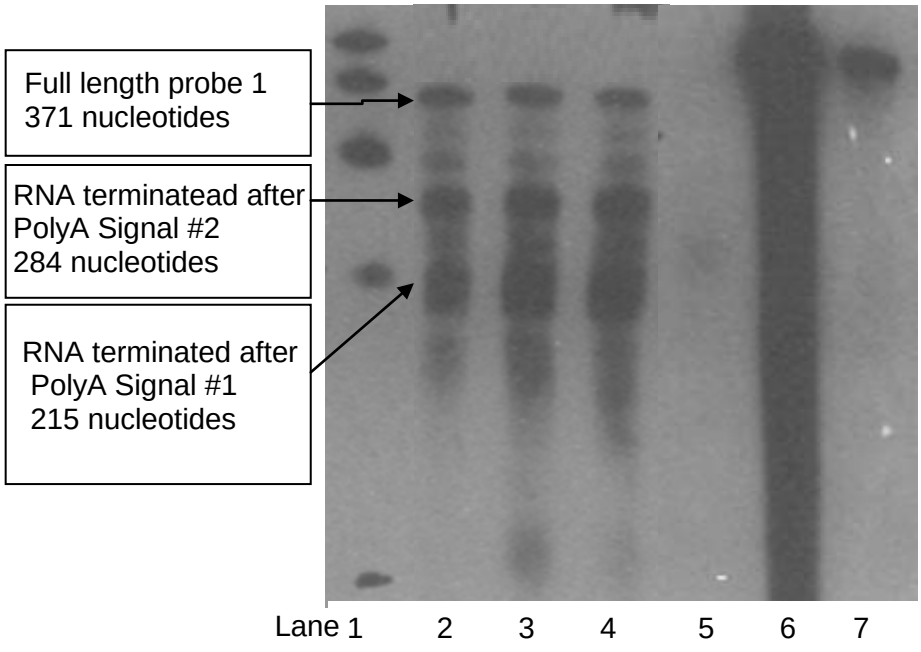
Full length probe 1
371 nucleotides
RNA terminatead after
PolyA Signal #2
284 nucleotides
RNA terminated after
PolyA Signal #1
215 nucleotides
Lane 1 2 3 4 5 6 7

(c)

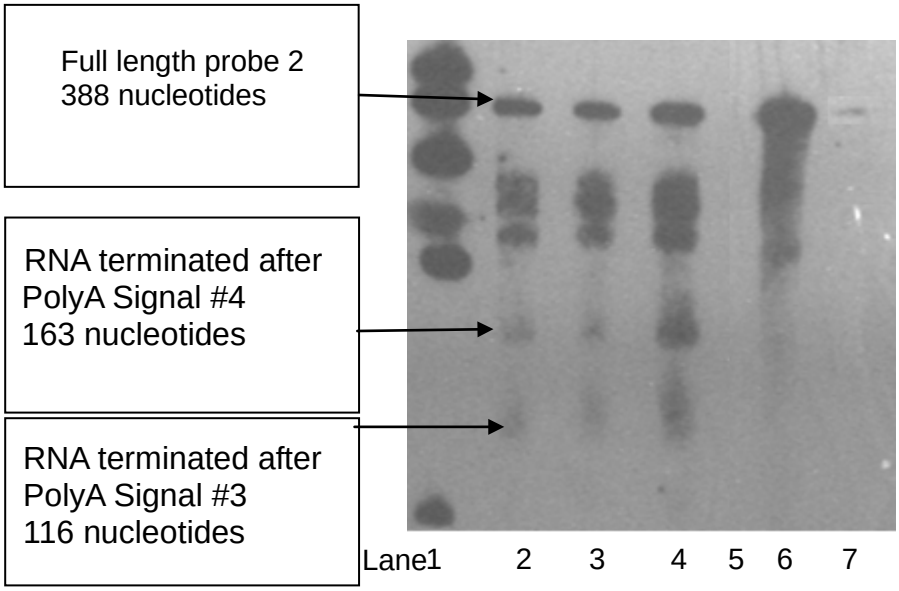
Full length probe 2
388 nucleotides
RNA terminated after
PolyA Signal #4
163 nucleotides
RNA terminated after
PolyA Signal #3
116 nucleotides
Lane1 2 3 4 5 6 7

(d)

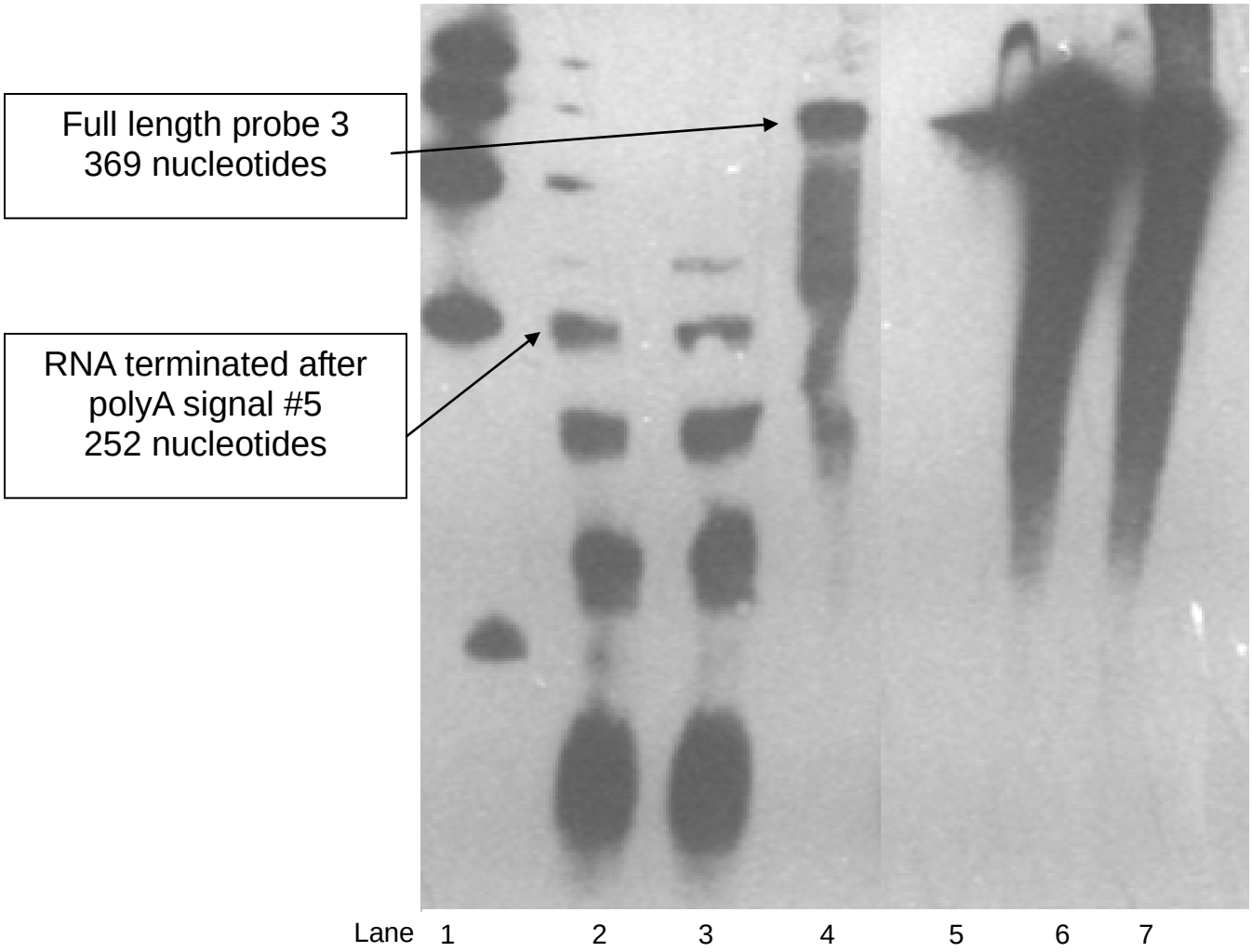

NAT1 mRNAs with intact polyadenylation tails contained in the public sequence databases including UCSC genomic browser, Unigene, and EST were examined. mRNAs ended 10-35 nucleotides beyond 4 different polyadenylation signals. These include polyadenylation signals located at positions 1088, 1209, 1248, and 1613. Three biotinylated RNA probes were used to determine the polyadenylation pattern of *NAT1*4*, *NAT1*10*, and *NAT1*10B* in transiently transfected UV5/1A1 cells via an RNase protection assay (Figure 16). RNase protection assays detected no difference in polyadenylation site usage between RNA

isolated from cells transfected with NATb/*NAT1*4 or* NATb/*NAT1*10*. Bands corresponding to polyadenylation signal 1 located at position 1028 (215 nucleotides), polyadenylation signal 2 located at position 1088 (284 nucleotides), polyadenylation signal 3 located at position 1209 (118 nucleotides), polyadenylation signal 4 located at position 1248 (163 nucleotides) and polyadenylation signal 5 located at position 1613 (252 nucleotides) were observed for all constructs. Full length probe 1 (371 nucleotides) and full length probe 2 (388 nucleotides) were observed for *NAT1*4*, *NAT1*10*, and *NAT1*10*B (Figure 16 b, c). Full length protection of probe 3 was observed only in *NAT1*10B* transfected cells (369 nucleotides) (Figure 16d). No band was observed in the lane with yeast RNA (negative control) for any probe.

The pcDNA5/FRT expression vector utilized in these experiments contained an SV40 polyadenylation signal for the hygromycin cassette. It was removed to ensure that the presence of *NAT1*10B* transcripts beyond the third probe were not vector-induced. Following removal of the SV40 polyadenylation signal from the pcDNA5/FRT, no significant ($p>0.05$) difference was observed in PABA *N*-acetylation in UV5/1A1 cells transiently transfected with *NAT1*10* or *NAT1*10B.*

All methods for figures 12 - 16 and can be found in the attached manuscript located in the appendix.

Discussion

Differences in expression and activity of the referent protein, NAT1 4, and the variants, NAT1 10 and NAT1 10B, were studied in UV5/*1A1* CHO cells transiently and stably transfected with NATb type mRNA. Increased *N*- and *O*- acetylation as well as increased mRNA and protein expression were observed in *NAT1*10* and *NAT1*10B* transfected cells when compared to *NAT1*4* transfected cells. This difference was observed in both transiently and stably transfected cells. This report also included examination of additional polymorphisms located in the 3'-UTR in an allele referred to in this paper as *NAT1*10B.* In addition to 1088T>A (rs1057126), 1095C>A (rs15561), and 1191G>T (rs4986993), *NAT1*10B* also has 1641A>C (rs8190865), a deletion ΔCT1647, 1716C>T (rs8190870) and 1735A>T. These polymorphisms were validated by their inclusion in the NCBI dbSNP database. Cells transfected with *NAT1*10B* resulted in higher *N*- and *O*- acetylation activity and protein expression compared to *NAT1*10*. Since these additional polymorphisms found in *NAT1*10B* are not screened for in association studies, it is possible that some of the discrepancies concerning *NAT1*10* phenotype could be attributed to misclassification of *NAT1*10B* as *NAT1*10*.

Alternative polyadenylation plays a large role in regulation of gene expression and it is known that 50% or more of human genes encode multiple transcripts derived from alternative polyadenylation sites (Tian et al., 2005). Differential processing at multiple polyadenylation sites can be influenced by physiological conditions such as cell growth, differentiation, and development or by pathological events such as cancer, however these mechanisms are largely unknown (Di Giammartino et al., 2011). There are 6 potential polyadenylation signals located in the region 3' to the NAT1 ORF. Previous studies have described the use of 2 consensus polyadenylation signals located at positions 1088 and 1209 in the NAT1 3'-UTR (Boukouvala and Sim, 2005) or most recently, the use of 3 NAT1 polyadenylation signals including the use of an additional polyadenylation signal at position 1613 (Wang et al., 2011). This study included a

survey of NCBI databases which found NAT1 transcripts that utilize 4 of the 6 potential polyadenylation signals located at positions 1088, 1209, 1248, and 1613. The 1088T>A SNP present in *NAT1*10* alters the 2nd polyadenylation signal (AATAAA – AAAAAA). It has been suggested (Boukouvala and Sim, 2005) that this change in polyadenylation signal may increase the stability of the *NAT1*10* RNA which could then result in differences between *NAT1*10* and *NAT1*4* in acetylation capacity. RNase protection assays were performed to map the polyadenylation pattern cells transfected with *NAT1*4*, *NAT1*10*, and *NAT1*10B* in NATb mRNA constructs. Bands were observed corresponding to the first 5 potential polyadenylation signals and no qualitative differences were observed between *NAT1*4* and *NAT1*10*. However, full length protection of probe 3 was observed for *NAT1*10B* but not for *NAT1*10* or *NAT1*4*. This indicates the presence of *NAT1*10B* transcripts that extend beyond probe 3. Other bands present may be due to either RNA cruciform structures or probe-probe interactions. Because NAT1 transcripts have been identified which utilize multiple polyadenylation signals both in this study and in NCBI databases, alternative polyadenylation usage likely plays an important role of NAT1 regulation.

Because the allelic frequency of *NAT1*10* allele is high in many populations, clearly defining the *NAT1*10* phenotype would allow cancer risk and other toxicities related to environmental arylamine exposure to be better understood. This study has shown that cells transfected with *NAT1*10* and NAT1*10B have higher *N*- and *O*- acetylation activity, NAT1 mRNA, and protein expression compared to cells transfected with *NAT1*4*. Additionally, higher ABP-induced DNA adducts and mutants were observed in cells transfected with *NAT1*10* compared to *NAT1*4.* However, no differences between *NAT1*4* and *NAT1*10* polyadenylation pattern were observed. Additionally, no differences in mRNA stability were observed between *NAT1*4, NAT1*10,* and *NAT1*10B* mRNA in stably transfected UV5/1A1 cells or in NAT1 endogenously expressed in HepG2 cells (Zhang et al., unpublished data). Other mechanisms

such as DNA-binding proteins must be responsible for the higher amount of *NAT1*10* mRNA, protein, acetylation activity, ABP-induced DNA adducts and mutants compared to *NAT1*4*. A difference was observed in the *NAT1*10B* polyadenylation pattern compared to *NAT1*10* and *NAT1*4*. This indicates additional mechanisms are involved in regulation of *NAT1*10B* compared to *NAT1*10.* Current screening methods do not differentiate between *NAT1*10* and *NAT1*10B* which could contribute to the ambiguous *NAT1*10* acetylation status. Further studies should be conducted to determine the responsible mechanisms for regulation of *NAT1*10* and *NAT1*10B*. Additional studies should also be conducted to examine the regulation of *NAT1*10* and *NAT1*10B* expressed in mRNA containing the 5'-UTR derived from the alternative promoter, NATa. The higher acetylation and ABP-induced mutants observed in NAT1 10 compared to NAT1 4 suggests that individuals possessing *NAT1*10* are at increased risk for cancers associated with arylamine exposure.

Key Research Outcomes

- Stable cell lines were created with NATb constructs (NATb/*NAT1*4,* NATb/*NAT1*10*, NATb/*NAT1*10B*, NATb/*NAT1*14*) and NATa constructs (NATa/*NAT1*4*, NATa/*NAT1*10*, NATa/*NAT1*10B*, NATa/*NAT1*14*).

- Cells transfected with NATa/*NAT1*4* resulted in significantly less N- and O-acetylation activity, protein and mRNA expression, ABP-induced cytotoxicity, DNA adduct formation and mutagenesis than cells transfected with NATb/*NAT1*4*.

- Cells transfected with *NAT1*10* and *NAT1*10B* resulted in higher PABA and ABP N-and O-acetylation activity, protein and mRNA expression than cells transfected with *NAT1*4*.

- Cells transfected with *NAT1*10* and *NAT1*10B* resulted in higher ABP induced adducts and cytotoxicity than cells transfected with *NAT1*4*.

- The kinetic parameters, k_m , v_{max}, and k_{cat} were determined for NAT1 4 and NAT1 14B both *in vitro* and *in situ.* Cells transfected with NAT1*4 resulted in 4-fold greater protein expression. Differences in intrinsic clearance, v_{max}/k_m between NAT1 4 and NAT1 14B are substrate dependent. Cancer risk related to *NAT1*14B* is likely also substrate dependent

Reportable Outcomes

Manuscripts

1. Millner, L.M., Doll, M.A., Cai, J., States, J.C., and Hein, D.W. (2011). NATb/NAT1*4 promotes greater arylamine N-acetyltransferase 1 mediated DNA adducts and mutations than NATa/NAT1*4 following exposure to 4-aminobiphenyl. Mol Carcinog. Published online August 11, 2011 as doi: 10.1002/mc.20836
2. Millner, L.M., Doll, M.A., Cai, J., States, J.C., and Hein, D.W. (2011). Phenotype of the Most Common "Slow Acetylator" Arylamine N-Acetyltransferase 1 Genetic Variant (*NAT1*14B)* is Substrate-Dependent. Drug Metabolism and Disposition. Published online October 18, 2011 as doi:10.1124/dmd.111.041855.
3. Millner, L.M., Doll, M.A., Stepp, M., Cai, J., States, J.C., and Hein, D.W. (2011). Functional analysis of arylamine *N*-acetyltransferase 1 (*NAT1*) *NAT1*10* haplotypes in a complete NATb mRNA construct. Carcinogenesis. Submitted and under review.

Published Abstracts

1. Lori M. Millner, Jean Bendaly, Mark A. Doll, David F. Barker, J. Christopher States and David W. Hein. Functional Effect of N-acetyltransferase Allele NAT1*10 in DNA Adduct Formation and Mutagenesis Following Exposure to Aromatic and Heterocyclic Amine Carcinogens. Abstracts, Ohio Valley Society of Toxicologists Meeting, Eli Lilly and Company, Indianapolis, Indiana, November 2, 2007.

5. Lori M. Millner, Jean Bendaly, Mark A. Doll, David F. Barker, J. Christopher States and David W. Hein. Functional effect of N-acetyltransferase 1 (NAT1*10) Polymorphism in DNA adduct formation and mutagenesis following exposure to aromatic and heterocyclic amine carcinogens. Abstracts, Society of Toxicology National Meeting, Seatle, WA. March 18, 2008.

6. Lori M. Millner, David F. Barker, Ashley L. Howarth, Mark A. Doll, J. Christopher States, David W. Hein. Translational Effects of Alternative NAT1 mRNA Isoforms. Abstracts, AACR Frontiers in Cancer Prevention Research International Conference, Washington, DC. November 16-19, 2008.

7. Lori M. Millner, David F. Barker, Mark A. Doll, J. Christopher States, and David W. Hein. Functional effects of N-acetyltransferase 1 (NAT1*10) polymorphisms. *FASEB J.* 2009 23:LB394.

8. Lori M. Millner, David F. Barker, Mark A. Doll, J. Christopher States and David W. Hein. Functional Effects of Alternative *N*-acetyltransferase (*NAT1*10*) mRNA Isoforms. Environmental Health Sciences Showcase, NIEHS, University of Cincinnati, Cincinnati, Ohio. September 25, 2009.

9. Lori M. Millner, Mark A. Doll, J. Christopher States and David W. Hein. Differences in Arylamine-induced Mutagenesis Associated with N-acetyltransferase 1 Alternative mRNA

Isoforms. Abstracts Midwest DNA Repair Symposium, University of Louisville, Louisville, KY, May 15, 2010.

10. Lori M. Millner, Mark A. Doll, Jian Cai, J. Christopher States and David W. Hein. Functional Effects of NAT1*14 Polymorphism in a NATb mRNA Construct. 5th International Workshop on Aryalmine N-acetyltrasferases, Université Paris Diderot, Paris France, September 2, 2010.

11. Lori M. Millner, Mark A. Doll, Jian Cai, J. Christopher States and David W. Hein. Differences in Arylamine-Induced Mutagenesis with N-acetyltransferase 1 Alternative mRNA Isoforms. 5th International Workshop on Aryalmine N-acetyltrasferases, Université Paris Diderot, Paris France, September 2, 2010.

12. Lori M. Millner, Mark A. Doll, Jian Cai, J. Christopher States and David W. Hein. Effects of *N*-acetyltransferase 1 (NAT1*10) polymorphisms in NATb and NATa derived mRNA constructs on DNA adducts and mutations from 4-aminobiphenyl. Society of Toxicology 50th Meeting. Washington, D.C. March 6 – 10, 2011.

13. Lori M. Millner, Mark A. Doll, Jian Cai, J. Christopher States and David W. Hein. Differences in Arylamine-induced Mutagenesis Associated with N-acetyltransferase 1 Alternative mRNA Isoforms. Era of Hope Department of Defense Conference, Orlando, Florida. August 2 – 6, 2011.

Conclusions

NATb/*NAT1*4* versus NATa/*NAT1*4*

Significantly more NAT1 activity, protein, mRNA, ABP-induced cytoxicity, DNA adducts and mutagenesis were detected in cells stably transfected with NATb/*NAT1*4* than in cells transfected with NATa/*NAT1*4* ($p<0.05$). DNA adduct and mutant levels following exposure to ABP are biological endpoints that are very relevant to cancer risk. Because DNA adduct and mutant levels were significantly higher in cells transfected with NATb/*NAT1*4* than cells transfected with NATa/*NAT1*4*, cancer risk may be altered in tissues that express both NATb and NATa transcripts following exposure to arylamine carcinogens due to altered gene expression. These results suggest that differential regulation occurs in the *NAT1* 5'-UTR which could contribute to overexpression in disease states, causing increased mutagenesis, enhanced tumor growth, and decreased chemotherapeutic sensitivity. This study focused only on the referent allele, *NAT1*4,* but future studies should investigate 5'-UTR control with other *NAT1* alleles to determine if any effect occurs between combinations of 5'-UTRs and alleles.

*NAT1*10* versus *NAT1*4*

*NAT1*10* is putatively considered to be a rapid acetylator, however there are many conflicting results about the acetylator phenotype of *NAT1*10*. One study reported significantly higher enzyme activity in urinary bladder and colon tissue for individuals heterozygous for *NAT1*10/*4* compared to those individuals homozygous for *NAT1*4* (Bell et al., 1995). Similar findings were reported in colorectal tissue. In contrast, another study employing recombinantly expressed alleles reported no difference between NAT1*10 and NAT1*4 activities (de Leon et al., 2000).

This study reports on *in vitro* and *in situ* N-acetylation experiments which show that NAT1 10 and NAT1 10B are rapid acetylators compared to the referent, NAT1 4. ABP-induced mutagenesis also show increased mutants in cells transfected with *NAT1*10* than in cells transfected with *NAT1*4. NAT1*10* has been of high interest because of its association with many different cancers and because it has a very high allelic frequency in many different populations. Our constructs are a useful tool in the study of *NAT1*10* and indicate that cancer risk associated with NAT*10 and NAT1*10B is higher than risk associated with NAT1*4. Additionally, this is the first study that has examined *NAT1*10B* and our research emphasizes importance of *NAT1*10B* and suggests that *NAT1*10B* should be including when genotyping for *NAT1*10*.

*NAT1*14B* versus *NAT1*4*

Previous studies have shown that NAT1*14 is associated with decreased protein expression and decreased acetylation activity (Fretland et al., 2001). These studies confirm that NAT1*14 results in decreased protein expression when compared to NAT1*4. Our studies also reported the kinetic values, k_m, v_{max}, and k_{cat}. We showed that there are substrate dependent differences in those parameters, and a person possessing *NAT1*14B* would be at altered cancer risk only following exposure to some substrates and not to others.

References

Barker, D.F., Husain, A., Neale, J.R., Martini, B.D., Zhang, X., Doll, M.A., States, J.C., and Hein, D.W. (2006). Functional properties of an alternative, tissue-specific promoter for human arylamine N-acetyltransferase 1. Pharmacogenet Genomics *16*, 515-525.

Bell, D.A., Badawi, A.F., Lang, N.P., Ilett, K.F., Kadlubar, F.F., and Hirvonen, A. (1995). Polymorphism in the N-acetyltransferase 1 (NAT1) polyadenylation signal: association of NAT1*10 allele with higher N-acetylation activity in bladder and colon tissue. Cancer Res *55*, 5226-5229.

Boissy, R.J., Watson, M.A., Umbach, D.M., Deakin, M., Elder, J., Strange, R.C., and Bell, D.A. (2000). A pilot study investigating the role of NAT1 and NAT2 polymorphisms in gastric adenocarcinoma. Int J Cancer *87*, 507-511.

Bouchardy, C., Mitrunen, K., Wikman, H., Husgafvel-Pursiainen, K., Dayer, P., Benhamou, S., and Hirvonen, A. (1998). N-acetyltransferase NAT1 and NAT2 genotypes and lung cancer risk. Pharmacogenetics *8*, 291-298.

Boukouvala, S., and Sim, E. (2005). Structural analysis of the genes for human arylamine N-acetyltransferases and characterisation of alternative transcripts. Basic Clin Pharmacol Toxicol *96*, 343-351.

Butcher, N.J., Arulpragasam, A., and Minchin, R.F. (2004). Proteasomal degradation of N-acetyltransferase 1 is prevented by acetylation of the active site cysteine: a mechanism for the slow acetylator phenotype and substrate-dependent down-regulation. J Biol Chem *279*, 22131-22137.

Chen, Y., Liu, L., Nguyen, K., and Fretland, A.J. (2011). Utility of intersystem extrapolation factors in early reaction phenotyping and the quantitative extrapolation of human liver microsomal intrinsic clearance using recombinant cytochromes P450. Drug Metab Dispos *39*, 373-382.

de Leon, J.H., Vatsis, K.P., and Weber, W.W. (2000). Characterization of naturally occurring and recombinant human N-acetyltransferase variants encoded by NAT1. Mol Pharmacol *58*, 288-299.

Dhaini, H.R., and Levy, G.N. (2000). Arylamine N-acetyltransferase 1 (NAT1) genotypes in a Lebanese population. Pharmacogenetics *10*, 79-83.

Di Giammartino, D.C., Nishida, K., and Manley, J.L. (2011). Mechanisms and consequences of alternative polyadenylation. Mol Cell *43*, 853-866.

Feng, Z., Hu, W., Rom, W.N., Beland, F.A., and Tang, M.S. (2002). 4-aminobiphenyl is a major etiological agent of human bladder cancer: evidence from its DNA binding spectrum in human p53 gene. Carcinogenesis *23*, 1721-1727.

Fretland, A.J., Doll, M.A., Leff, M.A., and Hein, D.W. (2001). Functional characterization of nucleotide polymorphisms in the coding region of N-acetyltransferase 1. Pharmacogenetics *11*, 511-520.

Fretland, A.J., Doll, M.A., Zhu, Y., Smith, L., Leff, M.A., and Hein, D.W. (2002). Effect of nucleotide substitutions in N-acetyltransferase-1 on N-acetylation (deactivation) and O-acetylation (activation) of arylamine carcinogens: implications for cancer predisposition. Cancer Detect Prev *26*, 10-14.

Gehring, N.H., Frede, U., Neu-Yilik, G., Hundsdoerfer, P., Vetter, B., Hentze, M.W., and Kulozik, A.E. (2001). Increased efficiency of mRNA 3' end formation: a new genetic mechanism contributing to hereditary thrombophilia. Nat Genet *28*, 389-392.

Hein, D.W., Leff, M.A., Ishibe, N., Sinha, R., Frazier, H.A., Doll, M.A., Xiao, G.H., Weinrich, M.C., and Caporaso, N.E. (2002). Association of prostate cancer with rapid N-acetyltransferase 1 (NAT1*10) in combination with slow N-acetyltransferase 2 acetylator genotypes in a pilot case-control study. Environ Mol Mutagen *40*, 161-167.

Hoffmann, D., Djordjevic, M.V., and Hoffmann, I. (1997). The changing cigarette. Prev Med *26*, 427-434.

Hughes, N.C., Janezic, S.A., McQueen, K.L., Jewett, M.A., Castranio, T., Bell, D.A., and Grant, D.M. (1998). Identification and characterization of variant alleles of human acetyltransferase NAT1 with defective function using p-aminosalicylate as an in-vivo and in-vitro probe. Pharmacogenetics *8*, 55-66.

Husain, A., Barker, D.F., States, J.C., Doll, M.A., and Hein, D.W. (2004). Identification of the major promoter and non-coding exons of the human arylamine N-acetyltransferase 1 gene (NAT1). Pharmacogenetics *14*, 397-406.

Husain, A., Zhang, X., Doll, M.A., States, J.C., Barker, D.F., and Hein, D.W. (2007). Functional analysis of the human N-acetyltransferase 1 major promoter: quantitation of tissue expression and identification of critical sequence elements. Drug Metab Dispos *35*, 1649-1656.

IARC (1987). Overall Evaluations of Carcinogenicity. Lyon, France: International Agency for Research on Cancer. 440 pp. IARC Monographs on the Evaluation of Carcinogenic Risk of

Chemicals to Humans *1-42, suppl 7.*

Mishra, P.J., Banerjee, D., and Bertino, J.R. (2008). MiRSNPs or MiR-polymorphisms, new players in microRNA mediated regulation of the cell: Introducing microRNA pharmacogenomics. Cell Cycle *7*, 853-858.

Morton, L.M., Schenk, M., Hein, D.W., Davis, S., Zahm, S.H., Cozen, W., Cerhan, J.R., Hartge, P., Welch, R., Chanock, S.J.*, et al.* (2006). Genetic variation in N-acetyltransferase 1 (NAT1) and 2 (NAT2) and risk of non-Hodgkin lymphoma. Pharmacogenet Genomics *16*, 537-545.

Nauwelaers, G., Bessette, E.E., Gu, D., Tang, Y., Rageul, J., Fessard, V., Yuan, J.M., Yu, M.C., Langouet, S., and Turesky, R.J. (2011). DNA Adduct Formation of 4-Aminobiphenyl and Heterocyclic Aromatic Amines in Human Hepatocytes. Chem Res Toxicol.

Northrop, D.B. (1999). Rethinking fundamentals of enzyme action. Adv Enzymol Relat Areas Mol Biol *73*, 25-55.

Payton, M.A., and Sim, E. (1998). Genotyping human arylamine N-acetyltransferase type 1 (NAT1): the identification of two novel allelic variants. Biochem Pharmacol *55*, 361-366.

Pizzuti, A., Argiolas, A., Di Paola, R., Baratta, R., Rauseo, A., Bozzali, M., Vigneri, R., Dallapiccola, B., Trischitta, V., and Frittitta, L. (2002). An ATG repeat in the 3'-untranslated region of the human resistin gene is associated with a decreased risk of insulin resistance. J Clin Endocrinol Metab *87*, 4403-4406.

Stephenson, N., Beckmann, L., and Chang-Claude, J. (2010). Carcinogen metabolism, cigarette smoking, and breast cancer risk: a Bayes model averaging approach. Epidemiol Perspect Innov *7*, 10.

Tian, B., Hu, J., Zhang, H., and Lutz, C.S. (2005). A large-scale analysis of mRNA polyadenylation of human and mouse genes. Nucleic Acids Res *33*, 201-212.

Wakefield, L., Robinson, J., Long, H., Ibbitt, J.C., Cooke, S., Hurst, H.C., and Sim, E. (2008). Arylamine N-acetyltransferase 1 expression in breast cancer cell lines: a potential marker in estrogen receptor-positive tumors. Genes Chromosomes Cancer *47*, 118-126.

Walraven, J.M., Trent, J.O., and Hein, D.W. (2008). Structure-function analyses of single nucleotide polymorphisms in human N-acetyltransferase 1. Drug Metab Rev *40*, 169-184.

Zheng, W., Deitz, A.C., Campbell, D.R., Wen, W.Q., Cerhan, J.R., Sellers, T.A., Folsom, A.R., and Hein, D.W. (1999). N-acetyltransferase 1 genetic polymorphism, cigarette smoking, well-done meat intake, and breast cancer risk. Cancer Epidemiol Biomarkers Prev *8*, 233-239.

Zhu, Y., and Hein, D.W. (2008). Functional effects of single nucleotide polymorphisms in the coding region of human N-acetyltransferase 1. Pharmacogenomics J *8*, 339-348.

Appendix 1

NATb/*NAT1*4* Promotes Greater Arylamine *N*-acetyltransferase 1 Mediated DNA Adducts and Mutations Than NATa/*NAT1*4* Following Exposure to 4-Aminobiphenyl

Lori M. Millner, Mark A. Doll, Jian Cai, J. Christopher States, and David W. Hein*

[1]*Department of Pharmacology and Toxicology, James Graham Brown Cancer Center and Center for Environmental Genomics and Integrative Biology, University of Louisville, Louisville, Kentucky*

N-acetyltransferase 1 (NAT1) is a phase II metabolic enzyme responsible for the biotransformation of aromatic and heterocyclic amine carcinogens such as 4-aminobiphenyl (ABP). NAT1 catalyzes *N*-acetylation of arylamines as well as the *O*-acetylation of *N*-hydroxylated arylamines. *O*-acetylation leads to the formation of electrophilic intermediates that result in DNA adducts and mutations. NAT1 is transcribed from a major promoter, NATb, and an alternative promoter, NATa, resulting in mRNAs with distinct 5′-untranslated regions (UTR). NATa mRNA is expressed primarily in the kidney, liver, trachea, and lung while NATb mRNA has been detected in all tissues studied. To determine if differences in 5′-UTR have functional effect upon NAT1 activity and DNA adducts or mutations following exposure to ABP, pcDNA5/FRT plasmid constructs were prepared for transfection of full-length human mRNAs including the 5′-UTR derived from NATa or NATb, the open reading frame, and 888 nucleotides of the 3′-UTR. Following stable transfection of NATb/*NAT1*4* or NATa/*NAT1*4* into nucleotide excision repair (NER) deficient Chinese hamster ovary cells, *N*-acetyltransferase activity (in vitro and in situ), mRNA, and protein expression were higher in NATb/*NAT1*4* than NATa/*NAT1*4* transfected cells ($P < 0.05$). Consistent with NAT1 expression and activity, ABP-induced DNA adducts and *hypoxanthine phosphoribosyl transferase* mutants were significantly higher ($P < 0.05$) in NATb/*NAT1*4* than in NATa/*NAT1*4* transfected cells following exposure to ABP. These differences observed between NATa and NATb suggest that the 5′-UTRs are differentially regulated.

Key words: 4-aminobiphenyl; *N*-acetyltransferase 1; alternative mRNA isoforms; arylamine DNA adducts; *hprt* mutants

INTRODUCTION

Human arylamine *N*-acetyltransferase 1 (NAT1) is a phase II cytosolic enzyme responsible for the biotransformation of many arylamine compounds including pharmaceuticals and environmental carcinogens. A common environmental carcinogen found in cigarette smoke is an aromatic amine, 4-aminobiphenyl (ABP) [1]. Arylamines such as ABP can be inactivated via *N*-acetylation [2]. However, if ABP is first hydroxylated by cytochrome p4501A1 (CYP1A1), the hydroxyl-ABP then can be further activated by NAT1-catalyzed *O*-acetylation resulting in *N*-acetoxy-ABP [2]. This compound is very unstable and spontaneously degrades to form a nitrenium ion that can react with DNA to produce bulky adducts. If these adducts are not repaired, mutagenesis can occur and result in cancer initiation.

The only known endogenous NAT1 substrate is *p*-aminobenzoylglutamate (PABG), a catabolite of folate [3]. *NAT1* has been associated with various birth defects [4,5] that may be related to deficiencies in folate metabolism. *NAT1* polymorphisms and maternal smoking have been associated with increased incidence of oral clefts, spina bifida and increased limb deficiency defects [6,7]. *NAT1* polymorphisms have also been associated with increased risk for breast [8,9], pancreatic [10,11], urinary bladder [12,13] and colorectal cancers [14,15], non-Hodgkin lymphoma [16,17], mammary cell growth [18] and breast cancer survival [19]. However, other studies have concluded that NAT1 polymorphism status is not associated with increased risk to bladder, esophageal, prostate, or gastric cancers [20–22]. NAT1 has also been implicated in cell growth and survival. Studies have shown that overexpression of NAT1 increased density dependent cell proliferation, and knockdown of NAT1 resulted in marked change in cell morphology, an increase in cell–cell contact inhibition and a loss of cell viability at confluence [18,23]. *NAT1*4* is referred to as the referent

*Correspondence to: University of Louisville Health Sciences Center, 505 South Hancock Street, at Clinical and Translational Research Building Room 303, Louisville, KY 40202-1617.

Received 28 April 2011; Revised 7 June 2011; Accepted 11 July 2011

DOI 10.1002/mc.20836

Published online in Wiley Online Library (wileyonlinelibrary.com).

allele because it was the most common allele in the population in which it was first identified [24]. To date, 26 human *NAT1* alleles have been identified (http://louisville.edu/medschool/pharmacology/consensus-human-arylamine-n-acetyltransferase-gene-nomenclature/). Although the effects of *NAT1* polymorphisms on catalytic activity have been studied, the results are ambiguous. Within single NAT1 genotypes, conflicting phenotypes have been reported, and the relationship between phenotype and genotype remains poorly understood. Since factors other than genotype are likely affecting phenotype, it is important to understand transcriptional and translational control of *NAT1*.

The *NAT1* gene spans 53 kb and contains nine exons (Figure 1a). Several *NAT1* transcripts have been identified containing various combinations of 5′-untranslated region (UTR) exons and are known to originate from two distinct promoters, NATa and NATb. NATb, the major promoter, is located 11.8 kb upstream of the open reading frame (ORF). NATb promotes transcription of Type II transcripts and the major transcript, Type IIA, has been detected in all tissues studied to date [25,26]. An alternative promoter, NATa, originates 51.5 kb upstream of the *NAT1* ORF and promotes transcription of Type I transcripts expressed primarily in kidney, lung, liver, and trachea [25,27]. The NAT1 gene is induced following exposure to androgens and NAT1 protein stability is affected by the presence of substrates [28].

Recent analyses of genome-wide Pol II distribution in Drosophila and mammalian systems have reported that regulation of many genes occurs after transcription initiation [29,30] providing evidence for regulatory control in the 5′-UTR that is distinct from promoter regulatory control. Recent studies have shown that between 30% and 50% of all human genes utilize alternative promoters [31,32] to allow for cell, tissue, and disease specific expression. To determine if differences in 5′-UTR have functional effect upon NAT1 activity, DNA adducts or mutations following exposure to ABP, pcDNA5/FRT plasmid constructs were prepared for transfection of full length human mRNAs including the 5′-UTR derived from NATa or NATb, the *NAT1*4* ORF, and 888 nucleotides of the 3′-UTR. The constructs were cloned into two expression vectors utilizing two different constitutive promoters (CMV and the EF1α promoters) to examine regulatory control located in the 5′-UTR. The cells transfected with NATa/*NAT1*4* and NATb/*NAT1*4* constructs were characterized for NAT1 mRNA and protein expression, *N*- and *O*-acetyltransferase activity (in vitro and in situ), ABP-induced DNA adducts and *hypoxanthine phosphoribosyl transferase (hprt)* mutations following exposure to ABP.

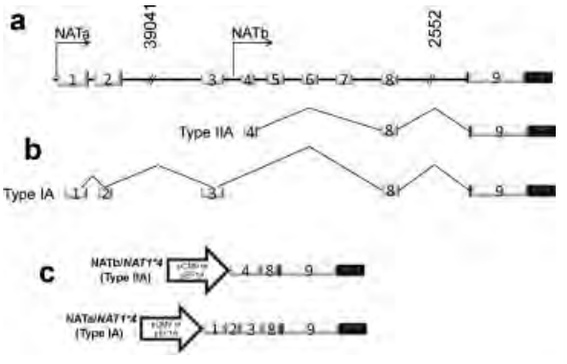

Figure 1. (a) Genomic organization of NAT1 gene; (b) Type IIA and Type IA NAT1 RNA (c) and representative NATb/*NAT1*4* and NATa/*NAT1*4* constructs (modified from Ref. [41]).

MATERIALS AND METHODS

Polyadenylation Site Removal

The bovine growth hormone (BGH) polyadenylation site from the pcDNA5/FRT (Invitrogen, Carlsbad, CA) vector was removed to allow the endogenous *NAT1* polyadenylation sites to be active. This was accomplished by digestion at 37°C with restriction endonucleases, *Apa*I and *Sph*I (New England Biolabs, Ipswich, MA), followed by overhang digestion with T4 DNA polymerase (Invitrogen) and ligation with T4 Ligase (Invitrogen).

NATb/*NAT1*4* and NATa/*NAT1*4* Constructs

NATb/*NAT1*4* and NATa/*NAT1*4* constructs were created utilizing gene splicing via overlap extension [33] by amplifying the 5′-UTR and the coding region/3′-UTR separately and then fusing the two regions together. Beginning with frequently used transcription start sites, the 5′-UTRs [26,27] were amplified from cDNA prepared from RNA isolated from homozygous *NAT1*4* HepG2 cells. All primer sequences used are shown in Table 1. The primers used to amplify the NATb 5′-UTR region were Lkm40P1 and NAT1 (3′) ORF Rev while the primers used to amplify the NATa 5′-UTR region were Lkm41P1 and NAT1 (3′) ORF Rev. The coding region and 3′-UTR were amplified as one piece from *NAT1*4* human genomic DNA with *NAT1*4*/*NAT1*4* genotype. The forward primer used to amplify the coding region/3′-UTR was NAT1 (3′) ORF Forward while the reverse primer was pcDNA5 distal Reverse. The two sections, the 5′-UTR and the coding region/3′UTR, were fused together via overlap extension and amplification of the entire product using nested primers. The forward nested primer for NATb was P1 Fwd Inr *Nhe*I while the forward nested primer for NATa was P3 Fwd Inr *Nhe*I. The reverse nested primer for both NATa and

Table 1. Primer Sequences

Primer name	Use	Sequence
Lkm40P1	NATb 5′-UTR forward specific PCR	5′-GGCCGCGGCATTCAGTCTAGTTCCTGGTTGCC-3′
P1 Fwd Inr *Nhe*I	NATb 5′-UTR forward specific nested PCR	5′-TTTAAAGCTAGCATTCAGTCTAGTCTAGTTCCTGGTTGCCGGCT-3′
Lkm41P3	NATa 5′-UTR forward specific PCR	5′-GGCCGCGGAACACATTCTGCTCAAATAAGCCT-3′
P3 Fwd Inr *Nhe*I	NATa 5′-UTR forward specific nested PCR	5′-TTAATGCTAGCAACACATTCTGCTCAAATAAAGCCTAGG-3′
NAT (3′) ORF Rev	NATa/NATb 5′-UTR reverse PCR	5′-TTCCTCACTCAGAGTCTTGAACTCTATT-3′
NAT1 (3′) ORF For	NAT1 coding region forward PCR	5′-AGACATCTCCATCATCTGTGTTTACTAGT-3′
pcDNA5 FRT distal Rev	NAT1 3′-UTR reverse PCR	5′-CGTGGGGATACCCCCTAGA
NAT1 KPN-Rev	NAT1 3′-UTR reverse nested PCR	5′-ATAGTAGGTACCTCTGAATTATAGATAAGCAAGATTCAGATTCT-3′
NATb Forward pEF1	NATb 5′-UTR forward specific pEF1a PCR	5′-AGTCGGATCCATTCAGTCTAGTTCCTGGTT-3′
NATa Forward pEF1	NATa 5′-UTR forward specific pEF1a PCR	5′-AGTCGGATCCAACACATTCTGCTCAAATAAAGCCTAGGCCAA-3′
NATa/b Reverse pEF1	NAT1 3′-UTR reverse pEF1a PCR	5′-TCGAGATATCAGCTCGGTACCTCTGAATTATAGA-3′
NAT1 total spliced Forward	NAT1 specific forward q-RT-PCR	5′-GAATTCAAGCCAGGAAGAAGCA-3′
NAT1 total spliced Reverse	NAT1 specific reverse q-RT-PCR	5′-TCCAAGTCCAATTTGTTCCTAGACT-3′
NAT1 TAQMAN probe for TS	TAQMAN probe for NAT1 total splice	6FAM-5′-CAATCTGTCTTCTGGATTAA-3′ MGBNFQ

NATb constructs was NAT1 Kpn Rev. Both forward nested primers included the *Kpn*I endonuclease restriction site and both reverse nested primers contained the *Nhe*I endonuclease restriction site to facilitate cloning. The pcDNA5/FRT vector and NATa/*NAT1*4* and NATb/*NAT1*4* allelic segments were digested at 37°C with restriction endonucleases *Kpn*I and *Nhe*I (New England Biolabs). The *NAT1* constructs were then ligated into pcDNA5/FRT using T4 ligase (Invitrogen). These same *NAT1* constructs were also cloned into a second expression vector, pEF1/5V-His (Invitrogen). The NATb/*NAT1*4* construct was amplified using the forward primer, NATb Forward pEF1, while the NATa/*NAT1*4* construct was amplified using the forward primer NATa Forward pEF1. Both forward primers contained the *Bam*HI restriction site. Both constructs were amplified using the reverse primer NATa/b Reverse pEF1 which contained the *Eco*RV restriction site. Both NATa/*NAT1*4* and *NATb*/*NAT1*4* and pEF1/5V-His were digested with the restriction endonucleases, *Bam*HI and *Eco*RV (New England Biolabs), followed by ligation into the vector using T4 ligase (Invitrogen). All constructs were sequenced to ensure integrity of allelic segments and junction sites.

Cell Culture

UV5-CHO cells, a nuclease excision repair (NER)-deficient derivative of AA8 which are hypersensitive to bulky DNA lesions, were obtained from the ATCC (catalog number: CRL-1865). Unless otherwise noted, cells were incubated at 37°C in 5% CO_2 in complete alpha-modified minimal essential medium (α-MEM, Lonza, Walkersville, MD) without L-glutamine, ribosides, and deoxyribosides supplemented with 10% fetal bovine serum (Hyclone, Logan, UT), 100 units/mL penicillin (Lonza), 100 μg/mL streptomycin (Lonza), and 2 mM L-glutamine (Lonza). The UV5/CHO cells used in this study were previously stably transfected with a single Flp recombination target (FRT) integration site [34]. The FRT site allowed stable transfections to utilize the Flp-In System (Invitrogen). When cotransfected with pOG44 (Invitrogen), a Flp recombinase expression plasmid, a site-specific, conserved recombination event of pcDNA5/FRT (containing either NATa/*NAT1*4* or NATb/*NAT1*4*) occurs at the FRT site. The FRT site allows recombination to occur immediately downstream of the hygromycin resistance gene, allowing for hygromycin selectivity only after Flp-recombinase mediated integration. The UV5/FRT cells were further modified by stable integration of human *CYP1A1* and NADPH-cytochrome P450 reductase gene (*POR*) [34]. They are referred to in this manuscript as UV5/*1A1* cells.

COS-1 cells, a SV-40 transformed fibroblast cell line derived from African green monkey kidney,

were also used for transient transfection. COS-1 cells were obtained from ATCC (catalog number: CRL-1650) and maintained at 37°C in 5% CO_2. COS-1 cells were cultured in complete Dulbecco's modified Eagle's medium 4.5 g/L glucose without L-glutamine (DMEM, Lonza) supplemented with 10% fetal bovine serum (Hyclone), 100 units/mL penicillin (Lonza), 100 μg/mL streptomycin (Lonza), and 2 mM L-glutamine (Lonza).

Transient Transfection

UV5/*1A1* and COS-1 cells were transiently transfected with pcDNA5/FRT (Invitrogen) or pEF1/V5-His (Invitrogen) containing NATa/*NAT1*4* and NATb/*NAT1*4* constructs using Lipofectamine reagent (Invitrogen) following the manufacturer's recommendations. UV5/*1A1* and COS-1 cells were cotransfected with pCMV-SPORT-βgal (β-galactosidase transfection control plasmid, Invitrogen). The cells were harvested the next day. Lysate was prepared by centrifuging the cells and resuspending pellet in homogenization buffer (20 mM $NaPO_4$ pH 7.4, 1 mM EDTA, 1 mM DTT, 0.1 mM PMSF, 2 μg/mL aprotinin, and 2 mM pepstatin A). The resuspended cell pellet was subjected to three rounds of freezing at −80°C and thawing at 37°C and then centrifuged at 15 000*g* for 10 min. The supernatant was used to measure *N*-acetyltransferase activity and β-galactosidase activity.

Stable Transfections

Stable transfections were carried out using the Flp-In System (Invitrogen) into UV5/*1A1* cells that were previously stably transfected with a FRT site (as noted above). The pcDNA5/FRT plasmids containing human NATa/*NAT1*4* or NATb/*NAT1*4* were cotransfected with pOG44 (Invitrogen), a Flp recombinase expression plasmid. UV5/*1A1* cells were stably transfected with pcDNA5/FRT containing NATa/*NAT1*4* and NATb/*NAT1*4* constructs using Effectene transfection reagent (Qiagen, Valencia, CA) following the manufacturer's recommendations. Since the pcDNA5/FRT vector contains a hygromycin resistance cassette, cells were passaged in complete α-MEM containing 600 μg/mL hygromycin (Invitrogen) to select for cells containing the pcDNA5/FRT plasmid. Hygromycin resistant colonies were selected approximately 10 d after transfection and isolated with cloning cylinders.

Measurement of *N*-Acetyltransferase Enzymatic Activity

In vitro assays using the NAT1 specific substrate para-aminobenzoic acid (PABA) or 4-aminobiphenyl (ABP) were conducted and acetylated products were separated utilizing HPLC [35]. Reactions containing 50 μL cell lysate, PABA or ABP (300 μM) and acetyl coenzyme A (1 mM) were incubated at 37°C for 10 min. Reactions were terminated by the addition of 1/10 volume of 1 M acetic acid and centrifuged at 15 000*g* for 10 min. Supernatant was injected into a (125 mm × 4 mm; 5 μM pore size) reverse phase C18 column. Reactants and products were eluted using a Beckman System Gold high performance liquid chromatograph (HPLC) system. HPLC separation of *N*-acetyl-PABA was achieved using a gradient of 96:4 sodium perchlorate pH 2.5:acetonitrile (ACN) to 88:12 sodium perchlorate pH 2.5:ACN over 3 min and was quantitated by absorbance at 280 nm. HPLC separation of *N*-acetyl-ABP was achieved using a gradient of 85:15 sodium perchlorate pH 2.5:ACN to 35:65 sodium perchlorate pH 2.5:ACN over 10 min and was quantitated by absorbance at 260 nm. Measurements were adjusted according to baseline measurements using lysates of the UV5/*CYP1A1* cell line. Both stably and transiently transfected cells were normalized by the amount of total protein. Assays involving transiently transfected cells and PABA used β-galactosidase activity to control for transfection efficiency. To correct for transfection efficiency, β-galactosidase plasmids (pCMV-sport-βgal) were cotransfected with pcDNA5/FRT or pEF1/5V-His. β-galactosidase activity was measured in reactions containing 30 μL cell lysate, 70 μL of 4 mg/mL *ortho*-nitrophenyl-β-D-galactopyranoside (ONPG), and 200 μL of cleavage buffer (60 mM Na_2HPO_4, 40 mM NaH_2PO_4, and 1 mM $MgSO_4$, pH 7.0). The reaction was incubated for 30 min at 37°C. The reaction was terminated by the addition of 500 μL of 1 M sodium carbonate and absorbance at 420 nm was measured. Protein concentrations were measured using the method of Bradford (Bio-Rad, Hercules, CA). The β-galactosidase activities were normalized to total protein and the resulting values were used to correct for the effect of any differences in transfection efficiency. In situ *N*-acetyltransferase activity was studied in a whole cell assay using media spiked with differing concentrations of PABA (10–300 μM). The cells were incubated at 37°C and media was collected after 5 h, 1/10 volume of 1 M acetic acid was added, and the mixture was centrifuged at 13 000*g* for 10 min. The supernatant was injected into the reverse phase HPLC column and *N*-acetyl-PABA was separated and quantitated as described above.

Measurement of *O*-Acetyltransferase Enzymatic Activity

N-hydroxy-4-aminobiphenyl (*N*-OH-ABP) *O*-acetyltransferase assays were conducted as previously described [34]. Assays containing 100 μg total protein, 1 mM acetyl coenzyme A, 1 mg/mL deoxyguanosine (dG), and 100 μM *N*-OH-ABP were incubated at 37°C for 10 min. Reactions were stopped with the addition of 100 μL of water saturated ethyl acetate and centrifuged at 13 000*g* for 10 min. The organic phase was removed,

evaporated to dryness and the residue was dissolved in 100 μL of 10% ACN. HPLC separation was achieved using a gradient of 80:20 sodium perchlorate pH 2.5:ACN to 50:50 sodium perchlorate pH 2.5:ACN over 3 min and dG-C8-ABP adduct was detected at 300 nm.

Measurement of NAT1 Protein

The amount of NAT1 produced in UV5/*1A1* cells stably transfected with NATa/*NAT1*4* or NATb/*NAT1*4* was determined by Western blot. Cell lysates were isolated as described above. Varying amounts of lysate were mixed 1:1 with 5% β-mercaptoethanol in Laemmli buffer (Bio-Rad), boiled for 5 min, and resolved by 12% SDS–PAGE. The proteins were then transferred by semi-dry electroblotting to polyvinylidene fluoride (PVDF) membranes. The membranes were probed with a polyclonal rabbit anti-hNAT1 ES195 (1:1000) kindly provided by Edith Sim [36] and with horseradish peroxidase (HRP)-conjugated secondary goat anti-rabbit IgG antibody (1:20 000) (Pierce, Rockford, IL). Supersignal West Pico Chemiluminescent Substrate was used for detection (Pierce) and densitometric analysis was performed using Quantity One Software (Bio-Rad).

Measurement of NAT1 mRNA

Total RNA was isolated from cells using the RNeasy kit (Qiagen) followed by removal of contaminating DNA by treatment with TurboDNase Free (Ambion, Austin, TX). Synthesis of cDNA was performed using qScript cDNA Synthesis Kit (Quanta Biosciences, Gaithersburg, MD) using 1 μg of total RNA in a 20 μL reaction per the manufacturer's protocol. Quantitative RT-PCR (RT-qPCR) assays were used to assess the relative amount of *NAT1* mRNA in cells stably transfected with NATa/*NAT1*4* compared to cells stably transfected with NATb/*NAT1*4*. The Step One Plus (Applied Biosystems, Foster City, CA) was used to perform qRT-PCR in reactions containing 1× final concentration of qScript One-Step Fast mix (Quanta Biosciences), 300 nM of each primer and 100 nM of probe in a total volume of 20 μL. For qRT-PCR of *NAT1* mRNA, a TaqMan probe was used with NAT1 Total Splice Forward and NAT1 Total Splice Reverse primers (Table 1) designed using Primer Express 1.5 software (Applied Biosystems). An initial incubation at 50°C was carried out for 2 min and at 94°C for 10 min followed by 40 cycles of 95°C for 15 s and 60°C for 1 min. TaqMan® Ribosomal RNA Control Reagents for quantitation of the endogenous control, 18S rRNA (Applied Biosystems) were used to determine ΔCt (*NAT1* Ct −18S rRNA Ct). ΔΔCt was determined by subtraction of the smallest ΔCt and relative amounts of *NAT1* mRNA were calculated using $2^{-\Delta\Delta Ct}$ as previously described [27].

Measurement of NAT1 mRNA Stability

Dishes (100 × 20 mm^2) containing 8×10^6 stably transfected NATa/*NAT1*4* and NATb/*NAT1*4* cells were treated with complete α-MEM media spiked with 10 μg/mL of the transcription inhibitor, Actinomycin D (Sigma, St. Louis, MO). Cells were collected at 0, 2, 4, 6, and 8-h time points and total RNA was isolated as described above. Relative *NAT1* mRNA levels were determined from cells transfected with NATa/*NAT1*4* or NATb/*NAT1*4* utilizing qRT-PCR assays as described above. The first-order rate decay constant (slope) of *NAT1* mRNA was determined by linear regression.

DNA Isolation and dG-C8-ABP Quantitation

DNA was isolated and dG-C8-ABP adducts were quantitated with modifications to a previously described method [34]. Stably transfected cells grown to approximately 80% confluency in 15 cm dishes were incubated in complete α-MEM media containing 1.56, 3.13, 6.25, 12.5 μM ABP or vehicle alone (0.5% DMSO) at 37°C. The cells were collected following 24 h of treatment, centrifuged for 5 min at 13 000*g*, and the pellet was resuspended in 2 volumes of homogenization buffer (20 mM sodium phosphate pH 7.4, 1 mM EDTA), 0.1 volumes of 10% SDS and 0.1 volume of 20 mg/mL Proteinase K and allowed to incubate overnight at 37°C. The DNA was extracted using phenol/chloroform:isoamyl alcohol and precipitated with isopropanol. The pellet was dried and resuspended in 500 μL of DNA adduct buffer (5 mM Tris pH 7.4, 1 mM $CaCl_2$, 1 mM $ZnCl_2$, and 10 mM $MgCl_2$). The DNA was quantitated by spectrophotometry at A_{260}. Five hundred pg of internal standard (dG-C8-ABP-d5, Toronto Research Chemicals, North York, Ontario, Canada) was added to 30 μg of sample DNA, treated with 10 units *DNase I* (US Biological, Swampscott, MA) for 1 h at 37°C followed by treatment with 10 units nuclease P1 (Sigma) for 6 h. The reactions were then treated with 10 units of alkaline phosphatase (Sigma) overnight at 37°C. The samples were then loaded onto Pep-Clean C-18 Spin Columns (Thermo Fisher Scientific), washed with 10% acetonitrile (ACN), eluted with 50% ACN by centrifugation at 2000*g* and dried. The samples were reconstituted with 25 μL 5% ACN in 2.5 mM NH_4HCO_3 just before analysis and 10 μL of the sample was analyzed by Accela LC System (Thermo Scientific, San Jose, CA) coupled with a LTQ-Orbitrap XL mass spectrometer (Thermo Scientific). Samples were loaded onto a 30 × 1 mm × 1.9 μm^2 Hypersil GOLD column (Thermo Scientific) and eluted with a 12.5-min binary solvent gradient (Solvent A: 5% ACN/0.1% formic acid and Solvent B: 95% ACN/0.1% formic acid) at 50 μL/min. The gradient started from 5%

Solvent B, increased linearly to 75% Solvent B in 10 min, and then remained at 75% B for 2.5 min. The eluates were ionized by electrospray isonization and dG-C8-ABP and dG-C8-ABP-d5 were detected with linear ion trap and detected by multiple reaction monitoring using the transitions of *m*/*z* 435.2 to *m*/*z* 319.2 (dG-C8-ABP) and *m*/*z* 440.2 to *m*/*z* 324.2 (dG-C8-ABP-d5). Concentrations of dG-C8-ABP were calculated from peak areas of dG-C8-ABP and dG-C8-ABP-d5 with a calibration curve from synthetic dG-C8-ABP and dG-C8-ABP-d5.

Measurement of Cytotoxicity and Mutagenesis

Assays for cell cytoxicity and mutagenesis were carried as previously described [37] with slight modifications. Cells were grown in HAT medium (30 mM hypoxanthine, 0.1 mM aminopterin, and 30 mM thymidine) for 12 doublings. Cells (1×10^6) were plated, allowed to grow for 24 h and were then treated with 1.56, 3.13, 6.25, or 12.5 μM ABP (Sigma) or vehicle alone (0.5% DMSO) in media. After 48 h, cells were plated to determine survival and mutagenic response to ABP. To determine cloning efficiency following each dose of ABP, 100 cells were plated in triplicate in 6 well-plates and allowed to grow for 7 d in nonselective media. Colonies were counted and expressed as percent of vehicle control. To determine mutagenic response following ABP exposure, 5×10^5 cells were plated and subcultured for 7 d and then seeded with 1×10^5 cells/100×20 mm dish (10 replicates) in complete αMEM containing 40 μM 6-thioguanine (Sigma). Mutant *hprt* cells were allowed to grow for 7 d and colonies were counted to determine ABP-induced mutants and corrected by cloning efficiency.

Statistical Analysis

Statistical differences were determined using either an unpaired student's *t*-test or one-way ANOVA using Prism Software by Graphpad (La Jolla, CA).

RESULTS

PABA *N*-Acetylation Following Transfection of NATb/*NAT1*4* or NATa/*NAT1*4*

PABA *N*-acetylation activity was 9-fold to 12-fold ($P < 0.05$) higher in CHO cells transfected with NATb/*NAT1*4* than NATa/*NAT1*4* following both transient and stable transfections (Figure 2a and b) utilizing the CMV promoter. Figure 2b shows average PABA *N*-acetylation for three stable clones of each NATb/*NAT1*4* and NATa/*NAT1*4*. One clone representative was selected from each group to conduct all further assays. To ensure that the difference was not promoter specific, *N*-acetylation

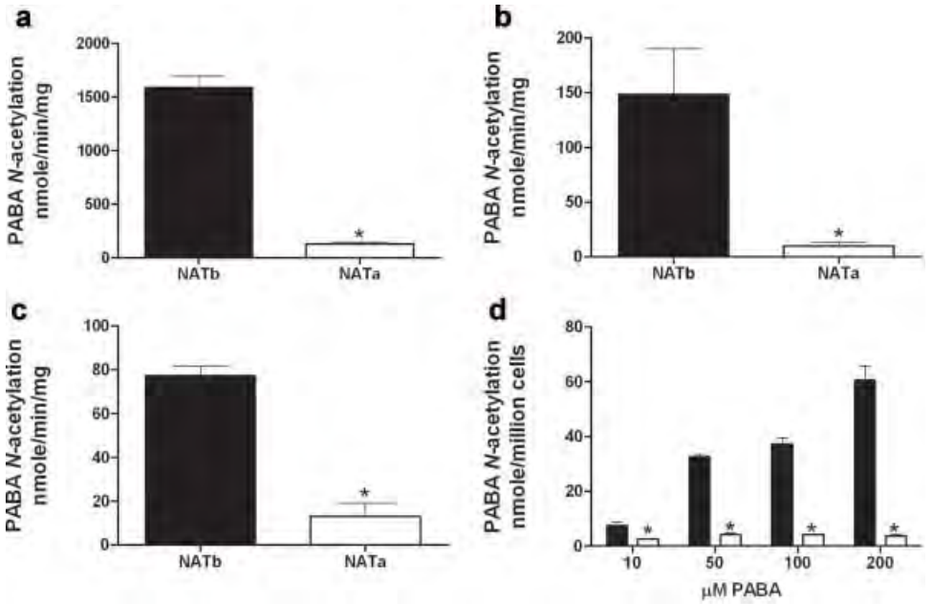

Figure 2. *N*-acetylation of PABA in UV5/1A1 cells expressing *CYP1A1* and NATb/*NAT1*4* (solid bars) or NATa/*NAT1*4* (open bars). (a) PABA *N*-acetylation activity following transient transfection with pcDNA5/FRT; (b) PABA NAT1 catalytic activity following stable transfection with pcDNA5/FRT of three different clones of each NATb/*NAT1*4* and NATa/*NAT1*4*; (c) PABA *N*-acetylation activity following transient transfection with pEF1/V5-His; (d) PABA *N*-acetylation in situ following stable transfection of pcDNA5/FRT. Each bar represents mean ± SEM for three transient transfections (a and c), three separate collections of three clones (b) or three separate collections of 1 clone (d). Asterisks (*) represent a significant difference ($P < 0.05$) (a, b, and d) or ($P < 0.0001$) (c) following a Student's *t*-test.

activity was also measured following transfection with constructs utilizing the EF1α promoter. PABA *N*-acetylation activity was sixfold ($P < 0.0001$) higher in CHO cells transiently transfected with NATb/*NAT1*4* than NATa/*NAT1*4* (Figure 2c) utilizing the EF1α promoter. To more accurately model in vivo *N*-acetylation and to confirm the in vitro results, an in situ assay was performed using PABA as the substrate in a dose response experiment (Figure 2d). The in situ assay showed that significantly ($P < 0.05$) more PABA *N*-acetylation activity was observed in cells stably transfected with NATb/*NAT1*4* than NATa/*NAT1*4* at all concentrations tested (Figure 2d) utilizing the CMV promoter. As shown in Figure 3, PABA *N*-acetylation activity also was significantly higher in COS-1 cells transiently transfected with NATb/*NAT1*4* than with NATa/*NAT1*4* utilizing either the CMV ($P < 0.005$) or EF1α ($P < 0.0001$) promoters.

ABP *N*-Acetylation and *N*-Hydroxy-ABP *O*-Acetylation Following Transfection of NATb/*NAT1*4* or NATa/*NAT1*4*

Cells stably transfected with NATb/*NAT1*4* were found to have sevenfold ($P < 0.0001$) higher ABP *N*-acetylation activity than cells stably transfected with NATa/*NAT1*4* (Figure 4a) utilizing the CMV promoter. *O*-acetyltransferase activity using *N*-OH-ABP as the substrate also was found to be sevenfold ($P < 0.05$) higher in cells stably transfected with NATb/*NAT1*4* than NATa/*NAT1*4* (Figure 4b) utilizing CMV promoter.

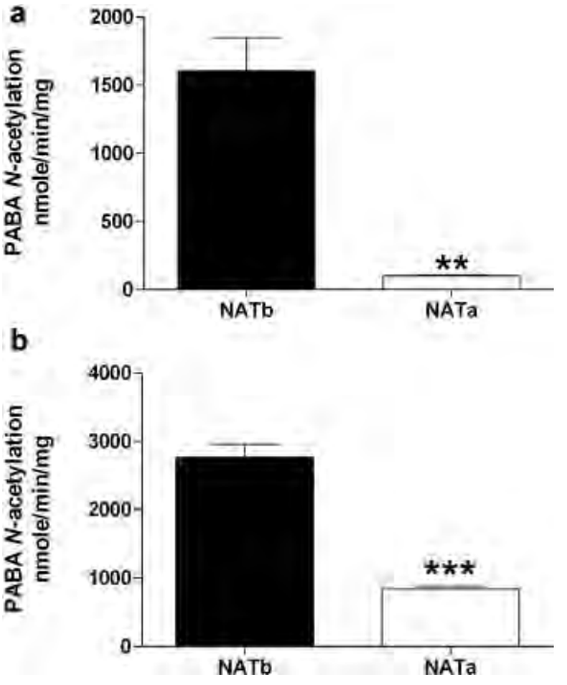

Figure 3. *N*-acetylation of PABA in COS-1 cells transiently transfected with (a) pcDNA5/FRT or (b) pEF1/V5-His containing NATb/*NAT1*4* or NATa/*NAT1*4*. Each bar represents mean ± SEM for three transient transfections. Asterisks (*) represent a significant difference either ($P < .005$) (a) or ($P < .0001$) (b) following a Student's *t*-test.

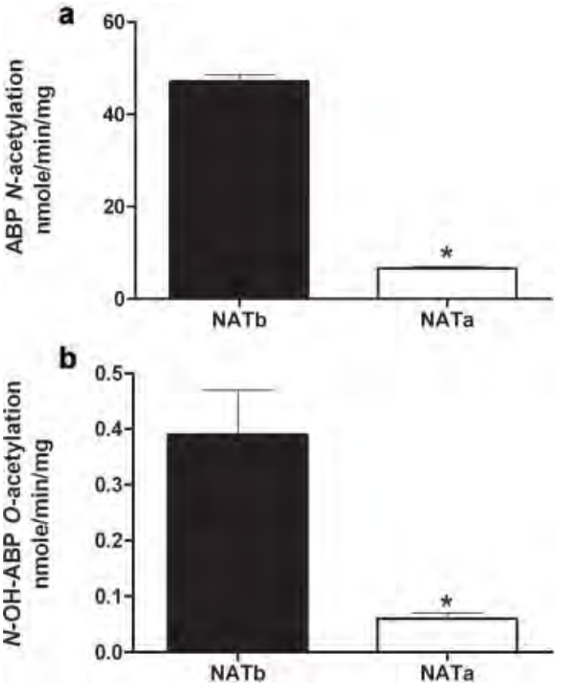

Figure 4. (a) *N*-acetylation of ABP and (b) *O*-acetylation of *N*-hydroxy-ABP in UV5/1A1 cells stably expressing *CYP1A1* and either NATb/*NAT1*4* (solid bars) or NATa/*NAT1*4* (open bars) in pcDNA5/FRT. Each bar represents mean ± SEM for three separate collections. Asterisks (*) represent a significant difference ($P < 0.0001$) (a) or ($P < 0.05$) (b) following a Student's *t*-test.

Expression of NAT1 Protein Following Transfection of NATb/*NAT1*4* or NATa/*NAT1*4*

NAT1 expression was determined by Western blot in cells stably transfected with NATb/*NAT1*4* and NATa/*NAT1*4* utilizing the CMV promoter. Fourfold ($P < 0.05$) more NAT1 was found in cells stably transfected with NATb/*NAT1*4* than cells transfected with NATa/*NAT1*4* following densitometric analysis (Figure 5).

Expression of NAT1 mRNA Following Transfection of NATb/*NAT1*4* or NATa/*NAT1*4*

As shown in Figure 6a, fourfold more NAT1 mRNA was detected in cells stably transfected with NATb/*NAT1*4* than in cells transfected with NATa/*NAT1*4* ($P < 0.05$) utilizing the CMV promoter. To determine the cause of the difference in NAT1 steady-state mRNA between cells stably transfected with NATb/*NAT1*4* and in cells transfected with NATa/*NAT1*4*, an mRNA stability assay was performed in the presence of actinomycin-D. No significant ($P > 0.05$) difference in the

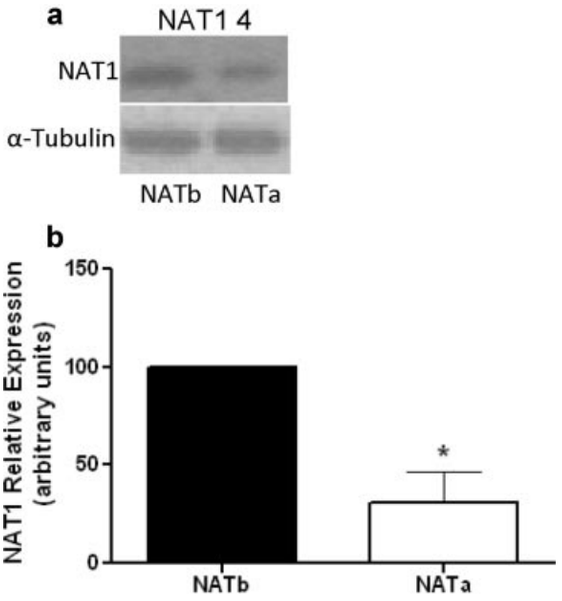

Figure 5. NAT1 protein expression in UV5/1A1 cells stably expressing *CYP1A1* and NATb/*NAT1*4* (solid bars) or NATa/*NAT1*4* (open bars) in pcDNA5/FRT. (a) Representative Western blot of 20 μg of total protein loaded; (b) percent intensity units (NATb defined as 100%) of densitometric analysis performed on three independent Western blots. Asterisks (*) represent a significant difference ($P < 0.05$) following a Student's *t*-test.

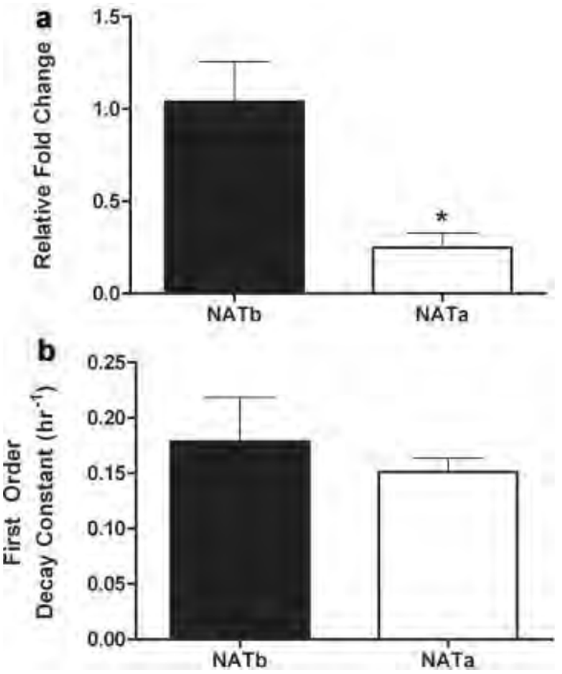

Figure 6. (a) NAT1 mRNA expression levels; (b) mRNA stability in UV5/1A1 cells stably expressing *CYP1A1* and NATb/*NAT1*4* (solid bars) or NATa/*NAT1*4* (open bars) in pcDNA5/FRT. Each bar represents mean ± SEM for (a) three or (b) nine determinations. Asterisks (*) represent a significant difference ($P < 0.05$) following a Student's *t*-test.

NAT1 mRNA first-order decay constant was observed between NAT1 mRNA derived from cells stably transfected with NATb/*NAT1*4* versus NATa/*NAT1*4* (Figure 6b).

Cytoxicity, dG-C8-ABP Adduct, and *hprt* Mutations From ABP in UV5/*1A1* Cells Stably Transfected With NATb/*NAT1*4* or NATa/*NAT1*4*

CYP1A1 mediated hydroxylation and NAT1 *O*-acetylation result in DNA adducts and mutations, if not repaired. Significantly ($P < 0.05$) greater cytoxicity (Figure 7a), dG-C8-ABP adducts (Figure 7b), and *hprt* mutants (Figure 7c) were detected in cells stably transfected with NATb/*NAT1*4* than NATa/*NAT1*4* utilizing the CMV promoter at each ABP concentration tested up to 12.5 μM.

DISCUSSION

As outlined in the Introduction Section, numerous studies report that *NAT1* genetic polymorphisms increase cancer risk following exposure to heterocyclic and aromatic amines. Due to the large variability in NAT1 activity that has been reported within a single genotype, it is becoming increasingly more apparent that factors other than genetic polymorphisms are affecting gene expression and cancer risk. One such factor is the use of alternative promoters to produce mRNAs with distinct 5′-UTRs. Recent studies have shown that between 30% and 50% of all human genes utilize alternative promoters [31,32] to allow for cell, tissue, and disease specific expression. *NAT1* has two promoters, NATa and NATb, which differ in promoter strength and tissue specificity [27,38]. Transcripts derived from NATa are found primarily in liver, lung, trachea, and kidney, while transcripts derived from NATb are found in all tissues studied to date [27,38]. It is possible that NATa transcripts are expressed in a wider range of tissues, but only when the cell is under specific environmental stress or disease states. For example, expression of NATa transcripts has recently been reported in several ER-positive breast cancer cell lines [39]. NATa transcripts may be selectively upregulated following certain environmental exposures or in specific tissues, such as breast, during certain disease states.

In the current study, two referent *NAT1*4* constructs were cloned to mimic the most common transcripts originating from each of the two alternative *NAT1* promoters, NATa and NATb (Figure 1a). Beginning with frequently used transcription start sites, the constructs include all exons found in the most common *NAT1* transcripts originating at the NATa or NATb promoters and represent Type Ia or Type IIa transcripts [26,27,40]. The NATa/*NAT1*4* and NATb/*NAT1*4* constructs have identical ORFs and 3′-UTRs. Both

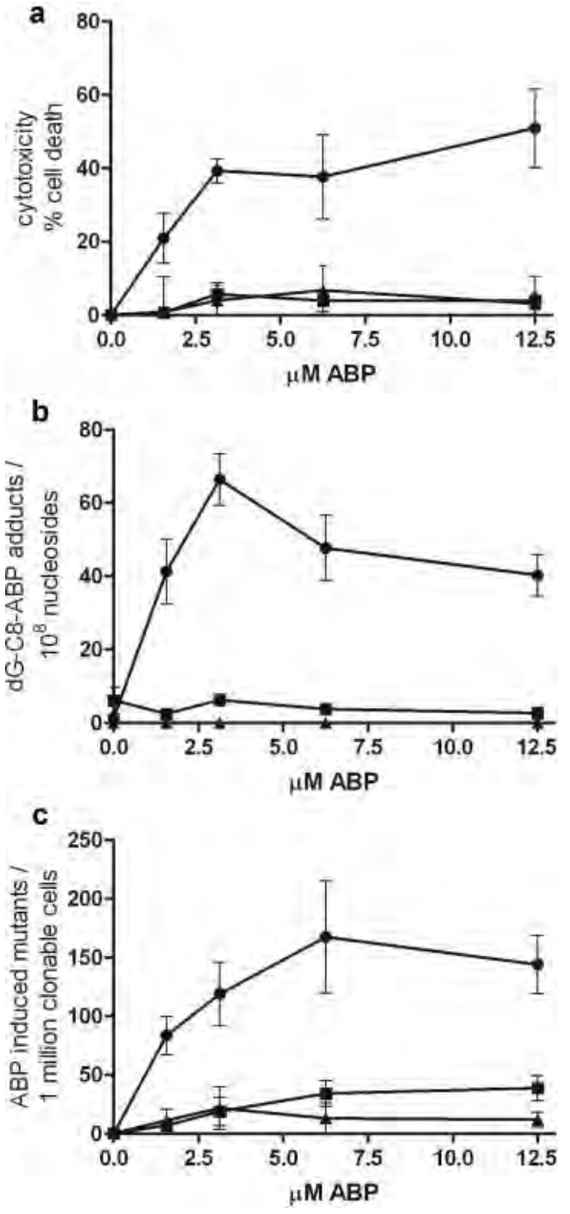

Figure 7. ABP-induced cytotoxicity, mutagenesis, and DNA adduct formation in CHO cells stably expressing *CYP1A1* only (triangles) and NATb/*NAT1*4* (circles) or NATa/*NAT1*4* (squares) in pcDNA5/FRT. Each data point represents mean ± SEM for three determinations. (a) ABP-induced cytotoxicity; (b) ABP-induced dG-C8-ABP adducts/10^8 nucleosides; (c) ABP-induced *hprt* mutant levels.

constructs include the entire ORF comprised of 870 nucleotides and 888 nucleotides of the 3′-UTR. The only difference between the two constructs is the 5′-UTR. The NATb 5′-UTR contains 117 nts and includes exon 4 and exon 8 while the NATa 5′-UTR contains 371 nts and includes exons 1, 2, 3, and 8 (Figure 1b and c).

Two constitutive promoters, the CMV and the EF1α promoter, were used to drive transcription of either the NATb/*NAT1*4* or NATa/*NAT1*4* full-length transcripts to examine regulatory control located in the 5′-UTRs. In this study, we report that cells transfected with NATb/*NAT1*4* had approximately four times greater NAT1 expression than cells transfected with NATa/*NAT1*4*. A four-fold difference in NAT1 mRNA expression also was observed, suggesting that transcriptional control is largely responsible for the functional differences observed between NATb/*NAT1*4* and NATa/*NAT1*4*. Recent studies have elucidated a large number of tissue- and cell-type specific isoforms of transcription factors and *cis*-acting factors. Alternative 5′-UTRs contribute to this intricate control of transcription allowing for very specific altered expression in tissues, cells, and even disease states [41]. The differences we observed were not caused by a specific interaction between the promoter and one of the 5′-UTRs because results were confirmed using two different constitutive promoters, CMV and EF1α.

There are many regulatory mechanisms that could be responsible for the observed differences in expression and functional effects including polymerase pausing, microRNA binding, and the presence of upstream ORFs and stem loops. A recent genome wide study has provided evidence that many genes are controlled after transcription initiation has occurred [29]. Polymerase pausing may be a widespread genetic control of gene expression [42,43]. Elongation of transcription is known to be nonuniform and RNA polymerases are prone to transient pausing that is sequence dependent [44,45]. Polymerase pausing could be examined in the NATa- and NATb-transfected cell lines by nuclear run-on or RIP-chip assays. A second possible mechanism of regulation is microRNA (miRNA) binding which regulates gene expression by catalyzing mRNA cleavage [45–47]. MicroInspector (miRNA target software) predicted only two miRNA binding sites in the NATb 5′-UTR located at positions 7 (has-miR-3937) and 46 (has-miR-198) while 54 miRNA binding sites were predicted throughout the NATa 5′-UTR. Regulation by these miRNAs could be analyzed by such methods as northern hybridization or microarray analysis. A third possible mechanism is regulation by upstream open reading frames (uORFs) which have been shown to reduce protein and mRNA expression [48]. Both NATa and NATb 5′-UTRs were examined for uORFs by the NCBI ORF Finder. The NATa 5′-UTR was predicted to have two uORFs, while the NATb 5′-UTR was predicted to have none. Studies including a luciferase reporter assay could be conducted to determine the transcriptional effects on the NATa 5′-UTR due to uORFs. Lastly, differential regulation of the NATa

and NATb 5′-UTRs could be due to the presence of stem loops [49]. NATa and NATb 5′-UTRs were both examined for the presence of stem loops by OligoCalc (Northwestern University, Evanston, IL) with a constraint of 5 base pair minimum. The NATa 5′-UTR has 42 potential stem-loop structures while the NATb 5′-UTR has only 7 potential stem-loop structures. Real time observation of transcription initiation and elongation [50] could be useful to determine the mechanism of the differential regulation observed between NATa and NATb 5′-UTRs.

Significantly more NAT1 activity, protein, mRNA, ABP-induced cytoxicity, DNA adducts and mutagenesis were detected in cells stably transfected with NATb/*NAT1*4* than in cells transfected with NATa/*NAT1*4* ($P < 0.05$). DNA adduct and mutant levels following exposure to ABP are biological endpoints that are very relevant to cancer risk. The findings that ABP-mediated DNA adduct and mutant levels were significantly higher in cells transfected with elevated NAT1 catalytic activity emphasizes the relative importance of NAT1-catalyzed *O*-acetylation of *N*-hydroxy-ABP in cancer risk. Associations between higher *N*-acetyltransferase 2 catalytic activity with higher ABP-mediated cytoxicity, DNA adduct formation, and mutagenesis also were recently reported [51]. The finding that these cancer risk indicators were higher in cells transfected with NATb/*NAT1*4* than cells transfected with NATa/*NAT1*4* suggest that differential regulation in the *NAT1* 5′-UTR also may modify ABP-mediated cancer risk. Because NATb transcripts are expressed ubiquitously, the minor transcript, NATa, may be expressed following environmental exposures or under certain disease states resulting in increased mutagenesis, enhanced tumor growth, and decreased chemotherapeutic sensitivity. For example, expression of NATa transcripts have recently been reported in several ER-positive breast cancer cell lines [39].

The findings of this study are significant due to their relevance to ABP-mediated carcinogenesis. However, translation of our results obtained in cell culture to human subjects will require additional studies to investigate tissue specificity. Although our study focused only on the referent allele, *NAT1*4*, future studies should investigate 5′-UTR control with other *NAT1* alleles, particularly those associated with increased cancer risk. Future investigations to determine mechanism(s) and location(s) of the differential regulation in the NAT1 5′-UTR also are needed.

ACKNOWLEDGMENTS

Portions of this work constitute partial fulfillment for the PhD in pharmacology and toxicology at the University of Louisville to Lori Millner. This work was supported by grants (R01-CA034627) from the National Cancer Institute (T32-ES011564 and P30-ES014443) from the National Institute for Environmental Health Sciences and (BC083107) from the Department of Defense Breast Cancer Research Program.

REFERENCES

1. International Agency for Research on Cancer. Overall evaluation of carcinogenicity: An update of IARC monographs, Supplement 7, Vols. 1–42. Monographs on the evaluation of carcinogenic risk to humans; 1987.
2. Hein DW, Doll MA, Rustan TD, et al. Metabolic activation and deactivation of arylamine carcinogens by recombinant human NAT1 and polymorphic NAT2 acetyltransferases. Carcinogenesis 1993;14:1633–1638.
3. Wakefield L, Cornish V, Long H, Griffiths WJ, Sim E. Deletion of a xenobiotic metabolizing gene in mice affects folate metabolism. Biochem Biophys Res Commun 2007; 364:556–560.
4. Jensen LE, Hoess K, Whitehead AS, Mitchell LE. The NAT1 C1095A polymorphism, maternal multivitamin use and smoking, and the risk of spina bifida. Birth Defects Res A Clin Mol Teratol 2005;73:512–516.
5. Lammer EJ, Shaw GM, Iovannisci DM, Van Waes J, Finnell RH. Maternal smoking and the risk of orofacial clefts: Susceptibility with NAT1 and NAT2 polymorphisms. Epidemiology 2004;15:150–156.
6. Carmichael SL, Shaw GM, Yang W, Iovannisci DM, Lammer E. Risk of limb deficiency defects associated with NAT1, NAT2, GSTT1, GSTM1, and NOS3 genetic variants, maternal smoking, and vitamin supplement intake. Am J Med Genet A 2006;140:1915–1922.
7. Jensen LE, Hoess K, Mitchell LE, Whitehead AS. Loss of function polymorphisms in NAT1 protect against spina bifida. Hum Genet 2006;120:52–57.
8. Millikan RC, Pittman GS, Newman B, et al. Cigarette smoking, N-acetyltransferases 1 and 2, and breast cancer risk. Cancer Epidemiol Biomarkers Prev 1998;7:371–378.
9. Zheng W, Deitz AC, Campbell DR, et al. N-acetyltransferase 1 genetic polymorphism, cigarette smoking, well-done meat intake, and breast cancer risk. Cancer Epidemiol Biomarkers Prev 1999;8:233–239.
10. Li D, Jiao L, Li Y, et al. Polymorphisms of cytochrome P4501A2 and N-acetyltransferase genes, smoking, and risk of pancreatic cancer. Carcinogenesis 2006;27:103–111.
11. Suzuki H, Morris JS, Li Y, et al. Interaction of the cytochrome P4501A2, SULT1A1 and NAT gene polymorphisms with smoking and dietary mutagen intake in modification of the risk of pancreatic cancer. Carcinogenesis 2008;29:1184–1191.
12. Sanderson S, Salanti G, Higgins J. Joint effects of the N-acetyltransferase 1 and 2 (NAT1 and NAT2) genes and smoking on bladder carcinogenesis: A literature-based systematic HuGE review and evidence synthesis. Am J Epidemiol 2007;166:741–751.
13. Gago-Dominguez M, Bell DA, Watson MA, et al. Permanent hair dyes and bladder cancer: Risk modification by cytochrome P4501A2 and N-acetyltransferases 1 and 2. Carcinogenesis 2003;24:483–489.
14. Shin A, Shrubsole MJ, Rice JM, et al. Meat intake, heterocyclic amine exposure, and metabolizing enzyme polymorphisms in relation to colorectal polyp risk. Cancer Epidemiol Biomarkers Prev 2008;17:320–329.
15. Bell DA, Stephens EA, Castranio T, et al. Polyadenylation polymorphism in the acetyltransferase 1 gene (NAT1) increases risk of colorectal cancer. Cancer Res 1995;55: 3537–3542.

16. Morton LM, Schenk M, Hein DW, et al. Genetic variation in N-acetyltransferase 1 (NAT1) and 2 (NAT2) and risk of non-Hodgkin lymphoma. Pharmacogenet Genomics 2006;16:537–545.
17. Kilfoy BA, Zheng T, Lan Q, et al. Genetic variation in N-acetyltransferases 1 and 2, cigarette smoking, and risk of non-Hodgkin lymphoma. Cancer Causes Control 2010;21: 127–133.
18. Adam PJ, Berry J, Loader JA, et al. Arylamine N-acetyltransferase-1 is highly expressed in breast cancers and conveys enhanced growth and resistance to etoposide in vitro. Mol Cancer Res 2003;1:826–835.
19. Ring BZ, Seitz RS, Beck R, et al. Novel prognostic immunohistochemical biomarker panel for estrogen receptor-positive breast cancer. J Clin Oncol 2006;24:3039–3047.
20. McGrath M, Michaud D, De Vivo I. Polymorphisms in GSTT1, GSTM1, NAT1 and NAT2 genes and bladder cancer risk in men and women. BMC Cancer 2006;6:239.
21. Wideroff L, Vaughan TL, Farin FM, et al. GST, NAT1, CYP1A1 polymorphisms and risk of esophageal and gastric adenocarcinomas. Cancer Detect Prev 2007;31: 233–236.
22. Kidd LR, Hein DW, Woodson K, et al. Lack of association of the N-acetyltransferase NAT1*10 allele with prostate cancer incidence, grade, or stage among smokers in Finland. Biochem Genet 2011;49:73–82.
23. Tiang JM, Butcher NJ, Cullinane C, Humbert PO, Minchin RF. RNAi-mediated knock-down of arylamine N-acetyltransferase-1 expression induces e-cadherin up-regulation and cell-cell contact growth inhibition. PLoS ONE 2011;6: e17031.
24. Vatsis KP, Weber WW. Structural heterogeneity of Caucasian N-acetyltransferase at the NAT1 gene locus. Arch Biochem Biophys 1993;301:71–76.
25. Boukouvala S, Sim E. Structural analysis of the genes for human arylamine N-acetyltransferases and characterisation of alternative transcripts. Basic Clin Pharmacol Toxicol 2005;96:343–351.
26. Husain A, Barker DF, States JC, Doll MA, Hein DW. Identification of the major promoter and non-coding exons of the human arylamine N-acetyltransferase 1 gene (NAT1). Pharmacogenetics 2004;14:397–406.
27. Barker DF, Husain A, Neale JR, et al. Functional properties of an alternative, tissue-specific promoter for human arylamine N-acetyltransferase 1. Pharmacogenet Genomics 2006;16:515–525.
28. Minchin RF, Hanna PE, Dupret JM, Wagner CR, Rodrigues-Lima F, Butcher NJ. Arylamine N-acetyltransferase I. Int J Biochem Cell Biol 2007;39:1999–2005.
29. Nechaev S, Fargo DC, dos Santos G, Liu L, Gao Y, Adelman K. Global analysis of short RNAs reveals widespread promoter-proximal stalling and arrest of Pol II in Drosophila. Science 2010;327:335–338.
30. Aida M, Chen Y, Nakajima K, Yamaguchi Y, Wada T, Handa H. Transcriptional pausing caused by NELF plays a dual role in regulating immediate-early expression of the junB gene. Mol Cell Biol 2006;26:6094–6104.
31. Takeda J, Suzuki Y, Nakao M, et al. H-DBAS: Alternative splicing database of completely sequenced and manually annotated full-length cDNAs based on H-Invitational. Nucleic Acids Res 2007;35:D104–D109.
32. Cooper SJ, Trinklein ND, Anton ED, Nguyen L, Myers RM. Comprehensive analysis of transcriptional promoter structure and function in 1% of the human genome. Genome Res 2006;16:1–10.
33. Horton RM, Hunt HD, Ho SN, Pullen JK, Pease LR. Engineering hybrid genes without the use of restriction enzymes: Gene splicing by overlap extension. Gene 1989;77:61–68.
34. Metry KJ, Zhao S, Neale JR, et al. 2-Amino-1-methyl-6-phenylimidazo [4,5-b] pyridine-induced DNA adducts and genotoxicity in chinese hamster ovary (CHO) cells expressing human CYP1A2 and rapid or slow acetylator N-acetyltransferase 2. Mol Carcinog 2007;46:553–563.
35. Hein DW, Doll MA, Nerland DE, Fretland AJ. Tissue distribution of N-acetyltransferase 1 and 2 catalyzing the N-acetylation of 4-aminobiphenyl and O-acetylation of N-hydroxy-4-aminobiphenyl in the congenic rapid and slow acetylator Syrian hamster. Mol Carcinog 2006;45: 230–238.
36. Stanley LA, Coroneos E, Cuff R, Hickman D, Ward A, Sim E. Immunochemical detection of arylamine N-acetyltransferase in normal and neoplastic bladder. J Histochem Cytochem 1996;44:1059–1067.
37. Wu RW, Tucker JD, Sorensen KJ, Thompson LH, Felton JS. Differential effect of acetyltransferase expression on the genotoxicity of heterocyclic amines in CHO cells. Mutat Res 1997;390:93–103.
38. Husain A, Zhang X, Doll MA, States JC, Barker DF, Hein DW. Functional analysis of the human N-acetyltransferase 1 major promoter: Quantitation of tissue expression and identification of critical sequence elements. Drug Metab Dispos 2007;35:1649–1656.
39. Wakefield L, Robinson J, Long H, et al. Arylamine N-acetyltransferase 1 expression in breast cancer cell lines: A potential marker in estrogen receptor-positive tumors. Genes Chromosomes Cancer 2008;47:118–126.
40. Butcher NJ, Arulpragasam A, Goh HL, Davey T, Minchin RF. Genomic organization of human arylamine N-acetyltransferase Type I reveals alternative promoters that generate different 5′-UTR splice variants with altered translational activities. Biochem J 2005;387:119–127.
41. Davuluri RV, Suzuki Y, Sugano S, Plass C, Huang TH. The functional consequences of alternative promoter use in mammalian genomes. Trends Genet 2008;24:167–177.
42. Core LJ, Waterfall JJ, Lis JT. Nascent RNA sequencing reveals widespread pausing and divergent initiation at human promoters. Science 2008;322:1845–1848.
43. Adelman K, La Porta A, Santangelo TJ, Lis JT, Roberts JW, Wang MD. Single molecule analysis of RNA polymerase elongation reveals uniform kinetic behavior. Proc Natl Acad Sci USA 2002;99:13538–13543.
44. Herbert KM, La Porta A, Wong BJ, et al. Sequence-resolved detection of pausing by single RNA polymerase molecules. Cell 2006;125:1083–1094.
45. Ambros V. The functions of animal microRNAs. Nature 2004;431:350–355.
46. Doench JG, Sharp PA. Specificity of microRNA target selection in translational repression. Genes Dev 2004;18: 504–511.
47. Zhang H, Kolb FA, Jaskiewicz L, Westhof E, Filipowicz W. Single processing center models for human Dicer and bacterial RNase III. Cell 2004;118:57–68.
48. Calvo SE, Pagliarini DJ, Mootha VK. Upstream open reading frames cause widespread reduction of protein expression and are polymorphic among humans. Proc Natl Acad Sci USA 2009;106:7507–7512.
49. Malys N, McCarthy JE. Translation initiation: Variations in the mechanism can be anticipated. Cell Mol Life Sci 2011; 68:991–1003.
50. Larson DR, Zenklusen D, Wu B, Chao JA, Singer RH. Real-time observation of transcription initiation and elongation on an endogenous yeast gene. Science 2011;332:475–478.
51. Bendaly J, Doll MA, Millner LM, et al. Differences between human slow N-acetyltransferase 2 alleles in levels of 4-aminobiphenyl-induced DNA adducts and mutations. Mutat Res 2009;671:13–19.

DMD Fast Forward. Published on October 18, 2011 as doi:10.1124/dmd.111.041855

Appendix 2

Phenotype of the Most Common "Slow Acetylator" Arylamine N-Acetyltransferase 1 Genetic Variant (*NAT1*14B)* is Substrate-Dependent

Lori M. Millner, Mark A. Doll, Jian Cai, J. Christopher States, and David W. Hein

Department of Pharmacology and Toxicology, James Graham Brown Cancer Center and Center for Environmental Genomics and Integrative Biology, University of Louisville, Louisville, Kentucky

Running Title Page

Running Title: *NAT1*14B* phenotype is substrate-dependent

Corresponding author: David W. Hein, Clinical and Translational Research – Room 303, University of Louisville Health Sciences Center, 505 South Hancock Street, Louisville, KY 40202-1617. Email: d.hein@louisville.edu; Tel: 502-852-6252; Fax: 502-852-7868

Number of text pages: 29

Number of Tables: 3

Number of Figures: 4

Number of words in Abstract: 178

Introduction: 712

Discussion: 1311

References: 40

Abbreviations: PABA, p-aminobenzoic acid; ABP, 4-aminobiphenyl; PCR, polymerase chain reaction; NAT1, N-acetyltransferase 1; NAT2, N-acetyltransferase 2; HPLC, high performance liquid chromatography; SNP, single nucleotide polymorphism; N-OH-ABP, N-hydroxy-4-aminobiphenyl; ORF, open reading frame; AcCoA, acetyl coenzyme A; CHO, Chinese hamster ovary; FRT, Flp Recombination Target; α-MEM, alpha-modified minimal essential medium; ACN, acetonitrile; dG, deoxyguanosine;

Abstract:

Human arylamine *N*-acetyltransferase 1 (NAT1) is a phase II cytosolic enzyme responsible for the activation or deactivation of many arylamine compounds including pharmaceuticals and environmental carcinogens. *NAT1* is highly polymorphic and has been associated with altered risk toward many cancers. *NAT1*14B* is characterized by a single nucleotide polymorphism in the coding region (rs4986782; 560G>A; R187Q). *NAT1*14B* is associated with higher frequency of smoking-induced lung cancer and is the most common "slow acetylator" arylamine N-acetyltransferase 1 genetic variant. Previous studies have reported decreased *N*- and *O*-acetylation capacity, and increased proteasomal degradation of NAT1 14B when compared to the referent, NAT1 4. The current study is the first to investigate *NAT1*14B* expression using constructs that completely mimic NAT1 mRNA by including the 5'- and 3'-UTRs together with the open reading frame of the referent, *NAT1*4,* or variant, *NAT1*14B*. Our results show that NAT1 14B is not simply associated with "slow acetylation". NAT1 14B-catalyzed acetylation phenotype is substrate dependent, and NAT1 14B exhibits higher *N*- and *O*-acetylation catalytic efficiency as well as DNA adducts following exposure to the human carcinogen, 4-aminobiphenyl.

Introduction

Human arylamine *N*-acetyltransferase 1 (NAT1) is a phase II cytosolic enzyme responsible for the biotransformation of many arylamine compounds including pharmaceuticals and environmental carcinogens (Hein et al., 2000). NAT1 catalyzes both arylamine *N*-acetylation and hydroxyarylamine *O*-acetylation. Genetic polymorphisms in NAT1 can alter the amount of NAT1 protein and result in modified enzymatic activity. In addition to bioactivation of arylamines, recent studies have provided evidence that NAT1 is involved in density dependent cell growth and survival. Studies have shown that overexpression of NAT1 increased density dependent cell proliferation, whereas knock-down of NAT1 resulted in marked change in cell morphology, an increase in cell-cell contact inhibition and a loss of cell viability at confluence (Adam et al., 2003; Tiang et al., 2011).

Molecular epidemiological studies have reported associations between NAT1 genetic polymorphisms and altered risk for developing several types of cancer including urinary bladder (Gago-Dominguez et al., 2003), breast (Ambrosone et al., 2007; Millikan et al., 1998; Zheng et al., 1999), colorectal (Bell et al., 1995; Lilla et al., 2006), lung (Wikman et al., 2001), non-Hodgkin lymphoma (Morton et al., 2006) and pancreatic (Li et al., 2006). The only known endogenous NAT1 substrate is p-aminobenzoylglutamate, a catabolite of folate (Wakefield et al., 2007). *NAT1* has been associated with various birth defects (Jensen et al., 2005; Lammer et al., 2004) that may be related to deficiencies in folate metabolism. The most common NAT1 variant allele associated with reduced acetylator phenotype is *NAT1*14B.* The allelic frequency for *NAT1*14B* in the Lebanese population was determined to be 23.8% (Dhaini and Levy, 2000), while American, German, French, and Canadian *NAT1*14B* allelic frequencies are less than 5% (Doll and Hein, 2002) *NAT1*14B* is likely to be very prevalent in other countries in the middle east, however allelic frequencies for many of those populations are not available.

*NAT1*14B* has been associated with an increased risk of smoking-induced lung cancer (Bouchardy et al., 1998).

*NAT1*14B* is characterized by a single nucleotide polymorphism (SNP) G560A (rs4986782) located in the open reading frame (ORF). G560A results in an amino acid substitution R187Q. Computational homology modeling based on the NAT1 crystal structure indicate that the side chain of R187 is partially exposed to the domain II beta barrel, the protein surface, and the active site pocket (Walraven et al., 2008). Interactions with these domains serve to stabilize the protein and help shape the active site pocket. The substitution of arginine for glutamine results in at least partial loss of these stabilizing hydrogen bonds resulting in destabilization of the NAT1 structure. Therefore, homology modeling predicts that NAT1 binding of acetyl coenzyme A (AcCoA), active site acetylation, substrate specificity and catalytic activity could be affected by the R187Q substitution (Walraven et al., 2008).

Previous studies have reported *NAT1*14B* to be associated with a reduced *N*-acetylation phenotype. For example, in peripheral blood mononuclear cells, NAT1 14B was reported to result in reduced *N*-acetyltransferase activities and protein levels (Hughes et al., 1998). Recombinant NAT1 14B expression in yeast demonstrated reduced *N*- and *O*-acetylation, protein levels and increased proteasomal degradation (Butcher et al., 2004; Fretland et al., 2001; 2002). NAT1 14 expressed in mammalian cells also resulted in decreased V_{max} but increased substrate K_m towards p-aminobenzoic acid (PABA) (Zhu and Hein, 2008).

Modifications in NAT1 protein activity are biologically relevant because formation of DNA adducts, tumor growth and drug resistance could be altered by differences in enzymatic activity. This study reports findings in constructs that completely mimic NAT1 mRNA by including the 5'-UTR transcribed by the major promoter (NATb) and 3'-UTRs and ORF of the referent, *NAT1*4,* and of the most common allele associated with reduced acetylation, *NAT1*14B*. This report describes NAT1 14B *N*-acetylation of the urinary bladder carcinogen 4-aminobiphenyl (ABP) and *O*-acetylation of *N*-OH-ABP. Initial pilot experiments were conducted following recombinant

expression in yeast (*Schizosaccaromyces pombe*) followed by more detailed studies utilizing recombinant expression in Chinese hamster ovary (CHO) cells. ABP is present in both mainstream (up to 23 ng per cigarette) and sidestream (up to 140 ng per cigarette) smoke (Hoffmann et al., 1997). Although strict federal regulations have banned industrial uses of ABP (IARC, 1987), ABP can still be found as a contaminant in color additives, paints, food colors, leather, textile dyes, diesel-exhaust particles, cooking oil fumes and commercial hair dyes (Nauwelaers et al., 2011).

Methods

Experiments in Yeast

***In situ N*-Acetylation Following Recombinant Expression of Human NAT1 in Yeast.** The ORFs of *NAT1*14B* and *NAT1*4* were recombinantly expressed in the pESP-3 yeast (*Schizosaccaromyces pombe*) expression system (Stratagene, La Jolla, CA). They were cultured in YES media (Teknova, Hollister, CA, 0.5% yeast extract, 3.0% glucose, 0.0225% adenine, 0.0225% histidine, 0.0225% leucine, 0.0225% uracil, and 0.0225% lysine). To ensure the amount of cells expressing *NAT1*4* and *NAT1*14B* was the same, cell cultures were both grown to an optical density (OD) of 0.40. Cell numbers were calculated based on OD, using the conversion of 1.0 OD (600 nm) corresponds to 2 x 10^7 cells (Stratagene). Aliquots (10 mL) from both the *NAT1*4* and *NAT1*14B* expressing cultures were each treated with ABP to make total volume concentrations of 10, 50 and 100 µM ABP. Samples (100 µl) were collected following 30 minute incubation with ABP. *N*-acetyl-ABP was separated and quantified by high performance liquid chromatography (HPLC) as described previously (Hein et al., 2006).

Experiments in CHO Cells

Polyadenylation Site Removal. The bovine growth hormone polyadenylation site from the pcDNA5/FRT (Invitrogen, Carlsbad, CA) vector was removed to allow the endogenous *NAT1* polyadenylation sites to be active. This was accomplished by digestion of pcDNA5/FRT at 37^{o}C with restriction endonucleases, ApaI and SphI (New England Biolabs, Ipswich, MA), followed by overhang digestion with T4 DNA polymerase (New England Biolabs) and ligation with T4 Ligase (New England Biolabs).

Preparation of NATb/*NAT1*4* Construct. NATb/*NAT1*4* construct was created utilizing gene splicing via overlap extension (Horton et al., 1989) by amplifying the 5'-UTR and the coding region/3'-UTR separately and then fusing the two regions together. Beginning with a

frequently used transcription start site of the NATb promoter, the 5'-UTR (Barker et al., 2006; Husain et al., 2004) was amplified from cDNA prepared from RNA isolated from homozygous *NAT1*4* HepG2 cells. All primer sequences used are shown in Table 1. The primers used to amplify the NATb 5'-UTR region were Lkm40P1 and NAT1 (3') ORF Rev. The coding region and 3'-UTR were amplified as one piece from *NAT1*4* human genomic DNA with *NAT1*4/NAT1*4* genotype. The forward primer used to amplify the coding region/3'-UTR was NAT1 (3') ORF Forward while the reverse primer was pcDNA5distal Reverse. The two sections, the 5'-UTR and the coding region/3'UTR, were fused together via overlap extension and amplification of the entire product using nested primers. The forward nested primer was P1 Fwd Inr NheI and the reverse nested primer was NAT1 Kpn Rev. The forward nested primer included the KpnI endonuclease restriction site and the reverse nested primer contained the NheI endonuclease restriction site to facilitate cloning. The pcDNA5/FRT vector and NATb/*NAT1*4* allelic segments were digested at 37^0C with restriction endonucleases KpnI and NheI (New England Biolabs). The NATb/*NAT1*4* construct was then ligated into pcDNA5/FRT using T4 ligase (New England Biolabs).

Preparation of NATb/*NAT1*14B.* To construct the NATb/*NAT1*14B* pcDNA5/FRT plasmid, the NATb/*NAT1*4* pcDNA5/FRT and a previously constucted *NAT1*14B* allelic construct expressed in a yeast vector, pESP-3 (Stratagene, La Jolla, CA) (Fretland et al., 2001), were both incubated at 37^oC with restriction enzymes, SbfI and AflII (New England Biolabs). Following restriction digestion, the NATb/*NAT1*4* pcDNA5/FRT and the 476 bp segment of *NAT1*14B* (including G560A) were gel purified and ligated utilizing T4 ligase (New England Biolabs). All constructs were sequenced to ensure integrity of allelic segments and junction sites. These constructs that contain NATb 5'-UTR, coding region of *NAT1*4* or *NAT1*14B*, and 3'-UTR are illustrated in Figure 1 and referred to as *NAT1*4* and *NAT1*14B* throughout this manuscript.

Cell Culture. UV5-CHO cells, a nuclease excision repair-deficient derivative of AA8 which are hypersensitive to bulky DNA lesions, were obtained from the ATCC (catalog number: CRL-1865). Unless otherwise noted, cells were incubated at 37^{o}C in 5% CO_2 in complete alpha-modified minimal essential medium (α-MEM, Lonza, Walkersville, MD) without L-glutamine, ribosides, and deoxyribosides supplemented with 10% fetal bovine serum (Hyclone, Logan, UT), 100 units/mL penicillin (Lonza), 100 µg/mL streptomycin (Lonza), and 2 mM L-glutamine (Lonza). The UV5/CHO cells used in this study were previously stably transfected with a single Flp Recombination Target (FRT) integration site (Bendaly et al., 2007). The FRT site allowed stable transfections to utilize the Flp-In System (Invitrogen). When co-transfected with pOG44 (Invitrogen), a Flp recombinase expression plasmid, a site-specific, conserved recombination event of pcDNA5/FRT (containing either NATa/*NAT1*4* or NATb/*NAT1*4)* occurs at the FRT site. The FRT site allows recombination to occur immediately downstream of the hygromycin resistance gene, allowing for hygromycin selectivity only after Flp-recombinase mediated integration. The UV5/FRT cells were further modified by stable integration of human *CYP1A1* and NADPH-cytochrome P450 reductase gene (Bendaly et al., 2007). They are referred to in this manuscript as UV5/*1A1* cells.

Stable Transfections. Stable transfections were carried out using the Flp-In System (Invitrogen) into UV5/*1A1* cells that were previously stably transfected with a FRT site (as noted above). The pcDNA5/FRT plasmids containing human NATb/*NAT1*4* or NATb/*NAT1*14B* were co-transfected with pOG44 (Invitrogen), a Flp recombinase expression plasmid. UV5/*1A1* cells were stably transfected with pcDNA5/FRT containing NATb/*NAT1*4* and NATb/*NAT1*14B* constructs using Effectene transfection reagent (Qiagen, Valencia, CA) following the manufacturer's recommendations. Since the pcDNA5/FRT vector contains a hygromycin resistance cassette, cells were passaged in complete α-MEM containing 600 µg/mL hygromycin

(Invitrogen) to select for cells containing the pcDNA5/FRT plasmid. Hygromycin resistant colonies were selected approximately 10 days after transfection and isolated with cloning cylinders.

Determination of *in vitro* (in-solution Biochemistry) Kinetic Parameters of *N*-Acetylation for NAT1 4 and NAT1 14B. Cells were collected by washing with 1xphosphate buffered saline (PBS) followed by adding 1 mL of of 0.25% Trypsin-EDTA and allowed to incubate for 5 min (Invitrogen). Cells were then collected and centrifuged at 3,000 Xg and washed with 1xPBS. Lysate was prepared by centrifuging the cells and resuspending pellet in homogenization buffer (20 mM $NaPO_4$ pH 7.4, 1 mM EDTA, 1 mM DTT, 0.1 mM PMSF, 2 µg/mL aprotinin and 2 mM pepstatin A). The resuspended cell pellet was subjected to 3 rounds of freezing at -80^{o}C and thawing at 37^{o}C and then centrifuged at 15,000xg for 10 min. *In vitro* assays using PABA or ABP were conducted and acetylated products were separated utilizing HPLC as previously described (Hein et al., 2006). Preliminary studies optimized reactions with respect to linearity of time and protein concentration. PABA and ABP kinetic constants were determined at a fixed concentration of 100 µM acetyl coenzyme A (AcCoA). PABA kinetic constants were determined using varying PABA concentrations between 11.7 – 3000 µM. ABP kinetic constants were determined using varying ABP concentrations between 11.7 – 3000 µM. Reactions containing substrate, AcCoA and enzyme were incubated at 37˚C for 10 min. Reactions were terminated by the addition of 1/10 volume of 1M acetic acid and centrifuged at 15,000Xg for 10 min. Measurements were adjusted according to baseline measurements using lysates of the UV5/*CYP1A1* cell line and normalized by the amount of total protein. Protein concentrations were measured using the method of Bradford (Bio-Rad, Hercules, CA). v_{max}, k_m, and k_{cat} were determined by fitting substrate concentration and velocity data to the hyperbolic Michaelis-Menten model. All calculations were determined using GraphPad Prism Software version 4 (Graphpad Software, La Jolla, California).

Determination of *in situ* (Whole-Cell Assay) Kinetic Parameters of NAT1 4 and NAT1 14B. *In situ* kinetic parameters were determined with a whole cell assay using media spiked with varying concentrations of PABA or ABP. PABA kinetic constants were determined using varying PABA concentrations between 2.25 – 300 µM. ABP kinetic constants were determined using varying ABP concentrations between 0.19 and 25 µM. The cells were incubated at 37ºC and media was collected after 1 h (PABA) or 22 min (ABP), 1/10 volume of 1M acetic acid was added, and the mixture was centrifuged at 13,000Xg for 10 min. Values were normalized to the amount of cells present at time of media removal. Following media removal, cells were washed with 1XPBS, trypsanized, and diluted in counting buffer (aqueous 1% sodium chloride). The number of cells was determined using a Z series Coulter Counter (Beckman Coulter, Indianopolis, IN). The supernatant was injected into the reverse phase HPLC column and *N*-acetyl-PABA and *N*-acetyl-ABP were separated and quantitated as described above. v_{max} and k_m were determined as described above.

Determination of *in vitro* Kinetic Parameters of *O*-acetylation for NAT1 4 and NAT1 14B. Cells and lysates were collected and prepared as described above. N-hydroxy-4-aminobiphenyl (*N*-OH-ABP) *O*-acetyltransferase assays were conducted and product was separated from substrate using HPLC as previously described (Hein et al., 2006). Assays containing 50 µg total protein, *N*-OH-ABP, AcCoA, and 1 mg/mL deoxyguanosine (dG) were incubated at 37^0C for 10 min. *N*-OH-ABP kinetic constants were determined at a fixed concentration of 100 µM AcCoA and *N*-OH-ABP concentrations between 0.78 and 200 µM. Reactions were stopped with the addition of 100 µL of water saturated ethyl acetate and centrifuged at 13,000xg for 10 min. The organic phase was removed, evaporated to dryness, redissolved in 100 µL of 10% ACN and injected onto the HPLC. v_{max}, k_m, and k_{cat} were determined as described above.

Measurement of NAT1 Protein. The amount of NAT1 produced in UV5/*1A1* cells stably transfected with *NAT1*4* or *NAT1*14B* was determined by western blot. Cells and lysates were collected and prepared as described above. Varying amounts of lysate were mixed 1:1 with 5% β-mercaptoethanol in Laemmli buffer (Bio-Rad), boiled for 5 min, and resolved by 12% SDS-PAGE. The proteins were then transferred by semi-dry electroblotting to polyvinylidene fluoride membranes. The membranes were probed with G5 (catalog #137204 Santa Cruz Biotechnology, Santa Cruz, CA), a monoclonal mouse anti-NAT1(1:200) antibody (), specific for an epitope mapping between amino acids 261-290 at the C-terminus of NAT1. Because the substitution R187Q lies outside this region, the antigenic site was not affected. Membrane were then probed with horseradish peroxidase-conjugated secondary donkey anti-mouse IgG antibody (1:2,000) (Santa Cruz). Supersignal West Pico Chemiluminescent Substrate was used for detection (Pierce). To determine a quantitative amount of NAT1 protein in lysate collected from cells stably transfected with *NAT1*4* or *NAT1*14B*, a standard curve was obtained from loading 1 - 140 ng of purified NAT1 (catalog #H00000009-p01 Abnova, Taipei, Taiwan). Intensities of varying amounts of lysate (55, 28, and 14 µg) from NAT1 4 and NAT1 14B were compared to intensities of the standard curve to determine the amount of NAT1 protein in the lysate. Kinetic properties of the NAT1 antibody binding of the purified protein and to NAT1 from sample lysate were assumed to be the same. Densitometric analysis was performed using Quantity One Software (Bio-Rad).

DNA Isolation and dG-C8-ABP Quantitation. Cells were prepared as described above. DNA was isolated and dG-C8-ABP adducts were quantitated as previously described (Millner et al., 2011). Stably transfected cells grown to approximately 80% confluency in 15 cm dishes were incubated in complete α-MEM media containing 1.56, 3.13, 6.25, 12.5 µM ABP or vehicle alone (0.5% DMSO) at 37°C. The cells were collected following 24 h of treatment,

centrifuged for 5 min at 260xg, and the pellet was resuspended in 2 volumes of homogenization buffer (20 mM sodium phosphate pH 7.4, 1 mM EDTA), 0.1 volumes of 10% SDS and 0.1 volume of 20 mg/mL Proteinase K and allowed to incubate overnight at 37^{o}C. The DNA was extracted using phenol/chloroform:isoamyl alcohol and precipitated with isopropanol. The pellet was dried and resuspended in 500 µL of DNA adduct buffer (5 mM Tris pH 7.4, 1 mM $CaCl_2$, 1 mM $ZnCl_2$, and 10 mM $MgCl_2$). The DNA was quantitated by spectrophotometry at A_{260}. Five hundred pg of internal standard (dG-C8-ABP-d5, Toronto Research Chemicals, North York, Ontario, Canada) was added to 30 µg of sample DNA, treated with 10 units *DNase I* (Sigma) for 1 h at 37^{o}C followed by treatment with 10 units nuclease P1 (Sigma) for 6 h. The reactions were then treated with 10 units of alkaline phosphatase (Sigma) overnight at 37^{o}C. The samples were then loaded onto PepClean C-18 Spin Columns (Thermo Fisher Scientific), washed with 10% ACN, eluted with 50% ACN by centrifugation at 2000xg and dried. The samples were reconstituted with 25 µL 5% ACN in 2.5 mM NH_4HCO_3 just before analysis and 10 µL of the sample was analyzed by Accela LC System (Thermo Scientific, San Jose, CA) coupled with a LTQ-Orbitrap XL mass spectrometer (Thermo Scientific, San Jose, CA). Samples were loaded onto a 30 × 1mm × 1.9 µm Hypersil GOLD column (Thermo Scientific, San Jose, CA) and eluted with a 12.5 min binary solvent gradient (Solvent A: 5% ACN/0.1% formic acid and Solvent B: 95% ACN/0.1% formic acid) at 50 µl/min. The gradient started from 5% Solvent B, increased linearly to 75% Solvent B in 10 min, and then remained at 75% B for 2.5 min. The eluates were ionized by electrospray ionization and dG-C8-ABP and dG-C8-ABP-d5 were detected with linear ion trap and detected by multiple reaction monitoring using the transitions of m/z 435.2 to m/z 319.2 (dG-C8-ABP) and m/z 440.2 to m/z 324.2 (dG-C8-ABP-d5). Concentrations of dG-C8-ABP were calculated from peak areas of dG-C8-ABP and dG-C8-ABP-d5 with a calibration curve from synthetic dG-C8-ABP and dG-C8-ABP-d5.

Measurement of Cytotoxicity. Assays for cell cytoxicity were carried out as described (Millner et al., 2011). Stably transfected cells expressing *NAT1*4* and *NAT1*14B* were grown in HAT medium (30 mM hypoxanthine, 0.1 mM aminopterin, and 30 mM thymidine) for 12 doublings. Cells ($1x10^6$) were plated, allowed to grow for 24 h and were then treated with 1.56, 3.13, 6.25 or 12.5 μM ABP (Sigma) or vehicle alone (0.5% DMSO) in media. After 48 h, cells were plated to determine survival following exposure to ABP. To determine cloning efficiency following each dose of ABP, 100 cells were plated in triplicate in 6 well-plates and allowed to grow for 7 days in non-selective media. Colonies were counted and expressed as percent of vehicle control.

Results

Initial experiments performed in yeast (*in situ*) resulted in higher NAT1 14B *N*-acetylation at 10 µM ($p<0.001$) and 50 µM ABP ($p<0.05$) compared to NAT1 4. There was no difference in *N*-acetylation between NAT1 14B and NAT1 4 following exposure to 100 µM ABP (Figure 2). The results of subsequent experiments performed in CHO cells are described below.

Kinetic parameters of the referent, NAT1 4, and the variant, NAT1 14B *in vitro* (per mg total protein in-solution biochemistry) are shown in Table 2. The apparent k_m of NAT1 14B was higher for PABA ($p<0.0001$) compared to NAT1 4 whereas the apparent k_m of NAT1 14B was lower for ABP ($p<0.0001$) and *N*-OH-ABP ($p<0.0001$) when compared to NAT1 4. The apparent v_{max} of NAT1 14B was lower for PABA ($p<0.0001$), ABP ($p<.0001$), and *N*-OH-ABP ($p<0.0001$) when compared to NAT1 4. The apparent v_{max}/k_m of NAT1 14B was lower for PABA ($p<0.0001$), higher for *N*-OH-ABP ($p<0.0001$), and not significantly different for ABP ($p>0.05$) when compared to NAT1 4.

The kinetic parameters, apparent k_m and k_{cat} also were determined *in vitro* (per mg NAT1 protein in solution biochemistry) for the referent, NAT1 4 and the variant, NAT1 14B (Table 2). The apparent k_{cat} of NAT1 14B was lower for PABA ($p<0.0001$) but higher for *N*-OH-ABP ($p<0.0001$) when compared to NAT1 4. There was no significant difference in apparent k_{cat} for ABP between NAT1 14B and NAT1 4 ($p>0.05$). The apparent k_{cat}/k_m of NAT1 14B was lower for PABA ($p<0.0001$) but higher for ABP ($p<0.05$) and N-OH-ABP ($p<0.0001$) when compared to NAT1 4.

Apparent k_m and v_{max} for PABA and ABP also were determined *in situ* (per million cells in a whole cell based assay) for the referent, NAT1 4, and the variant, NAT1 14B (Table 3). The apparent k_m of NAT1 14B was not significantly different for PABA ($p>0.05$) but was significantly lower for ABP ($p<0.0001$) when compared to NAT1 4. The apparent v_{max} of NAT1 14B was lower for PABA ($p<0.05$) and ABP ($p<0.0001$) when compared to NAT1 4. The apparent v_{max}/k_m of

NAT1 14B for PABA was significantly less ($p<0.05$) but was significantly higher for ABP ($p<0.05$) when compared to NAT1 4.

Expression of NAT1 14B and NAT1 4 was determined by western blot (Figure 3). The standard curve obtained by loading 1-140 ng of purified NAT1 protein (Abnova) was used to compare intensities of lysate from stably transfected cells. 55, 28, or 14 µg of total protein lysate, corresponded to 154, 77, and 38 ng of NAT1 4 protein and 38, 19, and 10 ng of NAT1 14B protein. Overall, NAT1 14B resulted in a 4-fold reduction in NAT1 protein compared to NAT1 4 ($p<0.001$).

ABP-induced cytotoxicity was also determined in cells stably transfected with *NAT1*4* or *NAT1*14B* (Figure 4a). Significantly more ABP-induced cytotoxicity was observed in *NAT1*14B* transfected cells following exposures to each ABP concentration. ABP-induced dG-C8-ABP adducts in cells stably transfected with *NAT1*4* and *NAT1*14B* were determined (Figure 4b). Significantly more dG-C8-ABP adducts were observed following exposures between 1.56 – 12.5 µM ABP in cells transfected with *NAT1*14B* than in cells transfected with *NAT1*4.*

Discussion

Smokers possessing *NAT1*14B* have been associated with increased risk for lung cancer compared to individuals possessing *NAT1*4* (Bouchardy et al., 1998). Previous studies have reported that *NAT1*14B* is associated with reduced *N*- and *O*-acetylation of various substrates including PABA, *p*-aminosalisylic acid, and various arylamine carcinogens (Fretland et al., 2001; Fretland et al., 2002; Hughes et al., 1998; Zhu and Hein, 2008). Recombinant NAT1 14B expression in yeast demonstrated lower *N*- and *O*-acetylation, NAT1-specific protein levels and increased NAT1 proteasomal degradation (Butcher et al., 2004; Fretland et al., 2001; Fretland et al., 2002). Similarly, NAT1 14B expressed in COS-1 cells also resulted in less NAT1 *N*- and *O*-acetylation, lower NAT1 protein level, and lower PABA $v_{max,}$ but higher PABA k_m when compared to the referent, NAT1 4 (Zhu and Hein, 2008). Our kinetic constant determinations performed in CHO cells confirmed that NAT1 14B results in a lower apparent v_{max} (both *in vitro* and *in situ*) for PABA when compared to the referent, NAT1 4. We also confirmed the higher PABA apparent k_m in NAT1 14B determined *in vitro* when compared to NAT1 4. In addition to PABA acetylation, we also report on *N*- and *O*-acetylation of ABP and *N*-OH-ABP. ABP is a human urinary bladder carcinogen found as a contaminant in cigarette smoke, food dyes, paints, textile dyes, engine exhaust, and commercial hair dyes (Nauwelaers, et al., 2011)

The arylamine substrate k_m of NAT1 is dependent on the AcCoA concentration because acetylation proceeds via a 'ping-pong bi-bi' reaction (Weber and Hein, 1985). AcCoA concentrations have been measured *in vivo* in the low micromolar range (Reeves et al., 1988). The lowest concentration of AcCoA (100 µM) was used that allowed repeatable and accurate measurements of acetylated product. In order to better mimic NAT1 catalyzed acetylation *in vivo*, kinetic constants were determined *in situ* (when possible) allowing the concentration of AcCoA to be provided by the cell.

Studies performed *in situ* using NAT1 14B and NAT1 4 produced in yeast did not result in lowered NAT1 14B *N*-acetylation of ABP (Figure 2) as previous studies had shown *in vitro*

(Fretland et al., 2002). This result was surprising as previous studies reported NAT1 14B activity and protein expression to be lower than NAT1 4. To further explore the NAT1 14B acetylation status, studies were conducted in stably transfected CHO cells.

When comparing apparent v_{max} (*in vitro*), the NAT1 14B apparent v_{max} was lower than the NAT1 4 for all substrates studied. The apparent v_{max} describes the maximum enzyme velocity extrapolated to maximum substrate concentrations. The lower apparent v_{max} for PABA, ABP, and *N*-OH-ABP indicate that at high substrate concentrations, NAT1 14B has a decreased ability to metabolize the substrate when compared to NAT1 4. The apparent v_{max}/k_m, or intrinsic clearance, describes an enzyme's ability to metabolize a substrate at substrate concentrations well below the k_m and has also been shown to correlate well to human liver clearance (Chen et al., 2011; Northrop, 1999). Although there are limitations in using v_{max}/k_m as a comparator of two enzymes, we determined apparent v_{max} for comparison at high substrate concentrations and apparent v_{max}/k_m for comparison at low substrate concentrations (Eisenthal et al., 2007). For PABA, the NAT1 14B apparent v_{max}/k_m was lower than NAT1 4. In contrast, no significant difference was observed between NAT1 14B and NAT1 4 apparent v_{max}/k_m towards the *N*-acetylation of ABP. Surprisingly, the NAT1 14B apparent v_{max}/k_m for the *O*-acetylation of *N*-OH-ABP was higher in *NAT1*14B* CHO cell lysate compared to *NAT1*4* CHO cell lysate. This indicates that the status of NAT1 14B intrinsic clearance compared to NAT1 4 intrinsic clearance is substrate dependent.

Transfection of *NAT1*14B* resulted in approximately a 4-fold less NAT1 protein expression compared to *NAT1*4*. When the amount of NAT1 protein was used to calculate apparent k_{cat} (determined *in vitro*), the results suggested that the lower NAT1 14B apparent v_{max} for these substrates is due to a reduction in NAT1 protein, not a reduction in the acetylation rate of the NAT1 14B enzyme. For example, although the NAT1 14B apparent v_{max} for *N*-OH-ABP was lower than the NAT1 4, the NAT1 14B apparent k_{cat} for *N*-OH-ABP was higher than NAT1 4. This difference in v_{max} compared to k_{cat} indicates that the lowered NAT1 14B apparent v_{max} is

caused by a reduction in protein expression. Butcher et. al (2004) reported that NAT1 14B and other NAT1 genetic variants associated with reduced enzymatic activity have reduced ability to be acetylated which resulted in an unstable NAT1 protein. Therefore, NAT1 14B was reported to be less stable and have increased proteasomal degradation compared to NAT1 4 (Butcher et al., 2004). Our study confirmed that NAT1 14B resulted in reduction of NAT1 protein.

Because determination of kinetic parameters is dependent upon AcCoA concentration, acetylation was measured *in situ* to allow the concentration of AcCoA to be provided by the cell. When comparing v_{max} (*in situ*), the NAT1 14B apparent v_{max} was lower than the NAT1 4 4 for PABA and ABP. When evaluated *in situ,* PABA NAT1 14B apparent v_{max}/k_m or intrinsic clearance was lower when compared to NAT1 4. In contrast, for ABP, the *in situ* NAT1 14B apparent v_{max}/k_m was higher when compared to NAT1 4. Because kinetic parameters of *N*-OH-ABP could not be determined *in situ*, an *in vitro* determination was performed. Like ABP, the NAT1 14B apparent v_{max}/k_m for *N*-OH-ABP was higher compared to NAT1 4. These findings indicate that differences in apparent v_{max}/k_m between NAT1 14B and NAT1 4 are substrate dependent. Risk for individuals possessing *NAT1*14B* is also likely exposure dependent. Increased apparent v_{max}/k_m indicates that NAT1 14B has an increased ability to metabolize ABP and *N*-OH-ABP at low substrate concentrations compared to NAT1 4 (Northrop, 1999). Since low substrate concentrations are relevant *in vivo*, the higher NAT1 14B apparent v_{max}/k_m suggests that differences between NAT1 14B and NAT1 4 catalyzed ABP acetylation should be observed *in vivo*. Therefore, risk for individuals possessing *NAT1*14B* is dependent on exposure type and can also be altered depending on exposure level.

NAT1 homology modeling predicted that the R187Q could affect NAT1 active site acetylation and enzymatic activity (Walraven et al., 2008). Because changes in binding of AcCoA and substrate specificity are likely altered due to the R187Q, it is not surprising that differences in intrinsic clearance between NAT1 14B and NAT1 4 were observed. We confirmed that R187Q modifies substrate affinity, albeit in opposite directions depending on substrate.

Further epidemiological studies are necessary to determine which carcinogen exposures result in increased risk for individuals possessing *NAT1*14B*. Kinetic parameters have been previously reported for an *N*-acetyltransferase 2 (NAT2) variant allele, *NAT2*7B.* (Hickman et al., 1995; Zang et al., 2007). Both papers reported differences in k_m for SMZ between NAT2 4 and NAT2 7B. Zang et al. also found that NAT2 7B *O*-acetylates *N*-OH-PhIP as effectively as NAT2 4, but does not *O*-acetylate *N*-OH-ABP as effectively as NAT2 4 (Zang et al., 2007). Our study is the first report of exposure dependent behavior for a variant of NAT1. Studies in our laboratory are currently underway to examine the interplay between NAT1 and NAT2 on ABP metabolism.

In addition to higher apparent v_{max}/k_m for NAT1 14B towards ABP and *N*-OH-ABP when compared to NAT1 4, ABP-induced DNA-adducts and cytoxicity were higher for NAT1 14B compared to NAT1 4. Measurement of DNA adduct levels following exposure to ABP is a biological endpoint very relevant to cancer risk. Because NAT1 14B resulted in increased ABP-induced DNA adducts, our results suggest that individuals possessing the *NAT1*14B* allele likely have increased risk compared to those who are homozygous for *NAT1*4* following low (environmental) dose exposure to ABP. NAT1 14B is not simply associated with "slow acetylation" but rather is substrate dependent, since NAT1 14B exhibits lower *N*-acetylation catalytic efficiency of PABA but higher *N*- and *O*-acetylation catalytic efficiency as well as DNA adducts following exposure to the human carcinogen ABP.

Author Contributions

Participated in research design: Millner, Doll, States, Hein.
Conducted experiments: Millner, Doll, Cai.
Performed data analysis: Millner, Cai, Hein.
Wrote or contributed to the writing of the manuscript: Millner, Doll, Cai, States, Hein.

References

Adam, P.J., Berry, J., Loader, J.A., Tyson, K.L., Craggs, G., Smith, P., De Belin, J., Steers, G., Pezzella, F., Sachsenmeir, K.F.*, et al.* (2003). Arylamine N-acetyltransferase-1 is highly expressed in breast cancers and conveys enhanced growth and resistance to etoposide in vitro. Mol Cancer Res *1*, 826-835.

Ambrosone, C.B., Abrams, S.M., Gorlewska-Roberts, K., and Kadlubar, F.F. (2007). Hair dye use, meat intake, and tobacco exposure and presence of carcinogen-DNA adducts in exfoliated breast ductal epithelial cells. Arch Biochem Biophys *464*, 169-175.

Barker, D.F., Husain, A., Neale, J.R., Martini, B.D., Zhang, X., Doll, M.A., States, J.C., and Hein, D.W. (2006). Functional properties of an alternative, tissue-specific promoter for human arylamine N-acetyltransferase 1. Pharmacogenet Genomics *16*, 515-525.

Bell, D.A., Stephens, E.A., Castranio, T., Umbach, D.M., Watson, M., Deakin, M., Elder, J., Hendrickse, C., Duncan, H., and Strange, R.C. (1995). Polyadenylation polymorphism in the acetyltransferase 1 gene (NAT1) increases risk of colorectal cancer. Cancer Res *55*, 3537-3542.

Bendaly, J., Zhao, S., Neale J.R., Metry, K.J., Doll, M.A., States, J.C., Pierce, W.M., Jr., and Hein, D.W. (2007) 2-Amino-3,8-dimethylimidazo-[4,5-f]quinoxaline-induced DNA adduct formation and mutagenesis in DNA repair-deficient Chinese hamster ovary cells expressing human cytochrome P4501A1 and rapid or slow acetylator N-acetyltransferase 2. Cancer Epidemiol Biomarkers Prev *16*, 1503-1509.

Bouchardy, C., Mitrunen, K., Wikman, H., Husgafvel-Pursiainen, K., Dayer, P., Benhamou, S., and Hirvonen, A. (1998). N-acetyltransferase NAT1 and NAT2 genotypes and lung cancer risk. Pharmacogenetics *8*, 291-298.

Butcher, N.J., Arulpragasam, A., and Minchin, R.F. (2004). Proteasomal degradation of N-acetyltransferase 1 is prevented by acetylation of the active site cysteine: a mechanism for the slow acetylator phenotype and substrate-dependent down-regulation. J Biol Chem *279*, 22131-22137.

Chen, Y., Liu, L., Nguyen, K., and Fretland, A.J. (2011). Utility of intersystem extrapolation factors in early reaction phenotyping and the quantitative extrapolation of human liver microsomal intrinsic clearance using recombinant cytochromes P450. Drug Metab Dispos *39*, 373-382.

Dhaini, H.R., and Levy, G.N. (2000). Arylamine N-acetyltransferase 1 (NAT1) genotypes in a Lebanese population. Pharmacogenetics *10*, 79-83.

Doll, M.A. and Hein, D.W. (2002) Rapid genotype method to distinguish frequent and/or functional polymorphisms in human N-acetyltransferase-1. Anal Biochem *301*, 328-332.

Eisenthal, R., Danson, M.J., and Hough, D.W. (2007). Catalytic efficiency and kcat/KM: a useful comparator? Trends Biotechnol *25*, 247-249.

Fretland, A.J., Doll, M.A., Leff, M.A., and Hein, D.W. (2001). Functional characterization of nucleotide polymorphisms in the coding region of N-acetyltransferase 1. Pharmacogenetics *11*, 511-520.

Fretland, A.J., Doll, M.A., Zhu, Y., Smith, L., Leff, M.A., and Hein, D.W. (2002). Effect of nucleotide substitutions in N-acetyltransferase-1 on N-acetylation (deactivation) and O-acetylation (activation) of arylamine carcinogens: implications for cancer predisposition. Cancer Detect Prev *26*, 10-14.

Gago-Dominguez, M., Bell, D.A., Watson, M.A., Yuan, J.M., Castelao, J.E., Hein, D.W., Chan, K.K., Coetzee, G.A., Ross, R.K., and Yu, M.C. (2003). Permanent hair dyes and bladder cancer: risk modification by cytochrome P4501A2 and N-acetyltransferases 1 and 2. Carcinogenesis *24*, 483-489.

Hein, D.W., Doll, M.A., Fretland, A.J., Leff, M.A., Webb, S.J., Xiao, G.H., Devanaboyina, U.S., Nangju, N.A., and Feng, Y. (2000). Molecular genetics and epidemiology of the NAT1 and NAT2 acetylation polymorphisms. Cancer Epidemiol Biomarkers Prev *9*, 29-42.

Hein, D.W., Doll, M.A., Nerland, D.E., and Fretland, A.J. (2006). Tissue distribution of N-acetyltransferase 1 and 2 catalyzing the N-acetylation of 4-aminobiphenyl and O-acetylation of N-hydroxy-4-aminobiphenyl in the congenic rapid and slow acetylator Syrian hamster. Mol Carcinog *45*, 230-238.

Hickman, D., Palamanda, J.R., Unadkat, J.D., and Sim, E. (1995). Enzyme kinetic properties of human recombinant arylamine N-acetyltransferase 2 allotypic variants expressed in Escherichia coli. Biochem Pharmacol *50*, 697-703.

Hoffmann, D., Djordjevic, M.V., and Hoffmann, I. (1997). The changing cigarette. Prev Med *26*, 427-434.

Horton, R.M., Hunt, H.D., Ho, S.N., Pullen, J.K., and Pease, L.R. (1989). Engineering hybrid genes without the use of restriction enzymes: gene splicing by overlap extension. Gene *77*, 61-68.

Hughes, N.C., Janezic, S.A., McQueen, K.L., Jewett, M.A., Castranio, T., Bell, D.A., and Grant, D.M. (1998). Identification and characterization of variant alleles of human acetyltransferase NAT1 with defective function using p-aminosalicylate as an in-vivo and in-vitro probe. Pharmacogenetics *8*, 55-66.

Husain, A., Barker, D.F., States, J.C., Doll, M.A., and Hein, D.W. (2004). Identification of the major promoter and non-coding exons of the human arylamine N-acetyltransferase 1 gene (NAT1). Pharmacogenetics *14*, 397-406.

IARC (1987). Overall Evaluations of Carcinogenicity. Lyon, France: International Agency for Research on Cancer. 440 pp. IARC Monographs on the Evaluation of Carcinogenic Risk of Chemicals to Humans *1-42, suppl 7.*

Jensen, L.E., Hoess, K., Whitehead, A.S., and Mitchell, L.E. (2005). The NAT1 C1095A polymorphism, maternal multivitamin use and smoking, and the risk of spina bifida. Birth Defects Res A Clin Mol Teratol *73*, 512-516.

Lammer, E.J., Shaw, G.M., Iovannisci, D.M., Van Waes, J., and Finnell, R.H. (2004). Maternal smoking and the risk of orofacial clefts: Susceptibility with NAT1 and NAT2 polymorphisms. Epidemiology *15*, 150-156.

Li, D., Jiao, L., Li, Y., Doll, M.A., Hein, D.W., Bondy, M.L., Evans, D.B., Wolff, R.A., Lenzi, R., Pisters, P.W.*, et al.* (2006). Polymorphisms of cytochrome P4501A2 and N-acetyltransferase genes, smoking, and risk of pancreatic cancer. Carcinogenesis *27*, 103-111.

Lilla, C., Verla-Tebit, E., Risch, A., Jager, B., Hoffmeister, M., Brenner, H., and Chang-Claude, J. (2006). Effect of NAT1 and NAT2 genetic polymorphisms on colorectal cancer risk associated with exposure to tobacco smoke and meat consumption. Cancer Epidemiol Biomarkers Prev *15*, 99-107.

Millikan, R.C., Pittman, G.S., Newman, B., Tse, C.K., Selmin, O., Rockhill, B., Savitz, D., Moorman, P.G., and Bell, D.A. (1998). Cigarette smoking, N-acetyltransferases 1 and 2, and breast cancer risk. Cancer Epidemiol Biomarkers Prev *7*, 371-378.

Millner, L,M,, Doll, M.A., Cai, J., States, J.C., and Hein, D.W. (2011). NATb/NAT1*4 promotes greater arylamine N-acetyltransferase 1 mediated DNA adducts and mutations than NATa/NAT1*4 following exposure to 4-aminobiphenyl. Mol Carcinog.(Epub Aug 11).

Morton, L.M., Schenk, M., Hein, D.W., Davis, S., Zahm, S.H., Cozen, W., Cerhan, J.R., Hartge, P., Welch, R., Chanock, S.J.*, et al.* (2006). Genetic variation in N-acetyltransferase 1 (NAT1) and 2 (NAT2) and risk of non-Hodgkin lymphoma. Pharmacogenet Genomics *16*, 537-545.

Nauwelaers, G., Bessette, E.E., Gu, D., Tang, Y., Rageul, J., Fessard, V., Yuan, J.M., Yu, M.C., Langouet, S., and Turesky, R.J. (2011). DNA Adduct Formation of 4-Aminobiphenyl and Heterocyclic Aromatic Amines in Human Hepatocytes. Chem Res Toxicol *24*, 913-925.

Northrop, D.B. (1999). Rethinking fundamentals of enzyme action. Adv Enzymol Relat Areas Mol Biol *73*, 25-55.

Reeves, P.T., Minchin, R.F., and Ilett, K.F. (1988). Induction of sulfamethazine acetylation by hydrocortisone in the rabbit. Drug Metab Dispos *16*, 110-115.

Tiang, J.M., Butcher, N.J., Cullinane, C., Humbert, P.O., and Minchin, R.F. (2011). RNAi-Mediated Knock-Down of Arylamine N-acetyltransferase-1 Expression Induces E-cadherin Up-Regulation and Cell-Cell Contact Growth Inhibition. PLoS One *6*, e17031.

Wakefield, L., Cornish, V., Long, H., Griffiths, W.J., and Sim, E. (2007). Deletion of a xenobiotic metabolizing gene in mice affects folate metabolism. Biochem Biophys Res Commun *364*, 556-560.

Walraven, J.M., Trent, J.O., and Hein, D.W. (2008). Structure-function analyses of single nucleotide polymorphisms in human N-acetyltransferase 1. Drug Metab Rev *40*, 169-184.

Weber, W.W., and Hein, D.W. (1985). N-acetylation pharmacogenetics. Pharmacol Rev *37*, 25-79.

Wikman, H., Thiel, S., Jager, B., Schmezer, P., Spiegelhalder, B., Edler, L., Dienemann, H., Kayser, K., Schulz, V., Drings, P.*, et al.* (2001). Relevance of N-acetyltransferase 1 and 2 (NAT1, NAT2) genetic polymorphisms in non-small cell lung cancer susceptibility. Pharmacogenetics *11*, 157-168.

Zang, Y., Doll, M.A., Zhao, S., States, J.C., and Hein, D.W. (2007). Functional characterization of single-nucleotide polymorphisms and haplotypes of human N-acetyltransferase 2. Carcinogenesis *28*, 1665-1671.

Zheng, W., Deitz, A.C., Campbell, D.R., Wen, W.Q., Cerhan, J.R., Sellers, T.A., Folsom, A.R., and Hein, D.W. (1999). N-acetyltransferase 1 genetic polymorphism, cigarette smoking, well-done meat intake, and breast cancer risk. Cancer Epidemiol Biomarkers Prev *8*, 233-239.

Zhu, Y., and Hein, D.W. (2008). Functional effects of single nucleotide polymorphisms in the coding region of human N-acetyltransferase 1. Pharmacogenomics J *8*, 339-348.

Footnotes

This work was supported by NIH grants [R01-CA034627] from the National Cancer Institute, [T32-ES011564 and P30-ES014443] from the National Institute for Environmental Health Sciences and [BC083107] from the Department of Defense Breast Cancer Research Program.

Portions of this work constitute partial fulfillment for the PhD in pharmacology and toxicology at the University of Louisville to Lori Millner.

Figure Legends

FIG. 1. NATb/*NAT1*4* and NATb/*NAT1*14B* constructs. (a) Schematic of NAT1 genomic structure and most common RNA transcribed by the NATb promoter. (b) Constructs including 5'-UTR, open reading frame (exon 9) and 3'-UTR.

FIG. 2. *In situ* ABP *N*-acetylation in yeast cultures recombinantly expressing *NAT1*4* and *NAT1*14B*. Each bar illustrates mean ± SEM for nmole acetylated ABP per million cells following 3 separate collections. Significant differences between *NAT1*4* and *NAT1*14B* expressing yeast cultures were determined by Student's t-test **$p<0.001$ and *$p<.05$.

FIG. 3. Western blot to determine relative protein expression of NAT1 4 and NAT1 14B. (a) Representative western blot; (b) densitometric analysis of western blot of 28 µg total protein loaded. Loading either 28 or 14 µg of total protein lysate, NAT1 14B resulted in approximately 4-fold less NAT1 protein than NAT1 4 ($p<0.001$). Bars represent mean ± SEM for 3 western blots and significance was determined by Student's t-test.

FIG. 4. ABP-induced cytotoxicity (a) and dG-C8-ABP adducts (b) in cells stably transfected with *NAT1*4* and *NAT1*14B*. Significantly more cytotoxicity was observed for NAT1 14B than NAT1 4 following all ABP exposures between 1.56 – 12.5 µM. Significantly more adducts were observed following all exposures examined in cells expressing NAT1 14B than in cells expressing NAT1 4. Values were adjusted for baseline values of UV5/*1A1* cells. Bars represent mean ± SEM for 3 determinations and significance was determined by Student's t-test. (*) $p<0.05$, (**) $p<0.001$, and (***) $p<0.0001$.

TABLE 1

Primers used to amplify NATb/*NAT1*4* construct

Primer Name	**Use**	**Sequence**
Lkm40P1	NATb 5-'UTR forward specific PCR	5'-GGCCGCGGCATTCAGTCTAGTTCCTGGTTGCC-3'
P1 Fwd Inr NheI	NATb 5'-UTR forward specific nested PCR	5'-TTTAAAGCTAGCATTCAGTCTAGTCTAGTTCCTGGTTGCCGGCT-3'
NAT1 (3') ORF Rev	NATa/NATb 5'-UTR reverse PCR	5'-TTCCTCACTCAGAGTCTTGAACTCTATT-3'
NAT1 (3') ORF For	NAT1 coding region forward PCR	5'-AGACATCTCCATCATCTGTGTTTACTAGT-3'
pcDNA5 FRTdistal Rev	NAT1 3'-UTR reverse PCR	5'-CGTGGGGATACCCCCTAGA-3'
NAT1 KPN-Rev	NAT1 3'-UTR reverse nested PCR	5'-ATAGTAGGTACCTCTGAATTATAGATAAGCAAAGATTCAGATTCT-3'

TABLE 2

NAT1 4 and NAT1 14B kinetic constants determined *in vitro* (per mg total protein)

Allele	**Substrate**	**$k_{m(app)}$**	**$v_{max(app)}$**	**$v_{max}/k_{m(app)}$**	**$k_{cat(app)}$**	**$k_{cat}/k_{m(app)}$**
		μM	nmole min^{-1} mg^{-1}	mL min^{-1} mg^{-1}	min^{-1}	min^{-1} μM^{-1}
*NAT1*4*	PABA	42.9±3.3	116±3	2.72±0.21	2400±57	56.5±4.3
*NAT1*14B*		430±1[a]	18.5±1.5[b]	0.043±0.002[b]	1550±97[b]	3.61±0.20[b]
*NAT1*4*	ABP	273±46	57.7±5.8	0.218±0.018	1200±122	4.52±0.38
*NAT1*14B*		65.6±3.9[b]	18.0±4.3[b]	0.280±.031	1760±128	22.9±0.23[c]
*NAT1*4*	*N*-OH-ABP	141±1.1	2.97±0.19	0.0211±0.0014	35.1±68	0.250±0.02
*NAT1*14B*		46.8±1.3[b]	1.76±0.03[b]	0.038±0.001[c]	147±7[a]	3.15±0.23[c]

PABA, ABP, and *N*-OH-ABP constants were determined at a fixed concentration of 100 μM AcCoA. Table values represent mean ± SEM for 3-6 individual determinations. Differences were tested for significance by Student's t-test. [a]significantly higher than NAT1 4 ($p<0.0001$); [b]significantly lower than NAT1 4 ($p<0.0001$); [c]significantly higher than NAT1 4 ($p<0.05$).

TABLE 3

NAT1 4 and NAT1 14B kinetic constants determined *in situ* (per million cells)

Allele	**Substrate**	**$k_{m(app)}$**	**$v_{max(app)}$**	**$v_{max}/k_{m(app)}$**
		μM	nmole min^{-1} million $cells^{-1}$	nmole min^{-1} million $cells^{-1}$ μM^{-1}
*NAT1*4*	PABA	95.5±1.1	0.16±0.01	1.71±0.08
*NAT1*14B*		72.1±11.1	0.101±0.018[a]	1.1±0.09[a]
*NAT1*4*	ABP	10.5±0.6	0.024±.0007	2.4±0.1
*NAT1*14B*		2.3±0.2[b]	0.0063±0.0005[b]	2.9±0.1[c]

Table values represent mean ± SEM for 3-6 individual determinations. Differences were tested for significance by Student's t-test.

[a]significantly lower than NAT1 4 ($p<0.05$); [b]significantly lower than NAT1 4 ($p<0.0001$); [c]significantly higher than NAT1 4 ($p<0.05$).

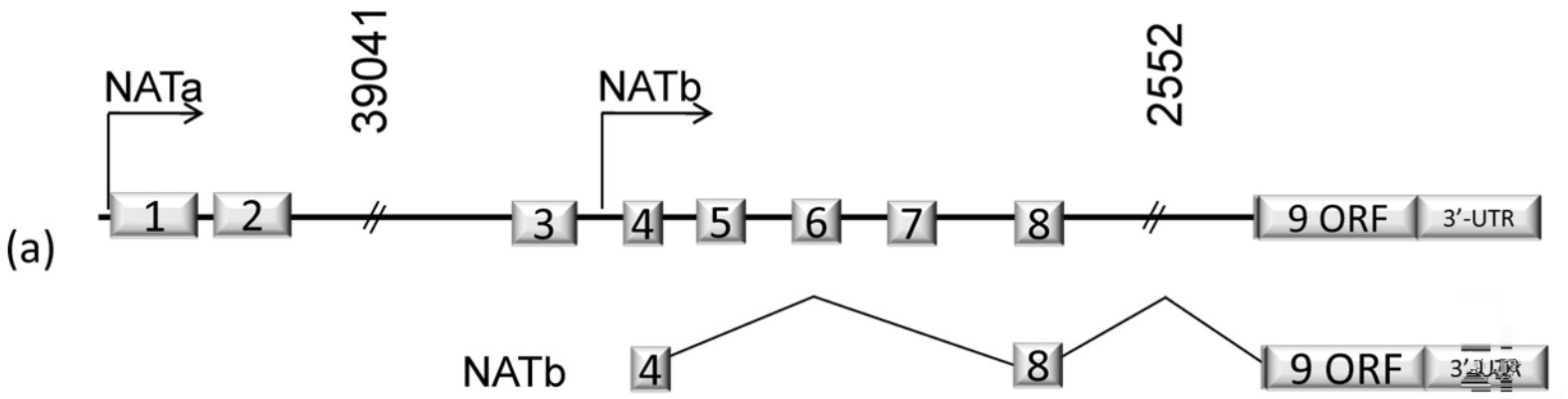
(a)
NATa
39041
NATb
2552
1
2
3
4
5
6
7
8
9 ORF
3′-UTR
NATb
4
8
9 ORF
3′-UTR

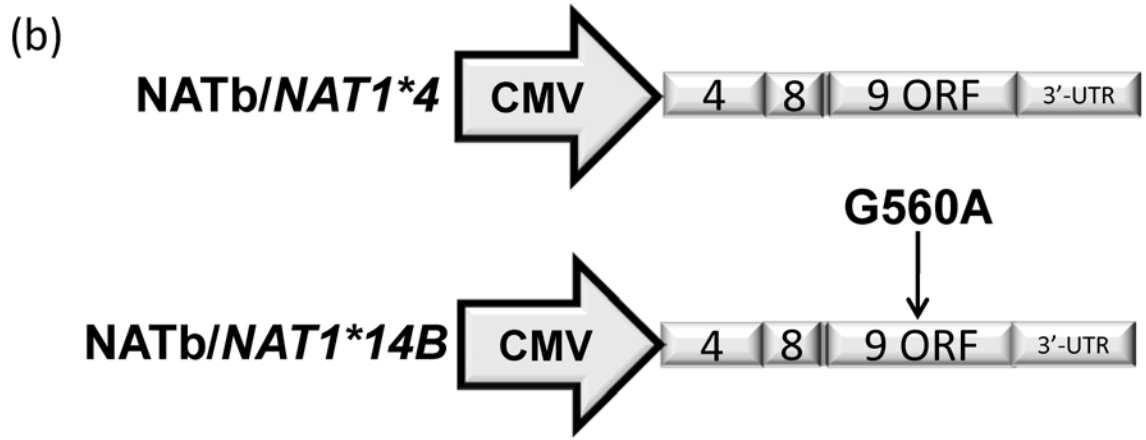
(b)
NATb/NAT1*4
CMV
4
8
9 ORF
3′-UTR
G560A
NATb/NAT1*14B
CMV
4
8
9 ORF
3′-UTR

Fig. 1

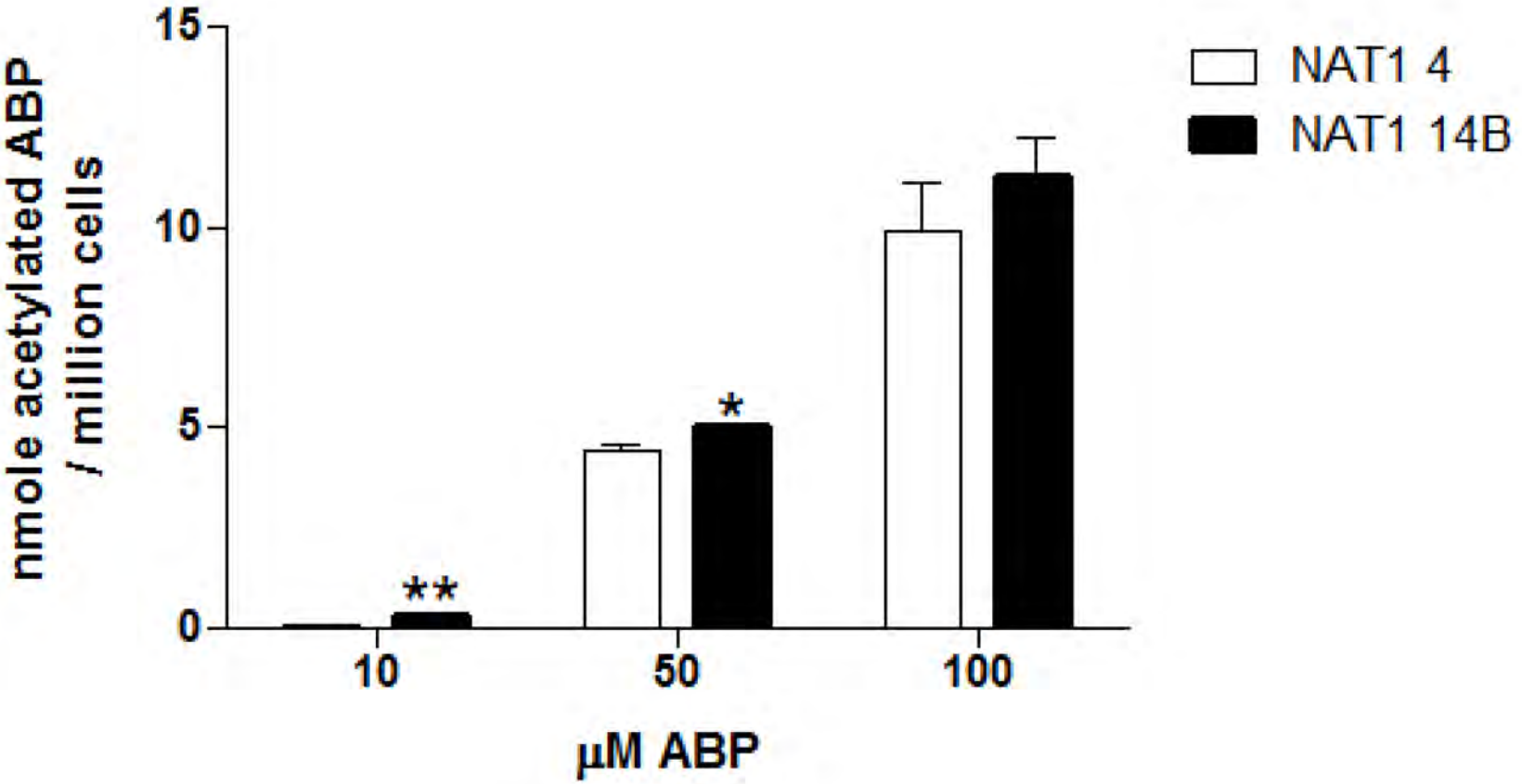
15
10
5
0
nmole acetylated ABP
/ million cells
**
*
10
50
100
µM ABP
NAT1 4
NAT1 14B

Fig. 2

Fig. 3

(a)


28µg
14µg
NAT1 4
NAT1 14B

(b)

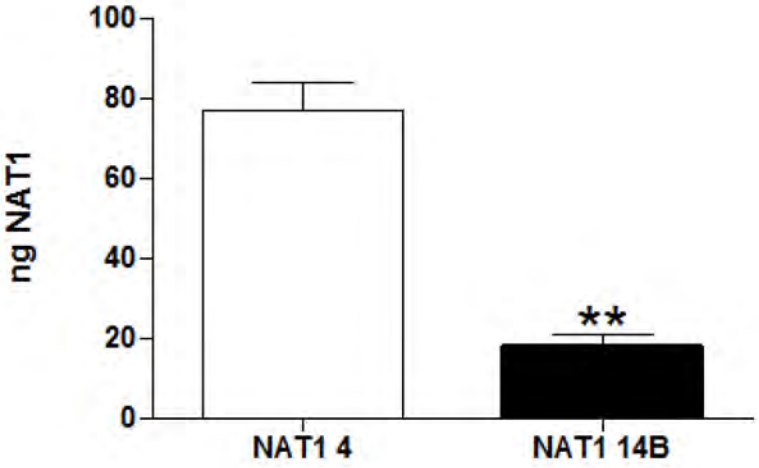
100
80
60
40
20
0
ng NAT1
**
NAT1 4
NAT1 14B

(a)

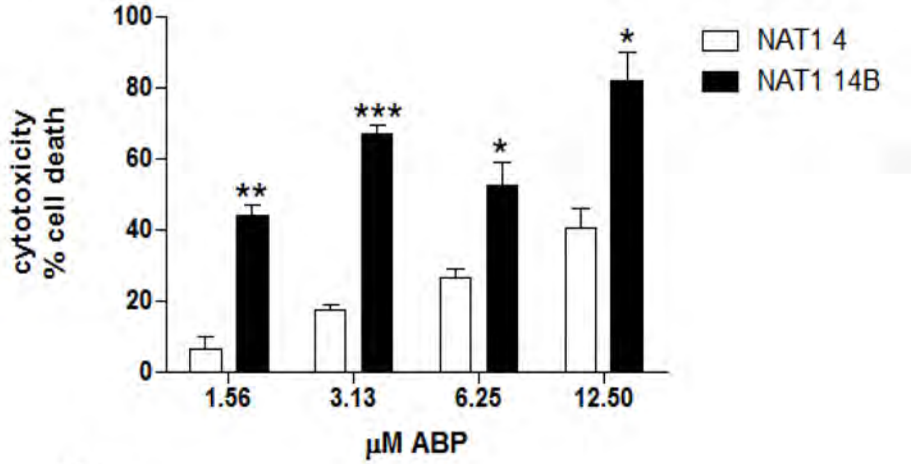
100
80
60
40
20
0
cytotoxicity
% cell death
**
***
*
*
1.56
3.13
6.25
12.50
µM ABP
NAT1 4
NAT1 14B

(b)

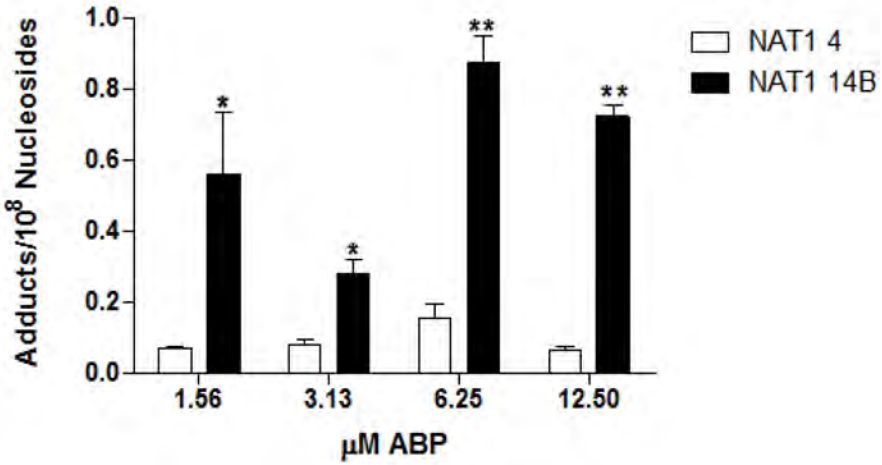
1.0
0.8
0.6
0.4
0.2
0.0
Adducts/10^8 Nucleosides
*
*
**
**
1.56
3.13
6.25
12.50
µM ABP
NAT1 4
NAT1 14B

Fig. 4

Functional analysis of arylamine N-acetyltransferase 1 (NAT1) NAT1*10 haplotypes in a complete NATb mRNA construct

Journal:	*Carcinogenesis*
Manuscript ID:	CARCIN-2011-00836
Manuscript Type:	Original Manuscript
Date Submitted by the Author:	29-Sep-2011
Complete List of Authors:	Millner, Lori; University of Louisville, Pharmacology and Toxicology Doll, Mark; University of Louisville, Pharmacology and Toxicology Stepp, Marcus; University of Louisville, Pharmacology and Toxicology States, J. Christopher; University of Louisville, Pharmacology and Toxicology Hein, David; University of Louisville, Pharmacology and Toxicology
Keywords:	N-acetyltransferase 1, Single nucleotide polymorphism, NAT1*10, genetic predisposition, 4-aminobiphenyl

Functional analysis of arylamine *N*-acetyltransferase 1 (*NAT1*) *NAT1*10* haplotypes in a complete NATb mRNA construct

Lori M. Millner, Mark A. Doll, Marcus W. Stepp, J. Christopher States, and David W. Hein*

Department of Pharmacology and Toxicology, James Graham Brown Cancer Center and Center for Environmental Genomics and Integrative Biology, University of Louisville, Louisville, Kentucky

*To whom correspondence should be addressed at University of Louisville Health Sciences Center, 505 South Hancock Street, at Clinical and Translational Research Building Room 303, Louisville, KY 40202-1617. Email: d.hein@louisville.edu; Tel: 502-852-6252; Fax: 502-852-7868.

Running Title: Functional analysis of *NAT1*10* vs *NAT1*4*

Abbreviations: NAT1, N-acetyltransferase 1;; UTR, untranslated region; ABP, 4-aminobiphenyl: hprt,, hypoxanthine phosphoribosyl transferasek ORF, open reading frame; SNP, single nucleotide polymorphism; CHO, Chinese hamster ovary; FRT, Flp recombination target; α-MEM, alpha-modified essential medium; PABA, p-aminobenzoic acid; AcCoA, acetyl coenzyme A; HPLC, high performance liquid chromatography; *N*-OH-ABP, *N*-hydroxy-4-aminobiphenyl; qRT-PCR, quantitative reverse transcriptase polymerase chain reaction; dG, deoxyguanosine.

Abstract

N-acetyltransferase 1 (NAT1) catalyzes *N*-acetylation of arylamines as well as the *O*-acetylation of *N*-hydroxylated arylamines. *O*-acetylation leads to the formation of electrophilic intermediates that result in DNA adducts and mutations. *NAT1*10* is the most common variant haplotype and is associated with increased risk for numerous cancers. NAT1 is transcribed from a major promoter, NATb, and an alternative promoter, NATa, resulting in mRNAs with distinct 5'-untranslated regions (UTRs). To best mimic *in vivo* metabolism and the effect of *NAT1*10* polymorphisms on polyadenylation usage, pcDNA5/FRT plasmid constructs were prepared for transfection of full length human mRNAs including the 5'-UTR derived from NATb, the open reading frame, and 888 nucleotides of the 3'-UTR. Following stable transfection of *NAT1*4, NAT1*10* and an additional *NAT1*10* variant (termed *NAT1*10B*) into nucleotide excision repair deficient Chinese hamster ovary cells, *N*- and *O*- acetyltransferase activity (*in vitro* and *in situ*), mRNA, and protein expression were higher in in cells transfected with *NAT1*10 and NAT1*10B* than in cells transfected with *NAT1*4* ($p<0.05$). Consistent with NAT1 expression and activity, cytotoxicity and *hypoxanthine phosphoribosyl transferase* mutants following 4-aminobiphenyl (ABP) exposures were higher in *NAT1*10* than in *NAT1*4* transfected cells. RNase protection assays showed no difference between *NAT1*4* and *NAT1*10*. However, protection of one probe by *NAT1*10B* was not observed with *NAT1*4* or *NAT1*10*, suggesting additional mechanisms that regulate *NAT1*10B*. The higher mutants in cells transfected with *NAT1*10* and *NAT1*10B* are consistent with an increased cancer risk for individuals possessing *NAT1*10* haplotypes.

Introduction

Human arylamine N-acetyltransferase 1 (NAT1) is a phase II cytosolic isozyme responsible for the biotransformation of many arylamine compounds including environmental and occupational carcinogens such as 4-aminobiphenyl (ABP) [1]. NAT1 has been implicated in several types of cancer due to its role in metabolic activation of arylamine carcinogens, and recent findings report NAT1 may be important for cell growth and survival of cancer cells [2]. NAT1 has been found in nearly all tissues studied [3,4]. NAT1 is capable of both *N*-acetylation and *O*-acetylation. *N*-acetylation often results in inactivation followed by urinary excretion. However, following *N*-hydroxylation, *O*-acetylation catalyzed by NAT1 generates an unstable *N*-acetoxyarylamine which undergoes heterolytic cleavage to yield a highly reactive nitrenium ion. These nitrenium ions are highly electrophilic and can react with DNA which if unrepaired, leads to mutations. Therefore, following exposure to arylamine carcinogens, the acetylator phenotype may modulate individual susceptibility to cancer and other diseases.

*NAT1*10* is the most common NAT1 variant haplotype and is presently defined (http://n-acetyltransferasenomenclature.louisville.edu) by two single nucleotide polymorphisms (SNPs) in the 3'-UTR, 1088T>A (rs1057126) and 1095C>A (rs15561). *NAT1*10* was associated with elevated NAT1 activity levels in human bladder [5], colon [5,6], liver [7,8], leukocytes [9] and β-lymphocytes [8] as well as increased *N*-acetylation capacity *in vivo* [10]. However, other studies did not replicate the increased catalytic activity associated with *NAT1*10* [11-13] resulting in a complete lack of consensus regarding *NAT1*10* phenotype [14]. Further research on SNPs in the 3′-UTR is needed to better understand their functional effects, which may be tissue-specific. There are no amino acid changes due to 3'-UTR polymorphisms, but the 1088T>A causes a change in the second consensus polyadenylation signal (AATAAA – AAAAAA). It has been speculated that this change in polyadenylation signal may give rise to higher acetylation activity [7]. The 3'-UTR of a gene contains binding sites for important translational regulatory elements

that include microRNAs, proteins or protein complexes, cytoplasmic polyadenylation elements (CPE) and polyadenylation signals (AAUAAA) [15]. It has been shown that SNPs in 3'-UTRs of dihydrofolate reductase, thrombin and resistin genes cause functional effects and alter disease risk [15-17].

In addition to the high allelic frequency, *NAT1*10* has been associated with increased risk for many different forms of cancer. *NAT1*10* allele or haplotype has been associated with increased risk for non-Hodgkin lymphoma [18,19] as well as for cancers of the urinary bladder [20], lung [21-23], colon/rectum [7,24-26], breast [27-29], prostate [30,31], stomach [32] and pancreas [33]. However, other studies have reported no association between *NAT1*10* and cancer risk [34-37]. Thus, the contribution of *NAT1*10* to increased cancer risk is not well understood. It is imperative that the phenotype of *NAT1*10* be clearly defined in order to resolve the association of *NAT1*10* genotype with increased cancer risk.

The NAT1 gene is located on the small arm of chromosome 8 [38] and spans 53 kilobases. NAT1 is encoded by a single intronless coding exon containing an open reading frame (ORF) of 870 base pairs. Several *NAT1* transcripts have been identified containing various combinations of the 9 noncoding 5'-untranslated region (UTR) exons and are known to originate from a major promoter NATb, and an alternative promoter, NATa. NATa originates 51.5 kb upstream of the single NAT1 ORF while NATb originates 11.8 kb upstream of the NAT1 ORF [5,39,40]. NATb transcripts are expressed in all tissues studied, while NATa transcripts have been identified in kidney, liver, lung and trachea. In addition to polymorphic variation, it may be necessary to consider transcriptional and translational regulation to further understand the variation associated with *NAT1*10* acetylation activity and effect on cancer risk. In contrast to previous studies which included only the *NAT1* open reading frame (ORF), the current study employs constructs that mimic the most common transcript originating from the NATb promoter. The constructs contain the ORF, the 3'-UTR and all 5' non coding exons found in the most

common *NAT1* transcript originating at the NATb promoter [39-41]. The NATb construct contains exons 4 and 8 (5' NCEs) and exon 9 (ORF). In addition to the 5'-UTR and the ORF, the NATb constructs also contain 888 nucleotides of the 3'-UTR. The NATb constructs were employed to provide a more comprehensive model of *in vivo* metabolism and to study any haplotype specific interactions between the 5'-UTR and *NAT1*10* polymorphisms. These constructs were utilized to compare *N*- and *O*- acetylation, mRNA levels, protein levels, polyadenylation patterns, and ABP-induced mutagenesis between cells transfected with *NAT1*4* and with variants of *NAT1*10.*

Materials and methods

Polyadenylation site removal

The bovine growth hormone polyadenylation site from the pcDNA5/FRT (Invitrogen, Carlsbad, CA) vector was removed to allow the endogenous *NAT1* polyadenylation sites to be active. This was accomplished by digestion of pcDNA5/FRT at 37ºC with restriction endonucleases, ApaI and SphI (New England Biolabs, Ipswich, MA), followed by overhang digestion with T4 DNA polymerase (New England Biolabs) and ligation with T4 Ligase (New England Biolabs).

*NATb/NAT1*4, NATb/NAT1*10 NATb/NAT1*10B construct*

The constructs were created utilizing gene splicing via overlap extension [42] by amplifying the 5'-UTR and the coding region/3'-UTR separately and then fusing the two regions together. Beginning with frequently used transcription start sites [39,40], the 5'-UTRs were amplified from cDNA prepared from RNA isolated from homozygous *NAT1*4* HepG2 cells. All primer sequences used are shown in Table I. The primers used to amplify the NATb 5'-UTR region were Lkm40P1 and NAT1 (3') ORF Rev. The coding region and 3'-UTR were amplified as one piece from homozygous *NAT1*4* or homozygous *NAT1*10* human genomic DNA. The forward primer used to amplify the coding region/3'-UTR was NAT1 (3') ORF Forward while the reverse primer was pcDNA5distal Reverse. The two sections, the 5'-UTR and the coding region/3'UTR, were fused together via overlap and amplification of the entire product using nested primers. The forward nested primer for NATb was P1 Fwd Inr NheI. The reverse nested primer was NAT1 Kpn Rev (*NAT1*4* and *NAT1*10*) or NAT1 Kpn Rev 10B (*NAT1*10B*). Both forward nested primers included the *Nhe1* endonuclease restriction site and both reverse nested primers contained the *Kpn1* endonuclease restriction site to facilitate cloning. The pcDNA5/FRT vector and NATb/*NAT1*4* allelic segments were digested at 37^{0}C with restriction

endonucleases *KpnI* and *NheI* (New England Biolabs). The *NAT1* constructs were then ligated into pcDNA5/FRT using T4 ligase (Invitrogen). All constructs were sequenced to ensure integrity of allelic segments and junction sites.

*NATb/NAT1*10 construction*

NATb/*NAT1*10* constructs were created using the same NATb 5'-UTRs amplified from cDNA prepared from *NAT1*4* homozygous RNA isolated from HepG2 cells, while the ORF (open reading frame) and region 3' to the ORF were amplified as one piece from *NAT1*10/NAT1*10* homozygous human genomic DNA. These two sections, the 5' UTR and the ORF/region 3' to the ORF were fused together using nested primers. Upon sequencing to ensure allelic and junction site integrity, it was discovered that one of the *NAT1*10* sources had 4 additional polymorphisms located in the region 3' to the ORF including 1571T>C, 1642A>C, 1647 ΔCT, and 1716C>T. These *NAT1* polymorphisms were verified against NCBI databases and are in linkage disequilibrium (http://egp.gs.washington.edu/). This haplotype is referred to as *NAT1*10B* and was used to compare *N*-acetylation activity with that of *NAT1*10* and *NAT1*4*.

Cell culture

UV5-Chinese hamster ovary (CHO) cells, a nuclease excision repair -deficient derivative of AA8 which are hypersensitive to bulky DNA lesions, were obtained from the ATCC (catalog number: CRL-1865). Unless otherwise noted, cells were incubated at 37^0C in 5% CO_2 in complete alpha-modified minimal essential medium (α-MEM, Lonza, Walkersville, MD) without L-glutamine, ribosides, and deoxyribosides supplemented with 10% fetal bovine serum (Hyclone, Logan, UT), 100 units/mL penicillin (Lonza), 100 µg/mL streptomycin (Lonza), and 2

mM L-glutamine (Lonza). The UV5-CHO cells used in this study were previously stably transfected with a single Flp Recombination Target (FRT) integration site [43]. The FRT site allowed stable transfections to utilize the Flp-In System (Invitrogen). When co-transfected with pOG44 (Invitrogen), a Flp recombinase expression plasmid, a site-specific, conserved recombination event of pcDNA5/FRT (containing either NATa/*NAT1*4* or NATb/*NAT1*4)* occurs at the FRT site. The FRT site allows recombination to occur immediately downstream of the hygromycin resistance gene, allowing for hygromycin selectivity only after Flp-recombinase mediated integration. The UV5/FRT cells were further modified by stable integration of human *CYP1A1* and NADPH-cytochrome P450 reductase gene [43]. They are referred to in this manuscript as UV5/*1A1* cells.

*Removal of the SV40 polyadenylation signal from NATb/NAT1*10B Constructs*

The SV40 polyadenylation signal was removed from the *NAT1*10B* pcDNA5/FRT constructs by incubation at 37º with restriction enzymes, SacII and SapI. The overhangs were filled in or removed using T4 DNA polymerase (New England Biolabs) and then ligated back together using T4 DNA ligase (New England Biolabs).

Transient transfections

UV5/*1A1* cells were transiently transfected with pcDNA5/FRT (Invitrogen) or pEF1/V5-His (Invitrogen) containing *NAT1*4, NAT1*10,* and *NAT1*10B* constructs using Lipofectamine reagent (Invitrogen) following the manufacturer's recommendations. UV5/1A1 cells were co-transfected with pCMV-SPORT-βgal (β-galactosidase transfection control plasmid, Invitrogen). The cells were harvested the next day. Lysate was prepared by centrifuging the cells and resuspending pellet in lysis buffer (0.2% Triton-X-100, 20 mM $NaPO_4$ pH 7.4, 1 mM EDTA, 1 mM DTT, 0.1 mM PMSF, 2 µg/mL aprotinin and 2 mM pepstatin A). The resuspended cell pellet

was centrifuged at 13,000xg for 10 min. The supernatant was used to measure NAT1 and β-galactosidase activities.

Stable transfections

Stable transfections were carried out using the Flp-In System (Invitrogen) into UV5/*1A1* cells that were previously stably transfected with a FRT site (as noted above). The pcDNA5/FRT plasmids containing human *NAT1*4, NAT1*10,* or *NAT1*10B* were co-transfected with pOG44 (Invitrogen), a Flp recombinase expression plasmid. UV5/*1A1* cells were stably transfected with pcDNA5/FRT containing NATb/*NAT1*4, NATb/NAT1*10* and NATb/*NAT1*10B* constructs using Effectene transfection reagent (Qiagen, Valencia, CA) following the manufacturer's recommendations. Since the pcDNA5/FRT vector contains a hygromycin resistance cassette, cells were passaged in complete α-MEM containing 600 μg/mL hygromycin (Invitrogen) to select for cells containing the pcDNA5/FRT plasmid. Hygromycin-resistant colonies were selected approximately 10 days after transfection and isolated with cloning cylinders.

Determination of in vitro N-acetylation for NAT1 4, NAT1 10, and NAT1 10B

Lysate was prepared as described above. *In vitro* assays using the NAT1 specific substrate para-aminobenzoic acid (PABA, 300 μM) or ABP (100 μM) were conducted and acetylated products were separated utilizing high performance liquid chromatography (HPLC) as previously described. *N*-acetylation activity was determined at a fixed concentration of 1 mM acetyl coenzyme A (AcCoA). Reactions containing substrate, AcCoA and enzyme were incubated at 37˚C for 10 min. Reactions were terminated by the addition of 1/10 volume of 1 M acetic acid and centrifuged at 15,000Xg for 10 min. Measurements were adjusted according to baseline measurements using lysates of the UV5/*CYP1A1* cell line and normalized by the amount of total protein. Protein concentrations were measured using the method of Bradford (Bio-Rad, Hercules, CA).

In situ N-acetylation by NAT1 4, NAT1 10, and NAT1 10B

In situ N-acetylation activities were determined by a whole cell assay using media spiked with varying concentrations of PABA or ABP between 10 and 300 µM. The cells were incubated at 37 ºC and media was collected after 1 h (PABA) or 22 min (ABP), 1/10 volume of 1M acetic acid was added, and the mixture was centrifuged at 13,000xg for 10 min. The supernatant was injected into the reverse phase HPLC column and *N*-acetyl-PABA or *N*-acetyl-ABP was separated and quantitated as previously described [44]. Values were normalized to the amount of cells present at time of media removal.

Determination of in vitro O-acetylation for NAT1 4 and NAT1 10 and NAT1 10B

N-hydroxy-4-aminobiphenyl (*N*-OH-ABP) *O*-acetyltransferase assays were conducted and product was separated and quantified by HPLC as previously described [45]. Assays (100 µl) containing 50 µg total protein, *N*-OH-ABP (100 µM), AcCoA (1 mM), and 1 mg/mL deoxyguanosine (dG) were incubated at 37^0C for 10 min. Reactions were stopped with the addition of 100 µL of water saturated ethyl acetate and centrifuged at 13,000xg for 10 min. The organic phase was removed and evaporated to dryness, and the residual was redissolved in 100 µL of 10% ACN and injected onto the HPLC for separation and quantitation of dG-C8-ABP adducts.

Measurement of NAT1 protein

The amount of NAT1 produced in UV5/*1A1* cells stably transfected with NATb/*NAT1*X* was determined by western blot as previously described [45]. Cell lysates were isolated as described above. Varying amounts of lysate were mixed 1:1 with 5% β-mercaptoethanol in Laemmli buffer (Bio-Rad), boiled for 5 min, and proteins were resolved by 12% sodium dodecyl sulfate polyacrylamide gel electrophoresis. The proteins were then transferred by semi-dry electroblotting to polyvinylidene fluoride membranes. The membranes were probed with G5, a

monoclonal mouse anti-NAT1(1:200) Santa Cruz Biotechnology, Santa Cruz, CA) and with horseradish peroxidase (HRP)-conjugated secondary donkey anti-mouse IgG antibody (1:2,000) (Santa Cruz). Supersignal West Pico Chemiluminescent Substrate was used for detection (Pierce). Densitometric analysis was performed using Quantity One Software (Bio-Rad).

Measurement of NAT1 mRNA

Total RNA was isolated from cells using the RNeasy kit (Qiagen) followed by removal of contaminating DNA by treatment with TurboDNase Free (Ambion, Austin, TX). Synthesis of cDNA was performed using qScript cDNA Synthesis Kit (Quanta Biosciences, Gaithersburg, MD) using 1 µg of total RNA in a 20 µL reaction per the manufacturer's protocol. Quantitative reverse transcriptase polymerase chain reaction (qRT-PCR) assays were used to assess the relative amount of *NAT1* mRNA in stably transfected cells. The Step One Plus (Applied Biosystems, Foster City, CA) was used to perform qRT-PCR in reactions containing 1x final concentration of qScript One-Step Fast mix (Quanta Biosciences), 300 nM of each primer and 100 nM of probe in a total volume of 20 µL. For qRT-PCR of *NAT1* mRNA, a TaqMan probe was used with NAT1 Total Splice Forward and NAT1 Total Splice Reverse primers (Table I) designed using Primer Express 1.5 software (Applied Biosystems). An initial incubation at 50°C was carried out for 2 minutes and at 94°C for 10 minutes followed by 40 cycles of 95°C for 15 seconds and 60°C for 1 minute. TaqMan® Ribosomal RNA Control Reagents for quantitation of the endogenous control, 18S rRNA, (Applied Biosystems) were used to determine ΔCt (*NAT1* Ct –18S rRNA Ct). ΔΔCt was determined by subtraction of the smallest ΔCt and relative amounts of *NAT1* mRNA were calculated using $2^{-\Delta\Delta Ct}$ as previously described [40].

Measurement of cytotoxicity and mutagenesis

Assays for cell cytotoxicity and mutagenesis were carried as previously described [45]. Cells were grown in HAT media (30 mM hypoxanthine, 0.1 mM aminopterin, and 30 mM

thymidine) for 12 doublings. Cells ($1x10^6$) were plated, allowed to grow for 24 h and were then treated with 1.56, 3.13, 6.25 or 12.5 µM ABP (Sigma) or vehicle alone (0.5% DMSO) in media. After 48 h, cells were plated to determine survival and mutagenic response to ABP. To determine cloning efficiency following each dose of ABP, 100 cells were plated in triplicate in 6 well-plates and allowed to grow for 7 days in non-selective media. Colonies were counted and expressed as percent of vehicle control. To determine mutagenic response following ABP exposure, $5x10^5$ cells were plated and sub-cultured for 7 days and then seeded with $1x10^5$ cells/100 mm dish (10 replicates) in complete Dulbecco's modified Eagle's medium (Lonza) containing 40 µM 6-thioguanine (Sigma). Mutant *hprt* cells were allowed to grow for 7 days and colonies were counted to determine ABP-induced mutants and corrected by cloning efficiency.

NAT1 mRNA stability assays

Six-well plates containing 1 x 10^6 stably transfected *NAT1*4*, *NAT1*10, and NAT1*10B* cells were treated with complete α-MEM media spiked with 5 µg/mL of the transcription inhibitor, Actinomycin D (Sigma, St. Louis, MO). Cells were collected at 0, 1, 2, 4, and 6 hour time points and total RNA was isolated as described above. Relative *NAT1* mRNA levels were determined from cells transfected with *NAT1*4*, *NAT1*10,* and *NAT1*10B* utilizing qRT-PCR assays as described above. The first-order rate decay constant (slope) of *NAT1* mRNA was determined by linear regression.

RNase protection assay

Biotinylated RNA probes that span the region 3' to the NAT1 ORF were prepared using the MAXIscript *In Vitro* Transcription kit (Applied Biosystems/Ambion, Austin, TX). RNase Protection Assays (RNAPs) were carried out using RPAIII Kits (Applied Biosystems/Ambion) according to the manufacturer's protocols. Briefly, total RNA was collected from transiently

transfected CHO cells and treated with Turbo DNase Free kit (Applied Biosystems/Ambion). Five µg of total RNA was allowed to hybridize overnight in molar excess of biotinylated RNA probes. The resulting RNA-probe mixture was treated with RNase A/T1 (kit) to degrade any non-hybridized RNA and any remaining probe. The Rnase digested hybridized mixture was then separated on a 12% polyacrylamide gel and transferred to a nitrocellulose membrane. The membrane was probed with Chemiluminescent Nucleic Acid Detection Module (ThermoScientific) and exposed to x-ray film to visualize protected probe fragments.

Statistical Analysis

Statistical differences were determined using either an unpaired Student's t-test or one-way ANOVA using Prism Software by Graphpad (La Jolla, CA).

Results

Upon sequencing two human sources of *NAT1*10* genomic DNA used to create the *NAT1*10* constructs, one source was found to contain 4 additional polymorphisms in the 3'-UTR. In addition to 1088T>A (rs1057126), 1095C>A (rs15561), and 1191G>T (rs4986993), the second source also possessed 1641A>C (rs8190865), a deletion ΔCT1647, 1716C>T (rs8190870) and 1735A>T.

NAT1 activity was examined using PABA, ABP, or *N*-OH-ABP as substrates. Significantly more *N*-acetylation of PABA (Figure 1) and ABP (Figure 2) was detected in NATb/*NAT1*10* and NATb/*NAT1*10B* than in NATb/*NAT1*4* ($p<0.05$) in both transiently and stably transfected UV5/1A1 cells. Significantly more *O*-acetylation of *N*-OH-ABP was also detected in *NAT1*10* and *NAT1*10B* than in *NAT1*4* ($p<0.05$) in stably transfected UV5/1A1 cells (Figure 2).

Western blots were performed to examine NAT1 expression in stably transfected UV5/1A1 cells (Figure 3). Significantly more NAT1 ($p<0.05$) was detected in NATb/*NAT1*10* and *NAT1*10B* than in *NAT1*4* transfected cells (Figure 3b). Significantly ($p<0.001$) more NAT1 mRNA was also observed in *NAT1*10* and *NAT1*10B* than *NAT1*4* transfected cells (Figure 3c). However, no differences were observed in stability between *NAT1*4*, *NAT1*10* and *NAT1*10B* mRNA (Figure 3d).

Cytotoxicity and hprt mutants were examined in cells stably transfected with *NAT1*4* and *NAT1*10* following exposure to ABP. Increased ABP-induced cytotoxicity (Figure 4a) and *hprt* mutants (Figure 4b) were observed in all NAT1 transfected cells compared to non-transfected cells. Cells transfected with *NAT1*10* resulted in higher ABP-induced *hprt* mutants than cells transfected with *NAT1*4* following exposure to 3.2, 6.3 and 12.5 μM ABP.

NAT1 mRNAs with intact polyadenylation tails contained in the public sequence databases including UCSC genomic browser, Unigene, and EST ended 10-35 nucleotides beyond 4 different polyadenylation signals located at positions 1088, 1209, 1248, and 1613. Three biotinylated RNA probes were used to determine the polyadenylation pattern of *NAT1*4*, *NAT1*10*, and *NAT1*10B* in transiently transfected UV5/1A1 cells via an RNase protection assay (Figure 5). RNase protection assays detected no difference in polyadenylation site usage between mRNA isolated from cells transfected with NATb/*NAT1*4 or* NATb/*NAT1*10*. Bands corresponding to polyadenylation signal 1 located at position 1028 (215 nucleotides), polyadenylation signal 2 located at position 1088 (284 nucleotides), polyadenylation signal 3 located at position 1209 (118 nucleotides), polyadenylation signal 4 located at position 1248 (163 nucleotides) and polyadenylation signal 5 located at position 1613 (252 nucleotides) were observed for all constructs. Full length probe 1 (371 nucleotides) and full length probe 2 (388 nucleotides) were observed for *NAT1*4*, *NAT1*10*, and *NAT1*10B* (Figure 5 b, c). Full length protection of probe 3 was observed only in *NAT1*10B* transfected cells (369 nucleotides) (Figure 5d). No band was observed in the lane with yeast RNA (negative control) for any probe.

The pcDNA5/FRT expression vector utilized in these experiments contained an SV40 polyadenylation signal for the hygromycin cassette. It was removed to ensure that the presence of *NAT1*10B* transcripts beyond the third probe were not vector-induced. Following removal of the SV40 polyadenylation signal from the pcDNA5/FRT, no significant ($p>0.05$) difference was observed in PABA *N*-acetylation in UV5/1A1 cells transiently transfected with *NAT1*10* or *NAT1*10B.*

Discussion

As described in the Introduction, *NAT1*10* has been associated with higher risk for many different forms of cancer including breast, colorectal, lung, pancreatic, prostate and urinary bladder cancers, gastric adenocarcinoma, and non-Hodgkin's lymphoma. Several studies suggest that *NAT1*10* has higher acetylation capacity than the referent haplotype, *NAT1*4*, while others have reported no difference. Because the allelic frequency of *NAT1*10* is high in many diverse populations [46-48], particularly among those of African descent [49,50], it is important to identify mechanisms responsible for the increased cancer risk associated with *NAT1*10*. To better understand the association of *NAT1*10* and cancer, *NAT1*10* acetylation activity was studied (*in vitro* and *in situ*) using complete NATb mRNA constructs to better mimic *in vivo* gene expression.

Differences in expression and activity of the referent protein, NAT1 4, and the variants, NAT1 10 and NAT1 10B, were studied in UV5/*1A1* CHO cells transiently and stably transfected with NATb type mRNA. Increased *N*- and *O*- acetylation as well as increased mRNA and protein expression were observed in cells transfected with *NAT1*10* and *NAT1*10B* when compared to cells transfected with *NAT1*4*. This difference was observed in both transiently and stably transfected cells. In addition to 1088T>A (rs1057126), 1095C>A (rs15561), and 1191G>T (rs4986993), we identified an *NAT1*10* variant haplotype (termed *NAT1*10B)* that also has 1641A>C (rs8190865), a deletion ΔCT1647, 1716C>T (rs8190870) and 1735A>T. Cells transfected with *NAT1*10B* resulted in higher *N*- and *O*- acetylation activity and protein expression compared to *NAT1*10*. Since these additional polymorphisms found in *NAT1*10B* are not assessed in association studies, it is possible that some of the discrepancies concerning *NAT1*10* phenotype could be attributed to misclassification of *NAT1*10B* as *NAT1*10*.

Alternative polyadenylation plays a role in regulation of gene expression, and it is known that 50% or more of human genes encode multiple transcripts derived from alternative polyadenylation sites [51]. Differential processing at multiple polyadenylation sites can be influenced by physiological conditions such as cell growth, differentiation, and development or by pathological events such as cancer, however these mechanisms are largely unknown [52]. There are 6 potential polyadenylation signals located in the region 3' to the NAT1 ORF. Previous studies have described the use of 2 consensus polyadenylation signals located at positions 1088 and 1209 in the NAT1 3'-UTR [4] or most recently, the use of 3 NAT1 polyadenylation signals including the use of an additional polyadenylation signal at position 1613 [8]. Our study included a survey of NCBI databases which identified NAT1 transcripts that utilize 4 of the 6 potential polyadenylation signals located at positions 1088, 1209, 1248, and 1613. The 1088T>A SNP present in *NAT1*10* alters the 2nd polyadenylation signal (AATAAA – AAAAAA). It has been suggested that this change in polyadenylation signal may increase the stability of the *NAT1*10* mRNA which could then result in differences between *NAT1*10* and *NAT1*4* in acetylation capacity [6]. However, we did not observe differences in NAT1 mRNA stability between *NAT1*4*, *NAT1*10,* or *NAT1*10B* haplotypes. RNase protection assays were performed to map the polyadenylation pattern cells transfected with *NAT1*4*, *NAT1*10*, and *NAT1*10B*. Bands were observed corresponding to the first 5 potential polyadenylation signals and no qualitative differences were observed between *NAT1*4* and *NAT1*10*. However, full length protection of probe 3 was observed for *NAT1*10B* but not for *NAT1*10* or *NAT1*4*, suggesting the presence of *NAT1*10B* transcripts that extend beyond probe 3. Other bands present may be due to either RNA cruciform structures or probe-probe interactions. Because NAT1 transcripts have been identified which utilize multiple polyadenylation signals both in this study and in NCBI databases, alternative polyadenylation usage may be important in NAT1 regulation.

*NAT1*10* has been associated with increased risk for many cancers. The higher acetylation activity observed in NAT1 10 compared to NAT1 4 in this study could be partly responsible for the increased risk associated with individuals possessing *NAT1*10*. Butcher et al. [53] suggested cell-type specific expression of an RNA-binding protein that would allow increased mRNA stability in some cell types. In addition, a recent study reported an association between higher *NAT1*10* activity and increased translation efficiency in HepG2 cells [8]. However, our study demonstrated higher *NAT1*10* and *NAT1*10B* acetylation associated with higher mRNA expression. Therefore, it is possible that DNA-binding proteins could bind to *NAT1*4, NAT1*10, and NAT1*10B* mRNA differently in certain cell types and therefore modify NAT1 differently in those cell types. *NAT1*10* expression appears to be under the control of multiple types of regulation which could be cell type dependent.

Because the allelic frequency of *NAT1*10* haplotype is high, clearly defining the *NAT1*10* phenotype would allow cancer risk and other toxicities related to environmental arylamine exposure to be better understood. This study has shown that cells transfected with *NAT1*10* and *NAT1*10B* have higher *N*- and *O*- acetylation activity, NAT1 mRNA, and protein expression compared to cells transfected with *NAT1*4*. Additionally, higher ABP-induced DNA adducts and mutants were observed in cells transfected with *NAT1*10* compared to *NAT1*4.* However, no differences between *NAT1*4* and *NAT1*10* polyadenylation pattern were observed. Additionally, no differences in mRNA stability were observed between *NAT1*4, NAT1*10,* and *NAT1*10B* in stably transfected UV5/1A1 cells or in NAT1 endogenously expressed in HepG2 cells (unpublished data). Other mechanisms such as DNA-binding proteins may be responsible for the higher amount of *NAT1*10* mRNA, protein, acetylation activity, ABP-induced DNA adducts and mutants compared to *NAT1*4*. A difference was observed in the *NAT1*10B* polyadenylation pattern compared to *NAT1*10* and *NAT1*4*, suggesting that additional mechanisms are involved in regulation of *NAT1*10B* compared to *NAT1*10.* Current

genotyping methods do not differentiate between *NAT1*10* and *NAT1*10B* which could contribute to divergent findings regarding the role of *NAT1*10* in cancer risk. Further studies should be conducted to determine the responsible mechanisms for regulation of *NAT1*10* and *NAT1*10B*. The higher acetylation and ABP-induced mutants observed in NAT1 10 compared to NAT1 4 is consistent with increased risk for cancers associated with arylamine exposure in individuals possessing *NAT1*10* haplotypes.

Funding

This work was supported by grants [R01-CA034627] from the National Cancer Institute; [T32-ES011564 and P30-ES014443] from the National Institute for Environmental Health Sciences; and [BC083107] from the Department of Defense Breast Cancer Research Program.

Acknowledgement

Portions of this work constitute partial fulfillment for the PhD in pharmacology and toxicology at the University of Louisville to Lori Millner.

Conflict of Interest: None declared.

References

1. Hein, D.W., Doll, M.A., Fretland, A.J., Leff, M.A., Webb, S.J., Xiao, G.H., Devanaboyina, U.S., Nangju, N.A. and Feng, Y. (2000) Molecular genetics and epidemiology of the NAT1 and NAT2 acetylation polymorphisms. *Cancer Epidemiol. Biomarkers Prev.*, **9**, 29-42.

2. Tiang, J.M., Butcher, N.J., Cullinane, C., Humbert, P.O. and Minchin, R.F. (2011) RNAi-mediated knock-down of arylamine N-acetyltransferase-1 expression induces E-cadherin up-regulation and cell-cell contact growth inhibition. *PloS One*, **6**, e17031.

3. Pacifici, G.M., Bencini, C. and Rane, A. (1986) Acetyltransferase in humans: development and tissue distribution. *Pharmacology*, **32**, 283-91.

4. Boukouvala, S. and Sim, E. (2005) Structural analysis of the genes for human arylamine N-acetyltransferases and characterisation of alternative transcripts. *Basic Clin Pharmacol. Toxicol.*, **96**, 343-51.

5. Badawi, A.F., Hirvonen, A., Bell, D.A., Lang, N.P. and Kadlubar, F.F. (1995) Role of aromatic amine acetyltransferases, NAT1 and NAT2, in carcinogen-DNA adduct formation in the human urinary bladder. *Cancer Res.*, **55**, 5230-7.

6. Bell, D.A., Badawi, A.F., Lang, N.P., Ilett, K.F., Kadlubar, F.F. and Hirvonen, A. (1995) Polymorphism in the N-acetyltransferase 1 (NAT1) polyadenylation signal: association of NAT1*10 allele with higher N-acetylation activity in bladder and colon tissue. *Cancer Res.*, **55**, 5226-9.

7. Zenser, T.V., Lakshmi, V.M., Rustan, T.D., Doll, M.A., Deitz, A.C., Davis, B.B. and Hein, D.W. (1996) Human N-acetylation of benzidine: role of NAT1 and NAT2. *Cancer Res.*, **56**, 3941-7.

8. Wang, D., Para, M.F., Koletar, S.L. and Sadee, W. (2011) Human N-acetyltransferase 1 *10 and *11 alleles increase protein expression through distinct mechanisms and associate with sulfamethoxazole-induced hypersensitivity. *Pharmacogenet. Genomics*, **21**, 652-64.

9. Zhangwei, X., Jianming, X., Qiao, M. and Xinhua, X. (2006) N-Acetyltransferase-1 gene polymorphisms and correlation between genotype and its activity in a central Chinese Han population. *Clin. Chim. Acta*, **371**, 85-91.

10. Hein, D.W., McQueen, C.A., Grant, D.M., Goodfellow, G.H., Kadlubar, F.F. and Weber, W.W. (2000) Pharmacogenetics of the arylamine N-acetyltransferases: a symposium in honor of Wendell W. Weber. *Drug Metab. Dispos.*, **28**, 1425-32.

11. Payton, M.A. and Sim, E. (1998) Genotyping human arylamine N-acetyltransferase type 1 (NAT1): the identification of two novel allelic variants. *Biochem. Pharmacol.*, **55**, 361-6.

12. Bruhn, C., Brockmoller, J., Cascorbi, I., Roots, I. and Borchert, H.H. (1999) Correlation between genotype and phenotype of the human arylamine N-acetyltransferase type 1 (NAT1). *Biochem. Pharmacol.*, **58**, 1759-64.

13. de Leon, J.H., Vatsis, K.P. and Weber, W.W. (2000) Characterization of naturally occurring and recombinant human N-acetyltransferase variants encoded by NAT1. *Mol. Pharmacol.*, **58**, 288-99.

14. Hein, D.W. (2009) N-acetyltransferase SNPs: emerging concepts serve as a paradigm for understanding complexities of personalized medicine. *Expert Opinion Drug Metab. Toxicol.*, **5**, 353-66.

15. Mishra, P.J., Banerjee, D. and Bertino, J.R. (2008) MiRSNPs or MiR-polymorphisms, new players in microRNA mediated regulation of the cell: Introducing microRNA pharmacogenomics. *Cell Cycle*, **7**, 853-8.

16. Pizzuti, A., Argiolas, A., Di Paola, R., Baratta, R., Rauseo, A., Bozzali, M., Vigneri, R., Dallapiccola, B., Trischitta, V. and Frittitta, L. (2002) An ATG repeat in the 3'-untranslated region of the human resistin gene is associated with a decreased risk of insulin resistance. *J. Clin. Endocrinol. Metab.*, **87**, 4403-6.

17. Gehring, N.H., Frede, U., Neu-Yilik, G., Hundsdoerfer, P., Vetter, B., Hentze, M.W. and Kulozik, A.E. (2001) Increased efficiency of mRNA 3' end formation: a new genetic mechanism contributing to hereditary thrombophilia. *Nat. Genet.*, **28**, 389-92.

18. Morton, L.M., Bernstein, L., Wang, S.S., Hein, D.W., Rothman, N., Colt, J.S., Davis, S., Cerhan, J.R., Severson, R.K., Welch, R., Hartge, P. and Zahm, S.H. (2007) Hair dye use, genetic variation in N-acetyltransferase 1 (NAT1) and 2 (NAT2), and risk of non-Hodgkin lymphoma. *Carcinogenesis*, **28**, 1759-64.

19. Morton, L.M., Schenk, M., Hein, D.W., Davis, S., Zahm, S.H., Cozen, W., Cerhan, J.R., Hartge, P., Welch, R., Chanock, S.J., Rothman, N. and Wang, S.S. (2006) Genetic variation in N-acetyltransferase 1 (NAT1) and 2 (NAT2) and risk of non-Hodgkin lymphoma. *Pharmacogenet. Genomics*, **16**, 537-45.

20. Taylor, J.A., Umbach, D.M., Stephens, E., Castranio, T., Paulson, D., Robertson, C., Mohler, J.L. and Bell, D.A. (1998) The role of N-acetylation polymorphisms in smoking-associated bladder cancer: evidence of a gene-gene-exposure three-way interaction. *Cancer Res.*, **58**, 3603-10.

21. Abdel-Rahman, S.Z., El-Zein, R.A., Zwischenberger, J.B. and Au, W.W. (1998) Association of the NAT1*10 genotype with increased chromosome aberrations and higher lung cancer risk in cigarette smokers. *Mutation Res.*, **398**, 43-54.

22. Wikman, H., Thiel, S., Jager, B., Schmezer, P., Spiegelhalder, B., Edler, L., Dienemann, H., Kayser, K., Schulz, V., Drings, P., Bartsch, H. and Risch, A. (2001) Relevance of N-acetyltransferase 1 and 2 (NAT1, NAT2) genetic polymorphisms in non-small cell lung cancer susceptibility. *Pharmacogenetics*, **11**, 157-68.

23. Gemignani, F., Landi, S., Szeszenia-Dabrowska, N., Zaridze, D., Lissowska, J., Rudnai, P., Fabianova, E., Mates, D., Foretova, L., Janout, V., Bencko, V., Gaborieau, V., Gioia-Patricola, L., Bellini, I., Barale, R., Canzian, F., Hall, J., Boffetta, P., Hung, R.J. and Brennan, P. (2007) Development of lung cancer before the age of 50: the role of xenobiotic metabolizing genes. *Carcinogenesis*, **28**, 1287-93.

24. Chen, J., Stampfer, M.J., Hough, H.L., Garcia-Closas, M., Willett, W.C., Hennekens, C.H., Kelsey, K.T. and Hunter, D.J. (1998) A prospective study of N-acetyltransferase genotype, red meat intake, and risk of colorectal cancer. *Cancer Res.*, **58**, 3307-11.

25. Ishibe, N., Sinha, R., Hein, D.W., Kulldorff, M., Strickland, P., Fretland, A.J., Chow, W.H., Kadlubar, F.F., Lang, N.P. and Rothman, N. (2002) Genetic polymorphisms in heterocyclic amine metabolism and risk of colorectal adenomas. *Pharmacogenetics*, **12**, 145-50.

26. Lilla, C., Verla-Tebit, E., Risch, A., Jager, B., Hoffmeister, M., Brenner, H. and Chang-Claude, J. (2006) Effect of NAT1 and NAT2 genetic polymorphisms on colorectal cancer risk associated with exposure to tobacco smoke and meat consumption. *Cancer Epidemiol. Biomarkers Prev.*, **15**, 99-107.

27. Ambrosone, C.B., Abrams, S.M., Gorlewska-Roberts, K. and Kadlubar, F.F. (2007) Hair dye use, meat intake, and tobacco exposure and presence of carcinogen-DNA adducts in exfoliated breast ductal epithelial cells. *Arch. Biochem. Biophys.*, **464**, 169-75.

28. Millikan, R.C., Pittman, G.S., Newman, B., Tse, C.K., Selmin, O., Rockhill, B., Savitz, D., Moorman, P.G. and Bell, D.A. (1998) Cigarette smoking, N-acetyltransferases 1 and 2, and breast cancer risk. *Cancer Epidemiol. Biomarkers Prev.*, **7**, 371-8.

29. Zheng, W., Deitz, A.C., Campbell, D.R., Wen, W.Q., Cerhan, J.R., Sellers, T.A., Folsom, A.R. and Hein, D.W. (1999) N-acetyltransferase 1 genetic polymorphism, cigarette smoking, well-done meat intake, and breast cancer risk. *Cancer Epidemiol. Biomarkers Prev.*, **8**, 233-9.

30. Hein, D.W., Leff, M.A., Ishibe, N., Sinha, R., Frazier, H.A., Doll, M.A., Xiao, G.H., Weinrich, M.C. and Caporaso, N.E. (2002) Association of prostate cancer with rapid N-acetyltransferase 1 (NAT1*10) in combination with slow N-acetyltransferase 2 acetylator genotypes in a pilot case-control study. *Environ. Mol. Mutagen.*, **40**, 161-7.

31. Rovito, P.M., Jr., Morse, P.D., Spinek, K., Newman, N., Jones, R.F., Wang, C.Y. and Haas, G.P. (2005) Heterocyclic amines and genotype of N-acetyltransferases as risk factors for prostate cancer. *Prostate Cancer Prostatic. Dis.,* **8**, 69-74.

32. Boissy, R.J., Watson, M.A., Umbach, D.M., Deakin, M., Elder, J., Strange, R.C. and Bell, D.A. (2000) A pilot study investigating the role of NAT1 and NAT2 polymorphisms in gastric adenocarcinoma. *Int. J. Cancer*, **87**, 507-11.

33. Li, D., Jiao, L., Li, Y., Doll, M.A., Hein, D.W., Bondy, M.L., Evans, D.B., Wolff, R.A., Lenzi, R., Pisters, P.W., Abbruzzese, J.L. and Hassan, M.M. (2006) Polymorphisms of cytochrome P4501A2 and N-acetyltransferase genes, smoking, and risk of pancreatic cancer. *Carcinogenesis*, **27**, 103-11.

34. Brockton, N., Little, J., Sharp, L. and Cotton, S.C. (2000) N-acetyltransferase polymorphisms and colorectal cancer: a HuGE review. *Am. J. Epidemiol.*, **151**, 846-61.

35. Gu, J., Liang, D., Wang, Y., Lu, C. and Wu, X. (2005) Effects of N-acetyl transferase 1 and 2 polymorphisms on bladder cancer risk in Caucasians. *Mutation Res.*, **581**, 97-104.

36. Sanderson, S., Salanti, G. and Higgins, J. (2007) Joint effects of the N-acetyltransferase 1 and 2 (NAT1 and NAT2) genes and smoking on bladder carcinogenesis: a literature-based systematic HuGE review and evidence synthesis. *Am. J. Epidemiol.*, **166**, 741-51.

37. Gong, C., Hu, X., Gao, Y., Cao, Y., Gao, F. and Mo, Z. (2011) A meta-analysis of the NAT1 and NAT2 polymorphisms and prostate cancer: a huge review. *Med. Oncol.*, **28**, 365-76.

38. Blum, M., Grant, D.M., McBride, W., Heim, M. and Meyer, U.A. (1990) Human arylamine N-acetyltransferase genes: isolation, chromosomal localization, and functional expression. *DNA Cell Biol.,* **9**, 193-203.

39. Husain, A., Barker, D.F., States, J.C., Doll, M.A. and Hein, D.W. (2004) Identification of the major promoter and non-coding exons of the human arylamine N-acetyltransferase 1 gene (NAT1). *Pharmacogenetics*, **14**, 397-406.

40. Barker, D.F., Husain, A., Neale, J.R., Martini, B.D., Zhang, X., Doll, M.A., States, J.C. and Hein, D.W. (2006) Functional properties of an alternative, tissue-specific promoter for human arylamine N-acetyltransferase 1. *Pharmacogenet. Genomics*, **16**, 515-25.

41. Husain, A., Zhang, X., Doll, M.A., States, J.C., Barker, D.F. and Hein, D.W. (2007) Functional analysis of the human N-acetyltransferase 1 major promoter: quantitation of tissue expression and identification of critical sequence elements. *Drug Metab. Dispos.*, **35**, 1649-56.

42. Horton, R.M., Hunt, H.D., Ho, S.N., Pullen, J.K. and Pease, L.R. (1989) Engineering hybrid genes without the use of restriction enzymes: gene splicing by overlap extension. *Gene*, **77**, 61-8.

43. Bendaly, J., Zhao, S., Neale, J.R., Metry, K.J., Doll, M.A., States, J.C., Pierce, W.M., Jr. and Hein, D.W. (2007) 2-Amino-3,8-dimethylimidazo-[4,5-f]quinoxaline-induced DNA adduct formation and mutagenesis in DNA repair-deficient Chinese hamster ovary cells expressing human cytochrome P4501A1 and rapid or slow acetylator N-acetyltransferase 2. *Cancer Epidemiol. Biomarkers Prev.*, **16**, 1503-9.

44. Hein, D.W., Doll, M.A., Nerland, D.E. and Fretland, A.J. (2006) Tissue distribution of N-acetyltransferase 1 and 2 catalyzing the N-acetylation of 4-aminobiphenyl and O-acetylation of N-hydroxy-4-aminobiphenyl in the congenic rapid and slow acetylator Syrian hamster. *Mol. Carcinog.*, **45**, 230-8.

45. Millner, L.M., Doll, M.A., Cai, J., States, J.C. and Hein, D.W. (2011) NATb/NAT1*4 promotes greater arylamine N-acetyltransferase 1 mediated DNA adducts and mutations than NATa/NAT1*4 following exposure to 4-aminobiphenyl. *Mol. Carcinog.,* Epub Aug 11.

46. Lo-Guidice, J.M., Allorge, D., Chevalier, D., Debuysere, H., Fazio, F., Lafitte, L.J. and Broly, F. (2000) Molecular analysis of the N-acetyltransferase 1 gene (NAT1*) using polymerase chain reaction-restriction fragment-single strand conformation polymorphism assay. *Pharmacogenetics*, **10**, 293-300.

47. Vaziri, S.A., Hughes, N.C., Sampson, H., Darlington, G., Jewett, M.A. and Grant, D.M. (2001) Variation in enzymes of arylamine procarcinogen biotransformation among bladder cancer patients and control subjects. *Pharmacogenetics*, **11**, 7-20.

48. Cascorbi, I., Roots, I. and Brockmoller, J. (2001) Association of NAT1 and NAT2 polymorphisms to urinary bladder cancer: significantly reduced risk in subjects with NAT1*10. *Cancer Res.*, **61**, 5051-6.

49. Loktionov, A., Moore, W., Spencer, S.P., Vorster, H., Nell, T., O'Neill, I.K., Bingham, S.A. and Cummings, J.H. (2002) Differences in N-acetylation genotypes between Caucasians and Black South Africans: implications for cancer prevention. *Cancer Detect. Prev.*, **26**, 15-22.

50. Kidd, L.C., Vancleave, T.T., Doll, M.A., Srivastava, D.S., Thacker, B., Komolafe, O., Pihur, V., Brock, G.N. and Hein, D.W. (2011) No association between variant N-acetyltransferase genes, cigarette smoking and prostate cancer susceptibility among men of African descent. *Biomark. Cancer*, **2011**, 1-13.

51. Tian, B., Hu, J., Zhang, H. and Lutz, C.S. (2005) A large-scale analysis of mRNA polyadenylation of human and mouse genes. *Nucleic Acids Res.*, **33**, 201-12.

52. Di Giammartino, D.C., Nishida, K. and Manley, J.L. (2011) Mechanisms and consequences of alternative polyadenylation. *Mol. Cell*, **43**, 853-66.

53. Butcher, N.J., Tiang, J. and Minchin, R.F. (2008) Regulation of arylamine N-acetyltransferases. *Curr. Drug Metab.*, **9**, 498-504.

Primer	Use	Sequence
Lkm40P1	NATb 5-'UTR forward specific PCR	5'-GGCCGCGGCATTCAGTCTAGTTCCTGGTTGCC-3'
P1 Fwd Inr NheI	NATb 5'-UTR forward specific nested PCR	5'TTTAAAGCTAGCATTCAGTCTAGTCTAGTTCCTGGTTGCCGGCT-3'
NAT1 (3') ORF Reverse	NATb 5'-UTR reverse PCR	5'-TTCCTCACTCAGAGTCTTGAACTCTATT-3'
NAT1 (3') ORF For	NAT1 coding region forward PCR	5'-AGACATCTCCATCATCTGTGTTTACTAGT-3'
pcDNA5 FRTdistal Reverse	NAT1 3'-UTR reverse PCR	5'-CGTGGGGATACCCCCTAGA-3"
NAT1 KPN-Rev	NAT1 3'-UTR reverse nested PCR	5'-ATAGTAGGTACCTCTGAATTATAGATAAGCAAAGATTCAGATTCT-3'
NAT1 KPN-Rev*10B	NAT1 3'-UTR reverse nested PCR	5'-ATAGTAGGTACCTCTGAATTATAGATAAGCAAAGATACAGATTCT-3'
NAT1 total spliced Forward	NAT1 specific forward q-RT-PCR	5'-GAATTCAAGCCAGGAAGAAGCA-3'
NAT1 total spliced Reverse	NAT1 specific reverse q-RT-PCR	5'-TCCAAGTCCAATTTGTTCCTAGACT-3'
NAT1 TAQMAN probe	TAQMAN probe for NAT1 total splice	6FAM-5'-CAATCTGTCTTCTGGATTAA-3'MGBNFQ

Table I. Primers used to construct *NAT1*4*, *NAT1*10*, and *NAT1*10B* in NATb Type transcript constructs and for RT-PCR. These allelic constructs were then ligated into pcDNA5/FRT expression vectors.

Legends to Figures

Fig. 1. PABA *N*-acetylation by NAT1 4 (open bars), NAT1 10 (closed bars) and NAT1 10B (gray bars). (a) PABA *N*-acetylation (*in vitro*) following transient transfection with pcDNA5/FRT; (b) PABA *N*-acetylation (*in vitro*) following stable transfection with pcDNA5/FRT; (c) PABA *N*-acetylation (*in situ)* following stable transfection with pcDNA5/FRT. Each bar represents mean ± S.E.M. for three transient transfections (a) or three separate collections performed in triplicate (b and c) Significantly higher than NAT1 4 denoted by *p<0.05 and ***p<0.0001 following analysis with one-way ANOVA.

Fig. 2. ABP *N*-acetylation and *N*-OH-ABP *O*-acetylation by NAT1 4 (open bars), NAT1 10 (closed bars) and NAT1 10B (gray bars) (following stable transfection in UV5/1A1 cells. (a) ABP *N*-acetylation (*in vitro*); (b) ABP *N*-acetylation (*in situ*); (c) *O*-acetylation of *N*-OH-ABP (*in vitro*). Each bar represents mean ± S.E.M. for three separate collections performed in triplicate. Significantly higher than NAT1 4 denoted by *p<0.05 and ***p<0.0001 following analysis with one-way ANOVA.

Fig. 3. Representative western blot of NAT1 4, NAT1 10, and NAT1 10B stable expression (a) and densitometric analysis (b). NAT1 mRNA expression levels in stably transfected NATb constructs (c) and NAT1 mRNA stability (d). Each bar represents mean ± SEM of 2 western blots or 3 collections of mRNA each performed in triplicate. Analysis done with Quantity One software (BioRad). Significantly higher than NAT1 4 denoted by *p<0.05, **p<0.001, and ***p<0.0001 following analysis with one-way ANOVA.

Fig. 4. (a) ABP-induced cytotoxicity and (b) ABP-induced *hprt* mutants per million cells in UV5/1A1 cells that were stably transfected. CYP1A1 *only* (●), CYP1A1/NAT1 4 (■), and CYP1A1/NAT1 10 (▲). Each data point represents mean ± S.E.M. for three determinations.

Fig. 5. RNase protection assays examining pattern of polyadenylation site usage. (a) Schematic representation of NAT1 3'-UTR and probes. (b) The 1st and 2nd polyadenylation sites mapped with probe 1. (c) The 3rd and 4th polyadenylation sites mapped with probe 2. (d) The 5th and 6th polyadenylation sites mapped with probe 3. Lane 1: biotinylated marker; lane 2: RNA isolated from transiently transfected *NAT1*4*; lane 3: *NAT1*10*; lane 4: *NAT1*10B:* Lanes 5-7 are control lanes; lane 5: yeast (no target) RNA; lane 6: no RNase; lane 7: probe alone. Lanes 2 – 5 were hybridized to probe and treated with RNAse.

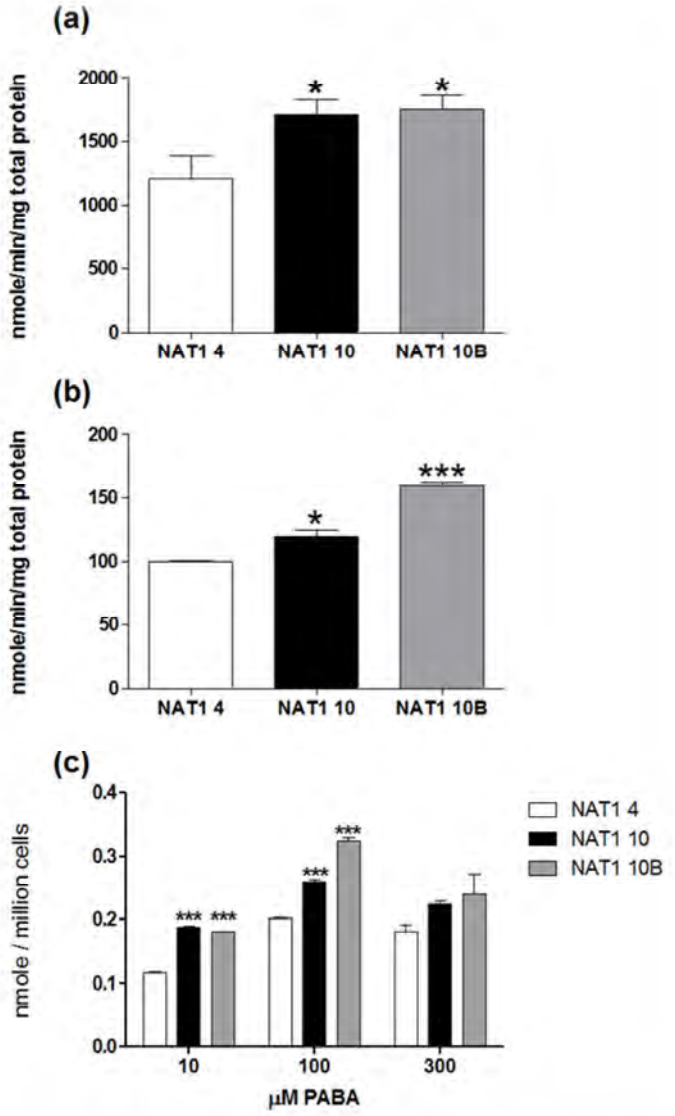

Fig. 1. PABA N-acetylation by NAT1 4 (open bars), NAT1 10 (closed bars) and NAT1 10B (gray bars). (a) PABA N-acetylation (in vitro) following transient transfection with pcDNA5/FRT; (b) PABA N-acetylation (in vitro) following stable transfection with pcDNA5/FRT; (c) PABA N-acetylation (in situ) following stable transfection with pcDNA5/FRT. Each bar represents mean ± S.E.M. for three transient transfections (a) or three separate collections performed in triplicate (b and c) Significantly higher than NAT1 4 denoted by *p<0.05 and ***p<0.0001 following analysis with one-way ANOVA.
158x256mm (300 x 300 DPI)

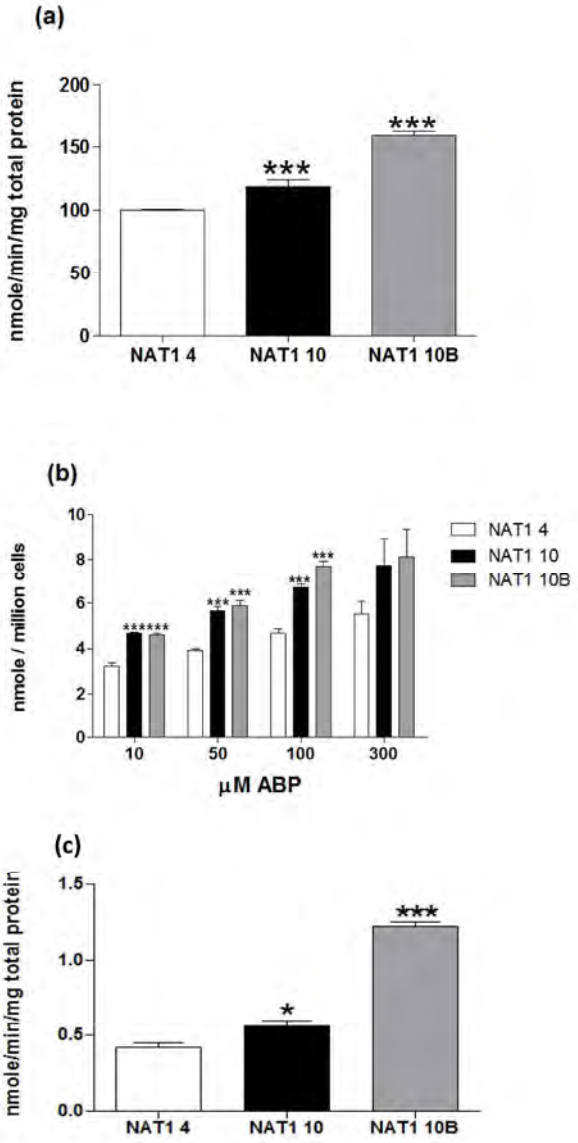

Fig. 2. ABP N-acetylation and N-OH-ABP O-acetylation by NAT1 4 (open bars), NAT1 10 (closed bars) and NAT1 10B (gray bars) (following stable transfection in UV5/1A1 cells. (a) ABP N-acetylation (in vitro); (b) ABP N-acetylation (in situ); (c) O-acetylation of N-OH-ABP (in vitro). Each bar represents mean ± S.E.M. for three separate collections performed in triplicate. Significantly higher than NAT1 4 denoted by *p<0.05 and ***p<0.0001 following analysis with one-way ANOVA.
180x343mm (300 x 300 DPI)

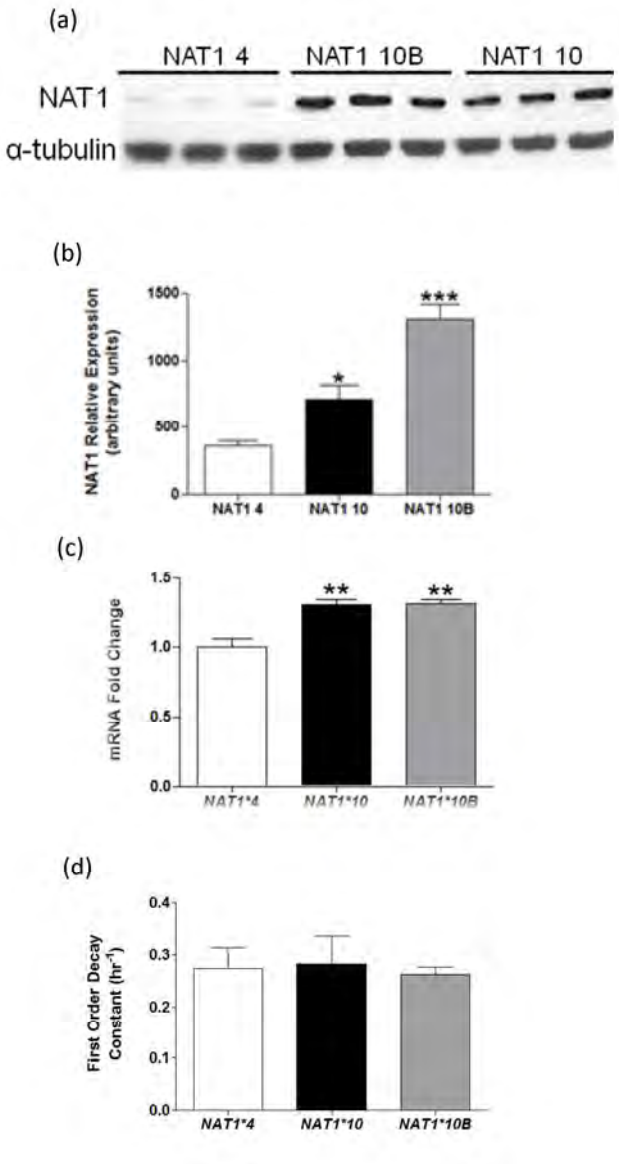

Fig. 3. Representative western blot of NAT1 4, NAT1 10, and NAT1 10B stable expression (a) and densitometric analysis (b). NAT1 mRNA expression levels in stably transfected NATb constructs (c) and NAT1 mRNA stability (d). Each bar represents mean ± SEM of 2 western blots or 3 collections of mRNA each performed in triplicate. Analysis done with Quantity One software (BioRad). Significantly higher than NAT1 4 denoted by *p<0.05, **p<0.001, and ***p<0.0001 following analysis with one-way ANOVA.
174x309mm (300 x 300 DPI)

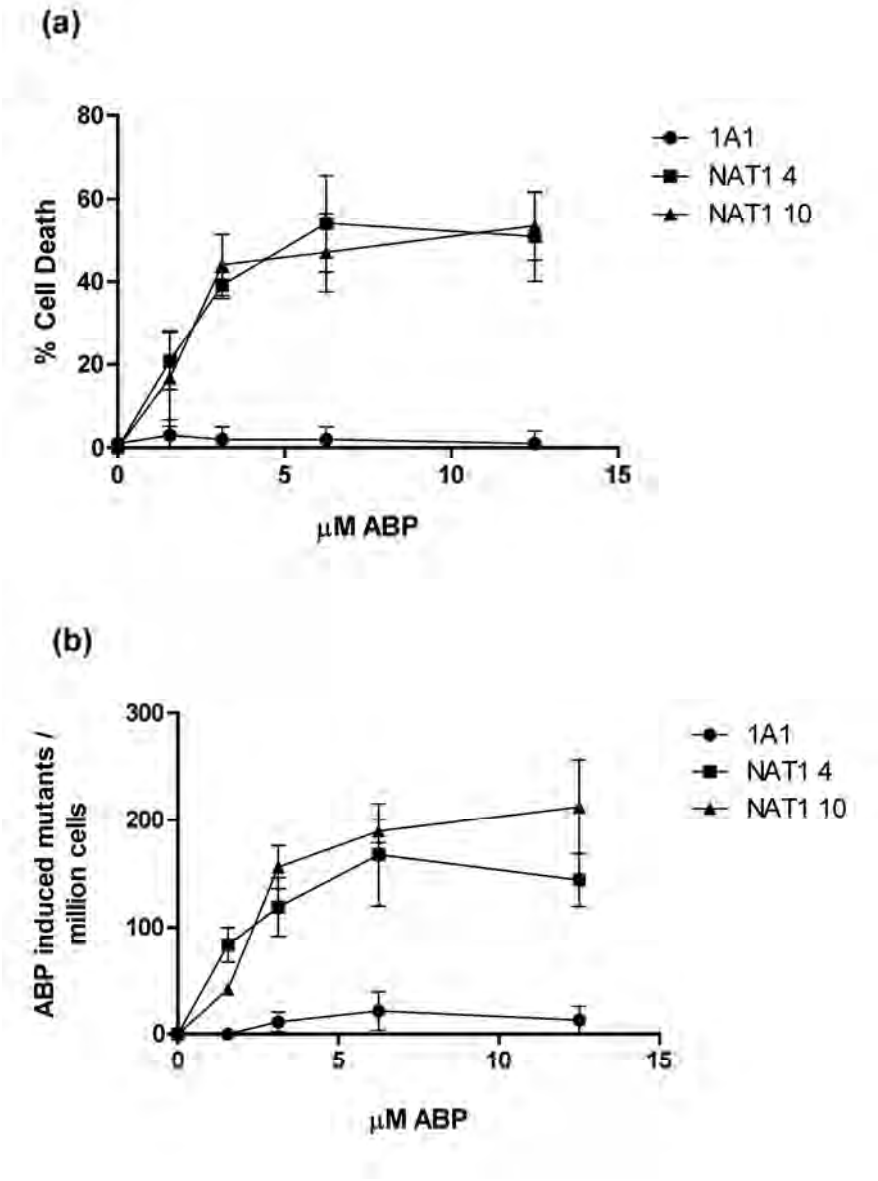

Fig. 4. (a) ABP-induced cytotoxicity and (b) ABP-induced hprt mutants per million cells in UV5/1A1 cells that were stably transfected. CYP1A1 only (circle), CYP1A1/NAT1 4 (square), and CYP1A1/NAT1 10 (triangle). Each data point represents mean ± S.E.M. for three determinations.
152x209mm (300 x 300 DPI)

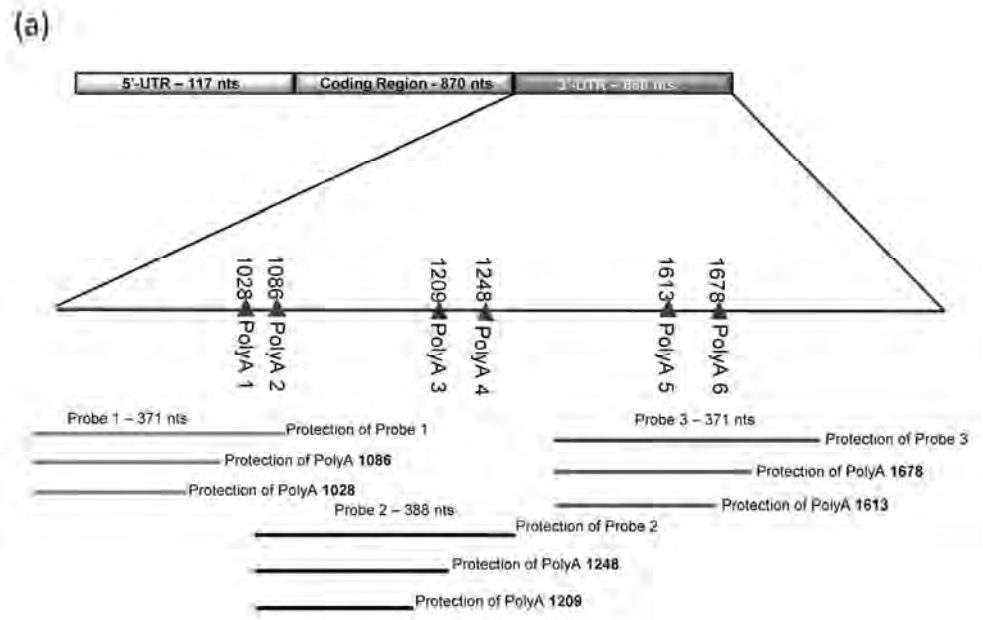

Fig. 5. RNase protection assays examining pattern of polyadenylation site usage. (a) Schematic representation of NAT1 3'-UTR and probes.
127x86mm (300 x 300 DPI)

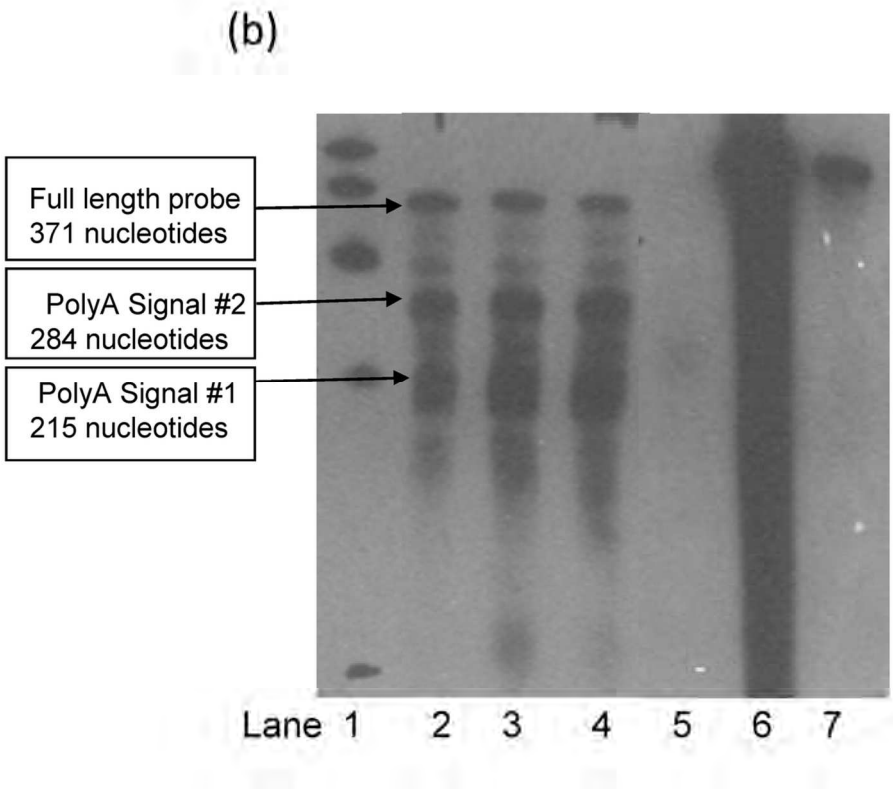

Fig. 5. RNase protection assays examining pattern of polyadenylation site usage. (b) The 1st and 2nd polyadenylation sites mapped with probe. Lane 1: biotinylated marker; lane 2: RNA isolated from transiently transfected NAT1*4; lane 3: NAT1*10; lane 4: NAT1*10B: Lanes 5-7 are control lanes; lane 5: yeast (no target) RNA; lane 6: no RNase; lane 7: probe alone. Lanes 2 – 5 were hybridized to probe and treated with RNAse.
111x90mm (300 x 300 DPI)

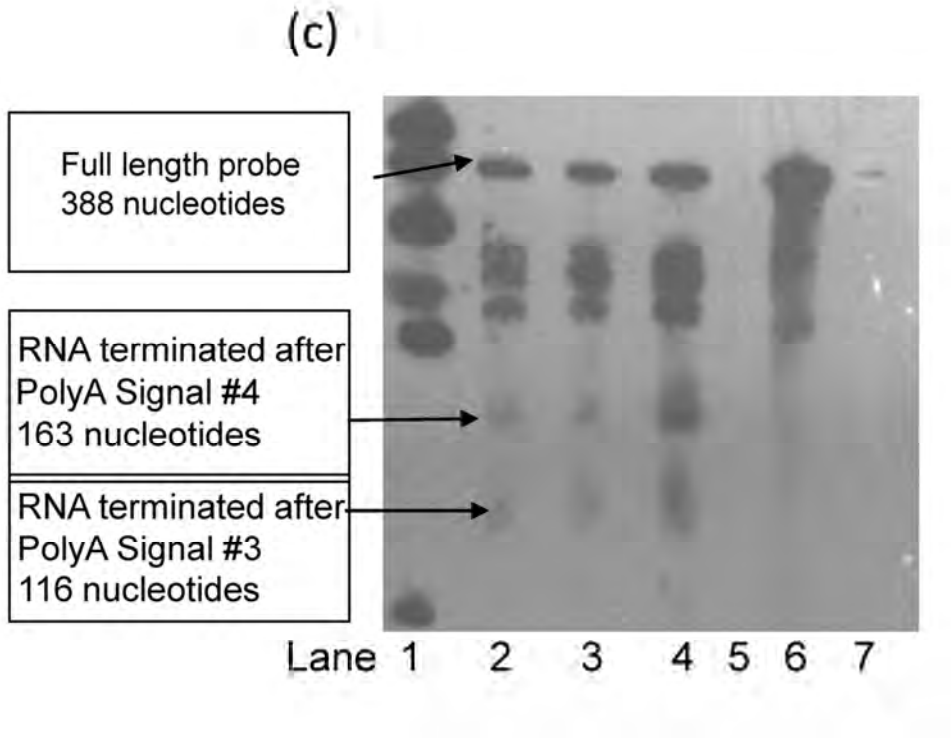

Fig. 5. RNase protection assays examining pattern of polyadenylation site usage. (c) The 3rd and 4th polyadenylation sites mapped with probe 2. Lane 1: biotinylated marker; lane 2: RNA isolated from transiently transfected NAT1*4; lane 3: NAT1*10; lane 4: NAT1*10B: Lanes 5-7 are control lanes; lane 5: yeast (no target) RNA; lane 6: no RNase; lane 7: probe alone. Lanes 2 – 5 were hybridized to probe and treated with RNAse.
95x75mm (300 x 300 DPI)

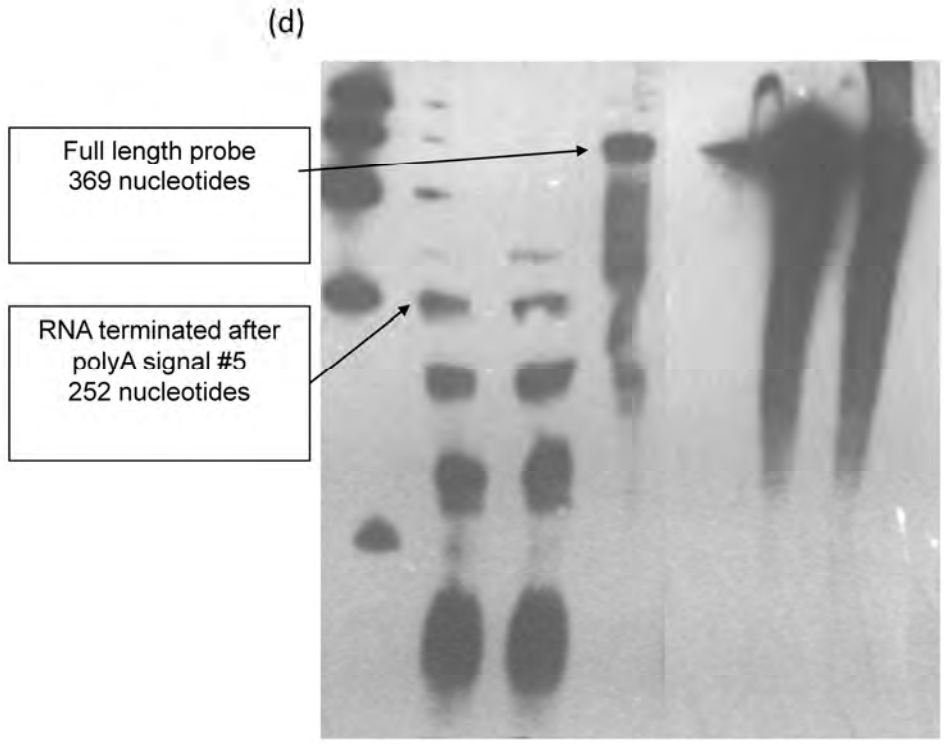

Fig. 5. RNase protection assays examining pattern of polyadenylation site usage. (d) The 5th and 6th polyadenylation sites mapped with probe 3. Lane 1: biotinylated marker; lane 2: RNA isolated from transiently transfected NAT1*4; lane 3: NAT1*10; lane 4: NAT1*10B: Lanes 5-7 are control lanes; lane 5: yeast (no target) RNA; lane 6: no RNase; lane 7: probe alone. Lanes 2 – 5 were hybridized to probe and treated with RNAse.
155x127mm (300 x 300 DPI)